Spring 1987

Microemulsions, lyotropic liquid crystals, and other association structures

Jiafu Fang

Department: Chemistry

MICROEMULSIONS, LYOTROPIC LIQUID CRYSTALS, AND OTHER ASSOCIATION STRUCTURES

BY

JIAFU FANG, 1952-

A DISSERTATION

Presented to the Faculty of the Graduate School of the

UNIVERSITY OF MISSOURI-ROLLA

In Partial Fufillment of the Requirements for the Degree

DOCTOR OF PHILOSOPHY

in

CHEMISTRY

1987

Raymond S. Berry

J. H. Wang

Garnin D. Haney

C. R. Hammel

J. N. Cogi

PUBLICATION DISSERTATION OPTION

This dissertation has been prepared in the style utilized by the Journal of Colloid and Interface Science and the Journal of Physical Chemistry. The body of the dissertation consists of four articles. Article I has been published by the Journal of Colloid and Interface Science in Vol. 109, 330(1986). Articles II and III have been accepted by the same journal for publication and are in press Article IV will be submitted to the Journal of Physical Chemistry. Introduction has been added for purposes normal to dissertation writing.

ABSTRACT

Phase diagrams have been determined showing the extent of the inverse micellar or microemulsion region for several ionic surfactants and some cosurfactants. Hexylamine has been found to be a very effective cosurfactant giving rise to very good water solubilizing capacity at extremely low surfactant concentrations and very low cosurfactant levels at rather high initial hydrocarbon levels.

A fairly extensive study of phase equilibria of the system composed of sodium dodecyl sulfate, hexylamine, heptane, and water has been carried out. The conductivity behavior of the inverse micellar or microemulsion phase of the system shows the percolation phenomenon. Low angle X-ray diffraction has been used to investigate the lamellar liquid crystalline phase. Equations are developed or modified to allow determination of the degree of interpenetration between the amphiphile bilayers and aqueous layers in the lamellar liquid crystal structure.

The association structures of water-in-oil (W/O) microemulsions containing sodium dodecyl sulfate, hexylamine, heptane, and aqueous sodium chloride have been investigated using time-average and dynamic light scattering techniques. Molecular weights, diffusion coefficients, and particle size of microemulsion droplets were determined. Modern theories of fluids have been used to interpret the behavior of scattered light intensity and diffusion coefficients.

ACKNOWLEDGEMENTS

The author would like to express his sincere thanks to Dr. Raymond L. Venable, Dr. Stig E. Friberg, and the other members of his advisory committee, Dr. Samir B. Hanna, Dr. Oliver K. Manuel, and Dr. Parthasakha Neogi for their guidance throughout the course of this work.

The author also gratefully acknowledges the earlier support provided by Xiamen(Amoy) University, Xiamen, Fujian, The People's Republic of China and research support from the Weldon Spring Endowment Fund of the University of Missouri.

Finally, I would like to express my deep gratitude to my parents, my brothers, my parents-in-law, and especially my wife, for their support, understanding, and patience for years during my pursuit of higher degrees.

TABLE OF CONTENTS

TABLE OF CONTENTS(continued)

TABLE OF CONTENTS(continued)

TABLE OF CONTENTS(continued)

LIST OF ILLUSTRATIONS

INTRODUCTION

LIST OF ILLUSTRATIONS(continued)

LIST OF ILLUSTRATIONS(continued)

LIST OF ILLUSTRATIONS(continued)

LIST OF ILLUSTRATIONS(continued)

LIST OF ILLUSTRATIONS(continued)

LIST OF ILLUSTRATIONS(continued)

ARTICLE III

Figures page

LIST OF ILLUSTRATIONS(continued)

Figures page

LIST OF ILLUSTRATION(continued)

Figures page

LIST OF ILLUSTRATIONS(continued)

ARTICLE IV

LIST OF ILLUSTRATIONS(continued)

LIST OF ILLUSTRATIONS(continued)

LIST OF TABLES

INTRODUCTION

Due to their unique molecular structures, amphiphilies (1) display a variety of association phenomena both in aqueous and nonaqueous solvents. An amphiphilic molecule usually consists of two moieties, one of which is soluble in water (hydrophilic) and the other is sparingly soluble or insoluble in water (hydrophobic) but soluble in apolar solvents such as hydrocarbons. The hydrophilic portion of the amphiphile is ionic or polar and the hydrophobic portion is usually a hydrocarbon chain. Common surfactants provide a typical example of such molecules. When amphiphilic molecules such as ionic surfactants are dissolved in water, they tend to aggregate themselvs into a macromolecular structure due to the hydrophobic effect(2) which arises from the energetically unfavorable interactions between the hydrocarbon tail and water. The aggregation will result in a minimum contact between the hydrocarbon tails and water molecules while the contact between the ionic head groups and water is maximum. A series of association structures may come about, depending on conditions such as the concentration of the amphiphile, temperature, salt concentration, addition of hydrocarbon and another much more hydrophobic amphiphile called a cosurfactant, e.g., an alcohol of intermediate chain length. These various association structures are normal micelles, lyotropic liquid crystals, and inverse micelles or microemulsions (3). In the following, some fundamental

aspects regarding molecular self-association of amphiphiles will be outlined first. Then a brief discussion about various association structures in surfactant-water binary systems follows. Special attention will be paid to three-component and four-component systems composed of surfactant, water, and cosurfactant or cosurfactant plus hydrocarbon in the case of quaternary systems.

A. SOME FUNDAMENTAL ASPECTS OF MOLECULAR SELF ASSOCIATION OF AMPHIPHILES

1. Thermodynamics of Micelle Formation(2-5)

When the total concentration of the surfactant reaches a certain point called the critical micellization concentration (CMC), micelles of different size form, as shown schematically in Figure 1. Consider that micelle formation is a chemical equilibrium and that micelles of different size can be treated as distinct chemical components in the system. The thermodynamic principles require that the chemical potential of an amphiphile in the micellar state be equal to that of the free monomer in the solution at equilibrium. It is convenient to use mole fraction as the concentration unit for each component in the solution(2). Suppose that the mole fraction of the amphiphile molecules in the micelles of aggregation number, N, is X_N. Then the mole fraction of the micelles of this size is X_N/N. Therefore one can respectively write the chemical potential for an amphiphile molecule in the aggregated state and in the free state

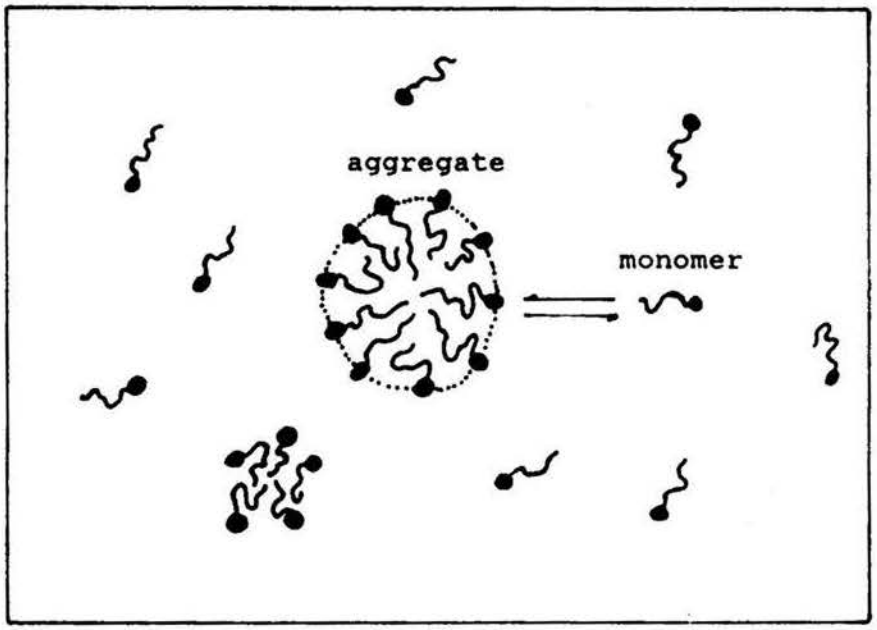

Figure 1. Association of N monomers into a micelle(3).

$$\mu_1 = \mu_1^o + kT\ln X_1 \tag{1}$$

$$\mu_N = \mu_N^o + \frac{kT}{N}\ln\frac{X_N}{N} \tag{2}$$

The concentration has been assumed low enough so that interactions between aggregates can be ignored. At equilibrium one obtains

$$\mu_N^o - \mu_1^o = kT\ln X_1 - \frac{kT}{N}\ln\frac{X_N}{N} \tag{3}$$

or

$$X_N = NX_1^N \exp\left[N\,\frac{(\mu_1^o - \mu_N^o)}{kT}\right] \tag{4}$$

The total concentration of the surfactant in the system, X_t, is

$$X_t = X_1 + X_{mic} = \sum_{N=1}^{\infty} X_N \tag{5}$$

where X_{mic} is the overall concentration of the surfactant in the micellar form and is given by

$$X_{mic} = \sum_{N=1}^{\infty} X_N \tag{6}$$

Eq. 4 is a micelle size distribution function. The optimal size, N^*, is defined as the size at which the derivative of X_N with respect to N is equal to zero at the prevailing free monomer concentration, X_1,

$$\left(\frac{\partial X_N}{\partial N}\right)_{X_1} = 0 \quad \text{at} \quad N = N^* \tag{7}$$

One can also relate the experimentally observable mean aggregation number, $\bar{N}$, to the total amphiphile concentration (4)

$$\bar{N} = \frac{\partial \ln(X_t - X_1)}{\partial \ln X_1} \tag{8}$$

The mean aggregation number is defined in terms of Eq.(4)

$$\bar{\bar{N}} = \sum_{N>1} NX_N / \sum_{N>1} X_N \tag{9}$$

For many micellar systems, the size distribution is narrow and $\bar{N}$ is close to N^*(6).

From Eq. 4 it is seen that the term $(\mu_1^\circ - \mu_N^\circ)$ determines the micelle size. Micelles with the optimal size form dominantly if μ_N° has a minimum at this size. μ_N° will take different forms for different shapes of micelles(3).

2. Micelle Shape and Size—Geometrical Considerations

Simple geometric considerations can allow approximate prediction of the micellar shape in terms of molecular parameters of the amphiphile(4,5,7). Since there must be no hole in the center of the micelle, the volume of the micelle of aggregation number N is always given by the volume of the hydrocarbon chain of the amphiphile times N, and one dimension of the micelle cannot exceed the double full extension of the hydrocarbon chain, l_c. Suppose that the interfacial area of the polar or ionic head of the amphiphile is a_o. Ninham and coworkers(5), after consideration of energetics, obtain the following predictive conditions for several possible associational structures:

$$\begin{array}{ll} \text{spherical micelles} & \upsilon/a_o l_c < 1/3 \\ \text{cylindrical micelles} & 1/3 < \upsilon/a_o l_c < 1/2 \\ \text{bilayers or vesicles} & 1/2 < \upsilon/a_o l_c < 1 \\ \text{inverted structures} & \upsilon/a_o l_c > 1 \end{array} \qquad (10)$$

where $\upsilon/a_o l_c$ is called the "packing ratio". Based on X-ray diffraction data(7), the volume per saturated hydrocarbon chain can be written as

$$\upsilon = 27.4 + 26.9n' \quad (\text{Å}^3) \qquad (11)$$

$$l_c = 1.5 + 1.265n' \quad (\text{Å}) \qquad (12)$$

where n' is some number less than the number of carbon atoms of the chain.

From Eq. 10 one sees that increasing the packing ratio increases the tendency to form nonspherical structures or inverted structures. This can be brought about by reducing a_o, shortening l_c, or increasing υ. To reduce the head group area, one can add salt or increase salt concentration in the case of ionic amphiphiles. Increase in temperature will enhance the thermal motion of the hydrocarbon chain and thus reduce l_c. Whereas increasing the degree of unsaturation of the hydrocarbon chain, particularly with cis double bonds, increases the volume of the chain. We will find that the packing ratio concept is useful in explaining a series of phase transitions from normal micelles to inverse micelles in three- or four-component systems.

The driving force for self association of amphiphilic molecules in aqueous solution is the hydrophobic effect, as mentioned previously. This hydrophobic effect sets, at the same time, the lower limit of micelle size. Micelles of very small aggregation number, e.g., N=2 or 3, are hard to form because a high degree of contact between the hydrocarbon chain and water cannot be avoided(7). On the other hand, very large micelles are difficult to form because of an enhanced repulsion between neighboring head groups in the case of ionic amphiphiles as the micelle size increases. In micelles formed from amphiphiles with uncharged head groups, the opposing force to self association is due to the preference for hydration. This opposing force sets an upper limit for micelle size. Therefore the micelles formed cannot have a purely statistical size distribution(7).

B. ASSOCIATION STRUCTURES IN BINARY SYSTEMS

Figure 2 gives a schematic partial phase diagram for an ionic alkyl chain surfactant in an aqueous system. Micelles do not form if the temperature is below a characteristic one called the critical micelle temperature (CMT)(8) and the surfactant precipitates as solid hydrated crystals at high concentrations. When the temperature is above CMT, the amphiphile dissolves as free monomers in solution at low concentrations and the bulk physical chemical properties of the solution behave as a simple electrolyte solution. However, when the amphiphile concentration reaches the

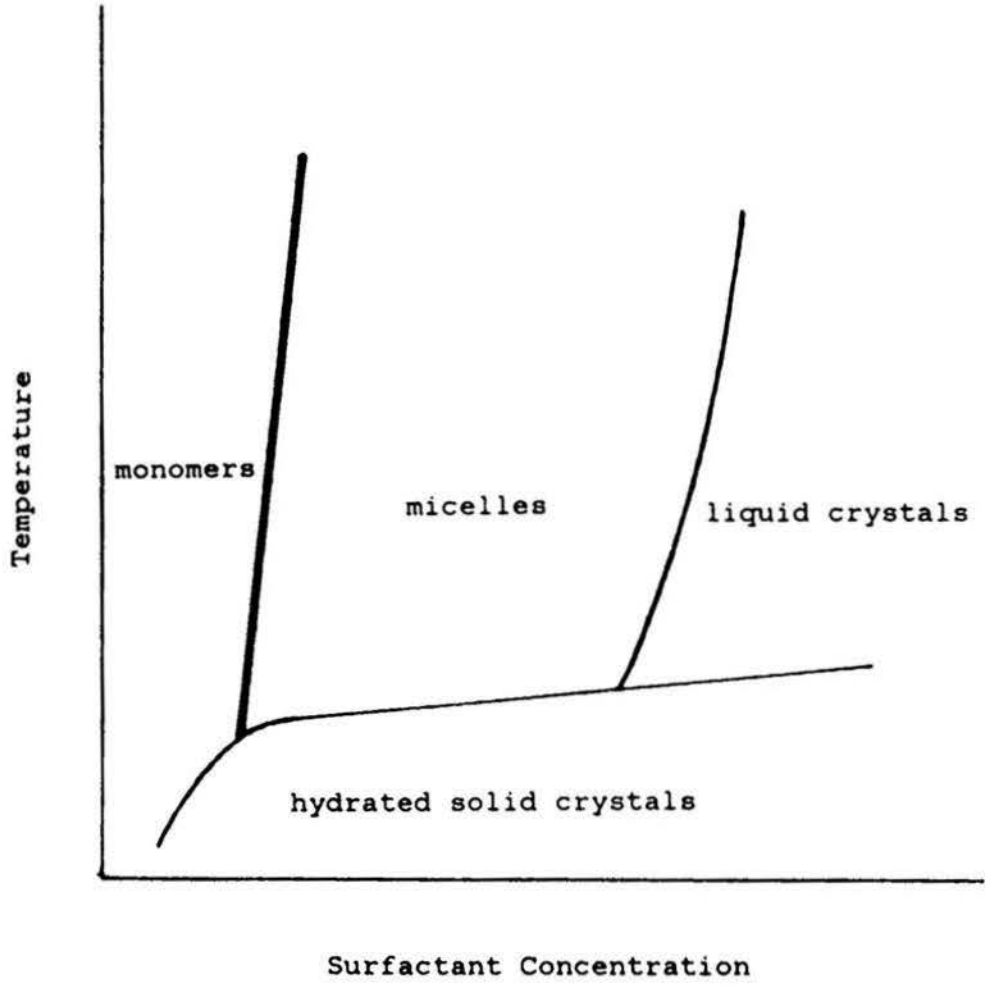

Figure 2. Schematic representation of a partial phase diagram for an ionic alkyl chain amphiphile-water system.

critical micellization concentration (CMC), which is actually a narrow concentration range, there is a sudden change in physical properties, such as turbidity, osmotic pressure, surface tension, conductivity, etc., indicating that an extensive association occurs(10). After the CMC, all added surfactant essentially aggregates into micelles and the concentration of free monomers basically remains constant at the CMC, as schematically shown in Figure 3. Normally, spherical micelles form first. When the concentration increases further, transition of micellar shape from sphere to cylinder may occur. For example, for the sodium dodecyl sulfate(SDS)-water system, this transition occurs at 25%(weight) SDS concentration at 25^{o}C and can be brought about at a lower concentration by addition of NaCl(8), as was mentioned in the previous section. Although, in the concentration range between 25% and 36% SDS the micellar shape is nonspherical, the solution remains optically isotropic because the cylindrical micelles are randomly oriented in space. However, upon additon of more SDS after 36%, a new phase comes about and is in equilibrium with the disordered cylindrical micelles if the SDS concentration is in the range of 36% to 40%. This new phase is the hexagonal liquid crystalline phase, as illustrated schematically in Figure 4. From 40% to 50% SDS, the system exists only in the hexagonal liquid crystalline phase. Above 50% SDS, the liquid crystalline phase becomes in equilibrium with solid SDS since there is no longer enough water to function as a solvent. We

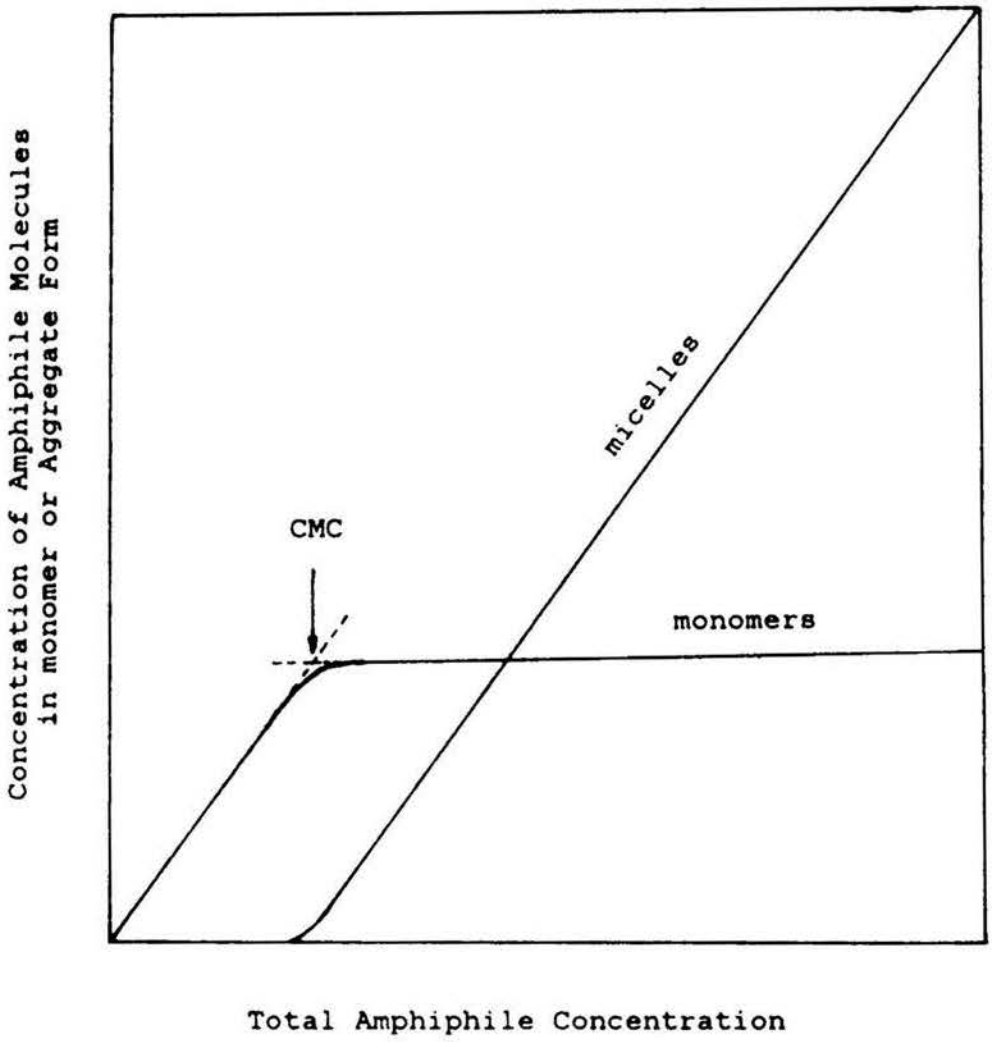

Figure 3. Monomer and aggregate concentration as a function of total amphiphile concentration.

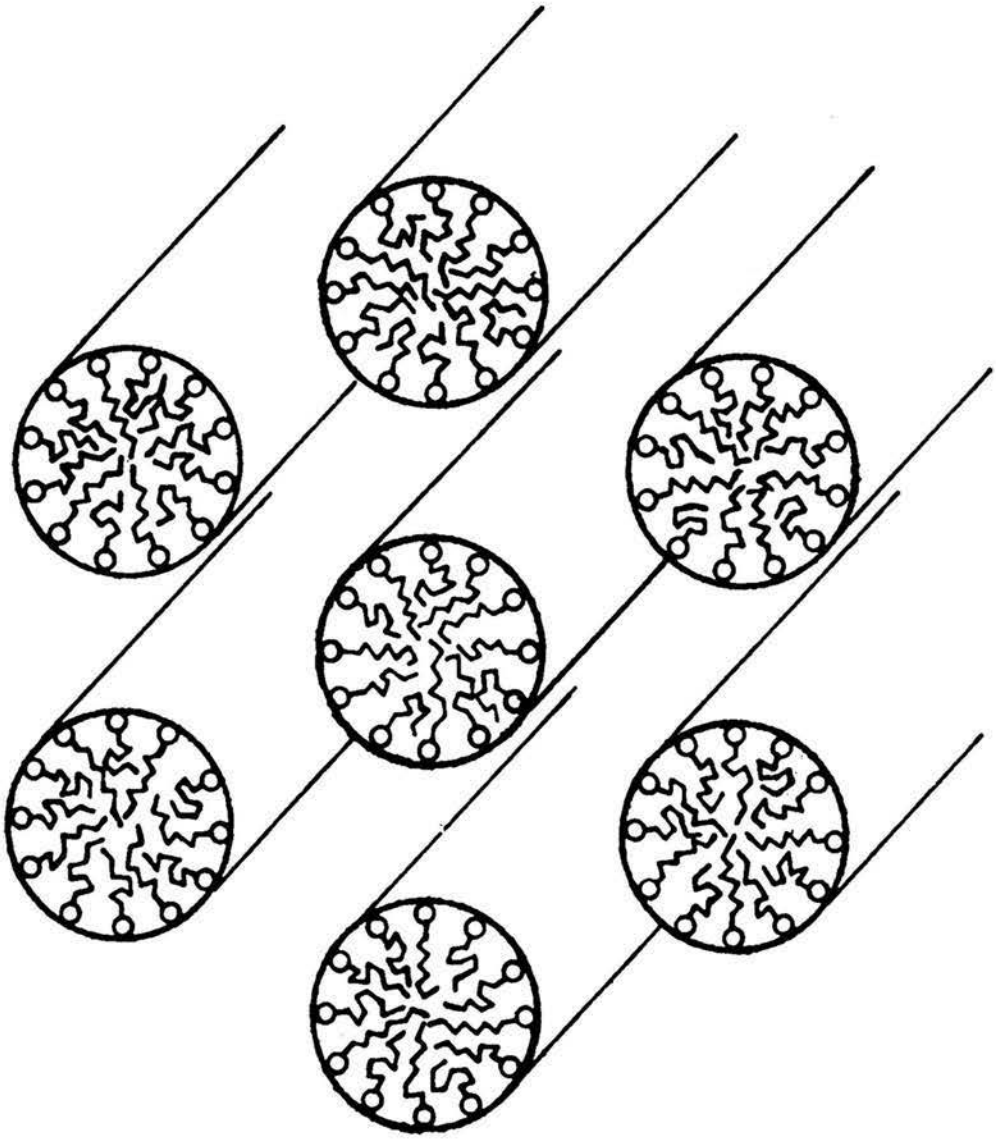

Figure 4. Schematic structure of the normal hexagonal liquid crystals.

will discuss more about liquid crystals in the next section when we deal with ternary or quaternary systems.

C. ASSOCIATION STRUCTURES AND PHASE BEHAVIOR IN THREE- AND FOUR-COMPONENT SYSTEMS—NORMAL MICELLES AND LIQUID CRYSTALS

1. Representation of Phase Diagrams

Under isothermal (and isobaric) conditions, phase equilibria of three-component systems are best represented in a triangular phase diagram. Each apex of the triangle represents a pure component and the concentration of this component in a mixture containing all the three constituents is read as the distance from the opposite base to the representive point of the mixture along a line between the center of the opposite base and the apex. The phase diagram can be conveniently expressed in weight percentages, although mole fraction may be more appropriate for interpretation of the phase behavior in terms of molecular interactions(11). The lever rule is valid in two-phase and three phase areas for ternary systems. To represent phase equilibria of a four-component system, a tetrahedron must be used as shown by Figure 5(12). Similar to the triangular representation of ternary systems, each apex of the tetrahedron represents a pure component. Since the diagram is three dimensional, it is cumbersome to use. Therefore, very often a triangular pseudophase diagram is used instead. The ratio of any two components of the system can be fixed and the combination of

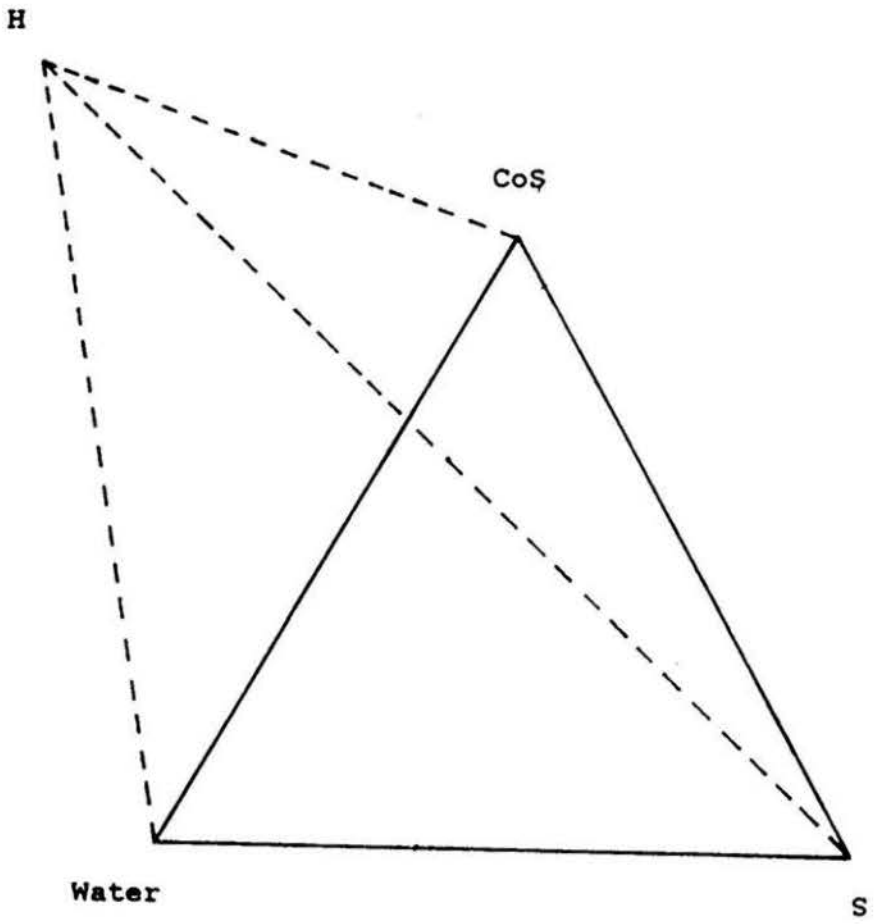

Figure 5. Three-dimensional phase diagram of a four-component system. S = Surfactant, CoS = Cosurfactant, H = Hydrocarbon.

these two components taken as a pseudocomponent. For reasons of convenience, the two miscible components (if any) are frequently mixed in the desired proportion when making the phase diagram. Other combinations are possible. For example, a pseudophase diagram can be made as the plane which is parallel to one of the four faces of the tetrahedron and bisects the other three edges.

2. Determination of Tie-lines

We are interested in tie-line determination in two isotropic liquid phase areas here because this is important in the study of critical phenomena in microemulsions, particularly for non-ionic systems(13-18). There is a simple method, among others, to determine the critical point by refractive index measurements. Figure 6 shows the phase diagram of a three-component system consisting of water, heptyltrimethylammonium bromide, and n-hexanol(19). L is an isotropic liquid region and the area ABCA is a two-phase region. Clearly, there is, on the equilibrium curve ABC, a critical point at which concentration fluctuation is maximum. To determine this critical point, it is necessary to draw tie-lines in this two-phase region. One finds the critical point if the tie-line merges into a single point. To draw tie-lines, a series of samples on the equilibrium curve ABC are prepared and the refractive index is measured for each sample. A working curve of refractive index vs. the compositions of samples is plotted. Then one needs to prepare a series of samples across the two-phase area and these samples split into

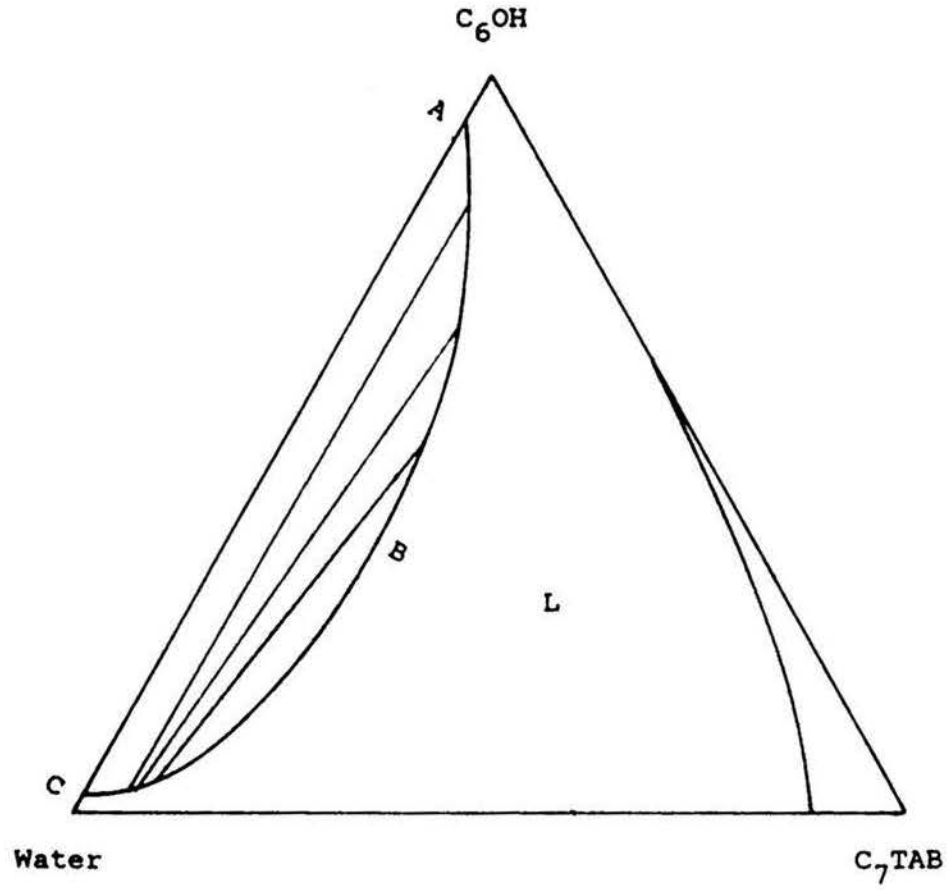

Figure 6. Phase diagram of the ternary system composed of water, heptyltrimethylammonium bromide(C_7TAB), and hexanol(C_6OH).

two phases at equilibrium. Refractive index is measured for each phase. Comparing this value of refractive index with the working curve, one finds the composition of this phase. Thus for each sample one tie-line is drawn. The critical point found in this way can be verified by light scattering measurements. A series of solutions in the one-phase region whose compositions are parallel to and close to the equilibrium curve ABC are prepared. The intensity of scattered light from the solution whose composition is closest to the critical point will have the highest value(20), as is schematically shown in Figure 7.

Notice that the above procedure for tie-line determination is not valid in the case of pseudophase diagrams of four- or five- component systems since tie-lines usually do not lie on the surface of the pseudophase diagram.

3. Normal Micellar Region

A typical phase diagram of a ternary system composed of an ionic surfactant, an alcohol of medium chain length, and water is presented in Figure 8(21). In Ekwall's terminology(22), the normal micellar region is denoted by L_1, E is the normal hexagonal liquid crystalline phase (see Figure 4), D represents the lamellar liquid crystal region, while the L_2 area is the so-called inverse micellar solution phase. We will have a brief discussion of each of these phases. In this section, the association structure of normal micelles will be treated.

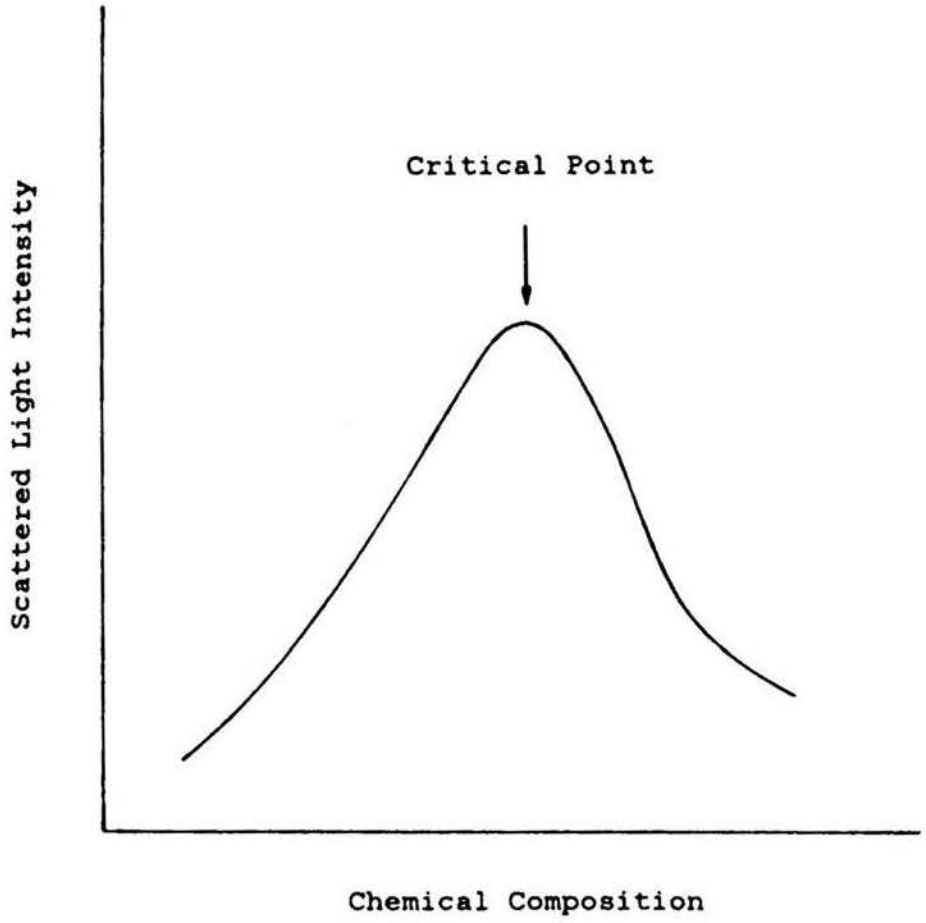

Figure 7. Schematic representation of scattered light intensity versus composition of solutions close and parallel to the equilibrium curve between two-phase and one-phase regions, at which a critical point exists.

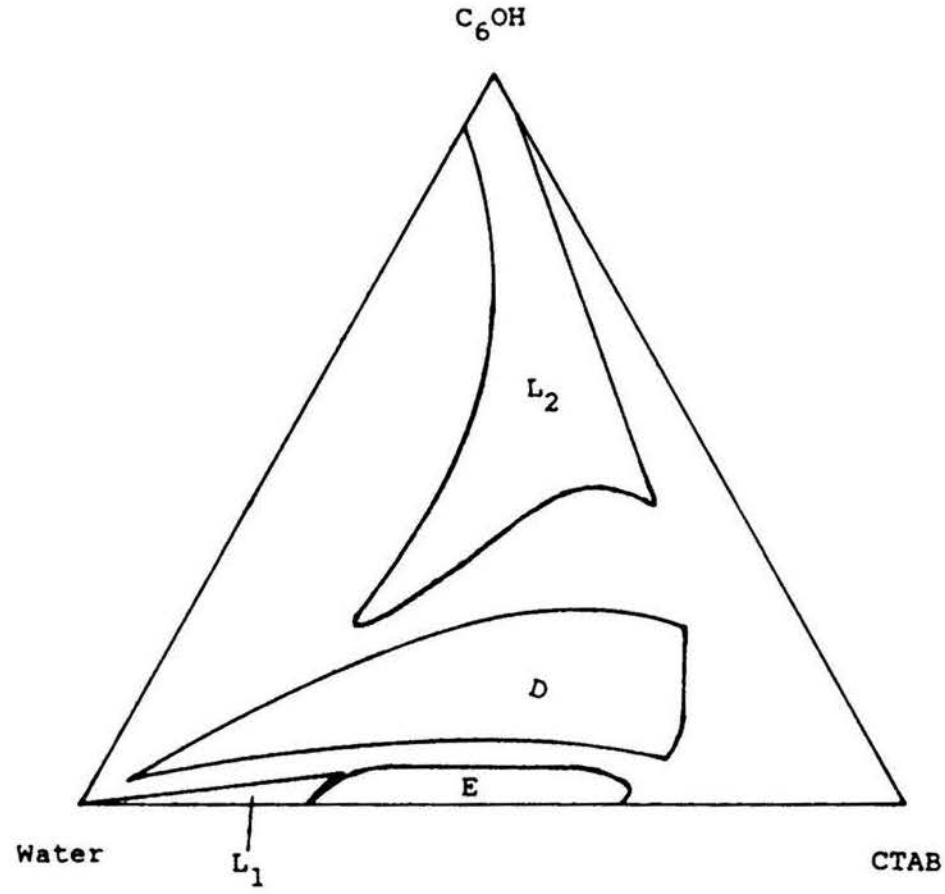

Figure 8. Phase diagram of water, n-hexanol, and cetyltrimethylammonium bromide(CTAB) system at 25°C (21).

The association structure of normal micelles in ternary systems is basically the same as that in binary systems, as discussed in section B. The ionic head groups of surfactant molecules stick out and contact with the aqueous continuous phase, while the hydrocarbon tails are hiding in the core of the micelle. Therefore it is possible to dissolve a certain amount of hydrocarbon or hydrophobic amphiphiles, such as alcohols, in the core of the micelle before the micelle is broken down. There should be a probability that some dissolved alcohol molecules in the micelle may insert between surfactant molecules in the surfactant layer with their polar heads pointing toward the surface of the micelle. In this way the micelle should gain some stability relative to the two-component system because the inserted neutral alcohol molecules help reduce the repulsion between neighboring ionic head groups of the surfactant molecules. Therefore the micelle size is expected to become larger compared to that of the corresponding binary system under otherwise equivalent conditions (2). However, solubility of hydrocarbons or alcohols will not be large , usually only a few percent, in normal micellar solutions(12).

4. Lytropic Liquid Crystals

The liquid crystalline state is an intermediate state between solid and liquid. The crystalline solid of an amphiphilic compound such as an ionic surfactant is characterized both by a long range order and a short range order. The liquid state is disordered in both the long and

short ranges, while the liquid crystalline state is disordered in the short range but ordered in the long range, as shown in Figure 9(23). There are two ways to obtain liquid crystals. For some organic compounds, a liquid crystalline state may be obtained by heating the solid or by cooling the liquid(24). These kinds of liquid crystals are termed thermotropic liquid crystals. A liquid crystal can also be obtained by addition of a solvent to a compound or a mixture of compounds, as seen in the binary system discussed previously and shown in Figure 8. Such liquid crystals are named lyotropic liquid crystals.

Depending on composition, an amphiphile system may have a variety of liquid crystal structures(22). The normal hexagonal and lamellar structures are most often seen. We will limit our discussion to these two structures. By "normal" we mean that the structure has a hydrocarbon core and a hydrophilic surface. The hexagonal has a two-dimensional periodicity and consists of an array of basically infinite cylinders, as shown in Figure 4. The lamellar structure is of one-dimensional periodicity and consists of infinitely expandable bilayers of amphiphile molecules intercalated by water layers at a repeating distance. The hydrocarbon tail of the amphiphile points to the center of the bilayer and the ionic or polar head toward the interface between the bilayer and water layer. Figure 10 gives a schematic representation of the lamellar liquid crystal structure(24). Clearly, liquid crystals are capable of dissolving hydrocarbons. The

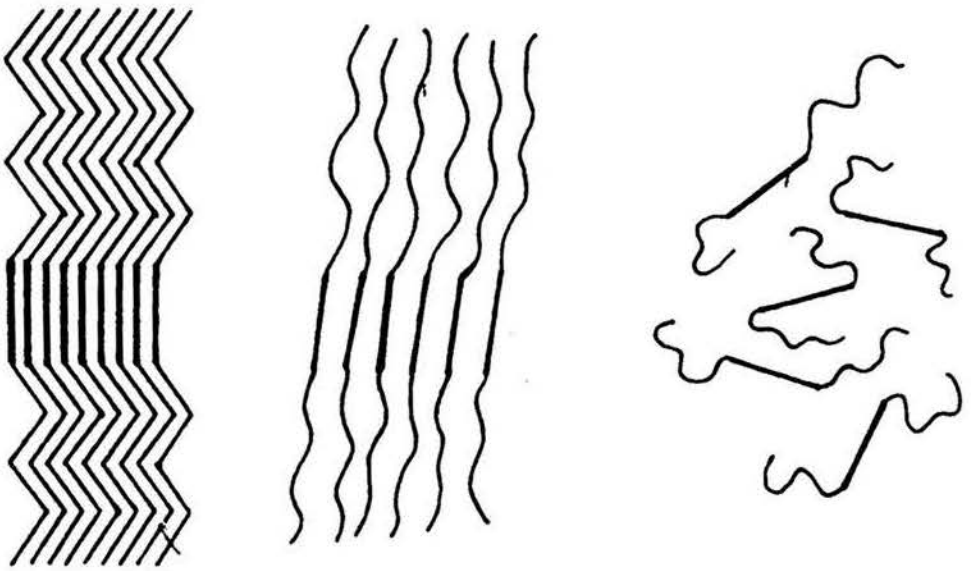

Figure 9. Schematic illustration of the crystalline (a), liquid crystalline (b), and liquid (c) states (23).

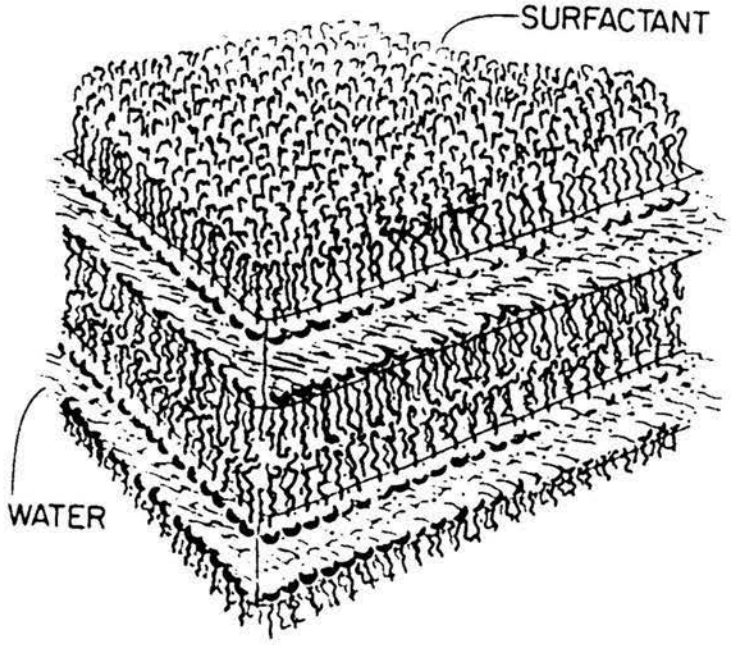

Figure 10. Schematic model of the lamellar liquid crystal structure (24).

dissolved hydrocarbon goes to the centers of the amphiphilic bilayers or the cores of cylinders in the case of the normal hexagonal structure. The orientation of cosurfactant molecules such as alcohol is the same as that of surfactant(23). Solubilized substances alter the stability of the liquid crystals. An alcohol cosurfactant of chain length in excess of six carbon atoms stabilizes the liquid crystals with the lamellar structure. The reason for this arises from the fact that the polar but neutral alcohol molecule is capable of reducing the destabilizing interactions of electrostatic repulsion between the ionic heads of surfactant molecules of like charge, as mentioned earlier. However, when the carbon atom number of the cosurfactant chain is less than six, the liquid crystalline phase is destabilized due to a high solubility of water in the reverse micellar solution(23). This destabilizing effect may also be appreciated by looking at the mobility of the cosurfactant molecule. A small alcohol molecule is easy to move around and this will lead to destabilization of the more ordered liquid crystal structure.

Because of the optically anisotropic nature of the liquid crystals discussed above, their existence is readily observed with the aid of two polarizing plastic sheets arranged with their planes of polarization perpendicular to each other and the sample in between them. A polarizing microscope is excellent for this purpose also. However, there exists an isotropic liquid crystalline phase for some

systems(22). So care should be exercised when using the above techniques. A powerful method in identification of liquid crystals is low angle X-ray diffraction, if a diffraction pattern of several reflections can be obtained(25). For the hexagonal structure with a two-dimensional periodicity, d-spacing is expressed as

$$d_{hk} = \frac{3}{2}a \frac{1}{(h^2+hk+k^2)^{1/2}} \quad (13)$$

where h and k are the Miller indices of the reflecting plane, and a is the lattice parameter of the unit cell. Therefore the diffraction pattern will appear such that the ratio of d values (positions of diffraction maxima) is $1:1/\sqrt{3}:1/\sqrt{4}:....$ For the one dimensional lamellar structure,

$$d = h/a \quad (14)$$

and the diffraction pattern is 1:1/2:1/3:... for the interlayer spacing ratio. According to the model given in Figure 10, it is easy to relate the interlayer spacing to the composition of the system

$$d = d_o/\phi_o \quad (15)$$

where d_o is the thickness of the amphiphile bilayer and ϕ_o the sum of the volume fractions of the substances forming the bilayers.

Figure 11 shows an example of a low angle X-ray diffraction pattern of a lamellar liquid crystalline phase. The sample consists of 30% water, 42% SDS , and 28%

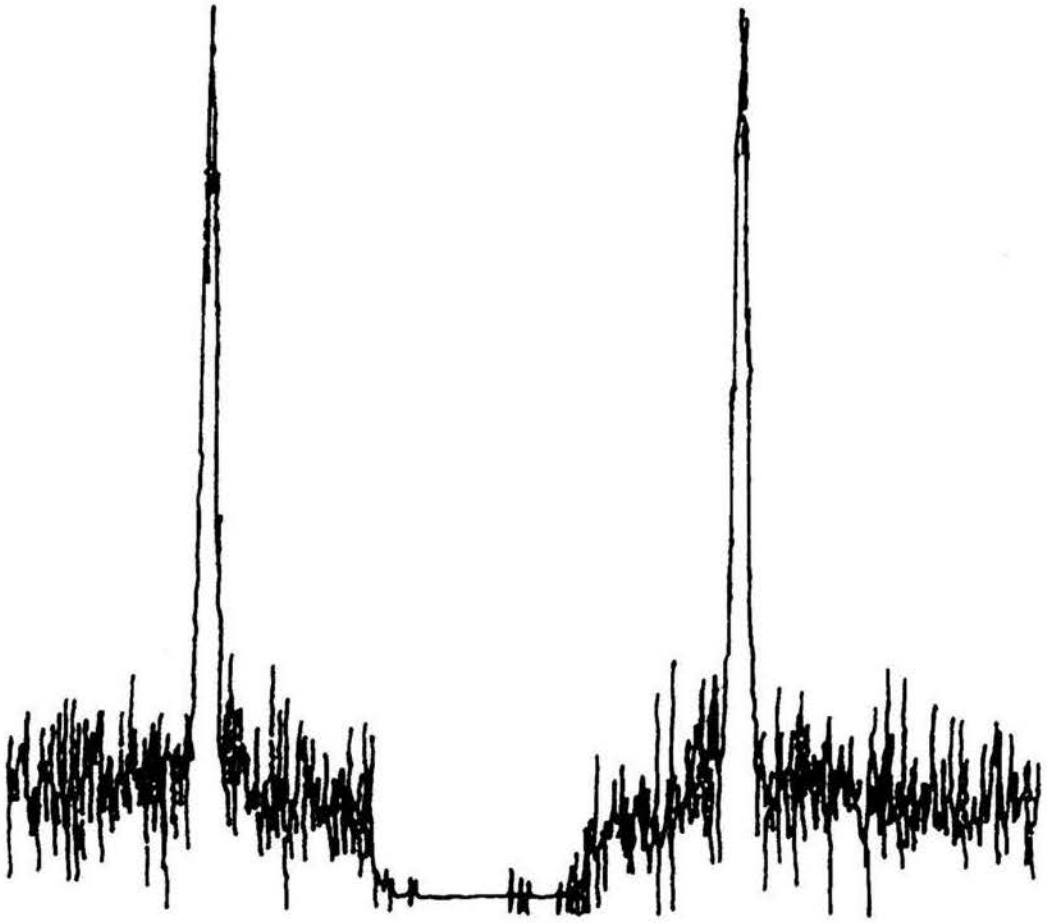

Figure 11. Low angle X-ray diffraction pattern of a lamellar liguid crystalline phase composed of 30% water, 28% SDS, and 42% hexylamine, collected using a Kiessig low angle camera from Richard Seifert with a tennelec position-sensitive-detection system (Model PSD-100). Radiation source: Ni-filtered Cuk_{α}. The dimension of the pattern has been reduced.

hexylamine. It is noted that only the first diffraction maximum is observed because other reflections are of low intensity and not observable in this case. The interlayer spacing is easily calculated using Bragg's law.

Eq. 15 can be written in terms of water weight fraction, f_w(26),

$$d = d_o(1 + \frac{\upsilon_w}{\upsilon_o} \frac{f_w}{1 + f_w}) \qquad (16)$$

where υ_w is the partial specific volume of water and υ_o is the mean partial specific volume of the constituents of the bilayers. Therefore one is able to deduce d_o and υ_w/υ_o from the intercept and slope of the plot of d versus $f_w/(1-f_w)$ if mutual penetration between bilayers and water layers is negligible.

D. INVERSE MICELLES AND MICROEMULSIONS

1. Inverse Micelles

In Figure 8 the isotropic solution area, L_2, extending from the cosurfactant corner is commonly called the inverse micellar solution region. However, this is not totally justified, as is pointed out by Friperg(27), since micellar droplets do not really form in the range of low water concentrations. Sizable inverse micelles form only when water concentration is high enough and in excess of that required for hydration of surfactant molecules. Therefore the inverse micellar region L_2 can microscopically be divided into two

areas, as shown in Figure 12. The area of low water concentration contains ion pairs of surfactant with a few water molecules associated with each ion pair in the cosurfactant solution(12). As water concentration increases, formation of inverse micelles gradually takes place over a rather wide range, in contrast to the critical micellization concentration (CMC) in the normal micelle phase which is a narrow amphiphile concentration range, as pointed out previously. That the solution in the low water concentration range of the L_2 region is a molecular dispersion of surfactant in cosurfactant solution can be verified by several experimental techniques. Light scattering and electron microscopy appear to be good tools(28). Figure 13 presents light scattering results from the three-component system we have chosen as a model system for this dissertation. The system is composed of sodium dodecyl sulfate, hexylamine, and water. The measurements of scattered light intensity were carried out by keeping the ratio of surfactant to cosurfactant constant and varying the water content. We see that the scattered light intensity from solutions with low water concentrations is very low, even lower than pure toluene liquid, and the intensity stays low over a large range of water concentration before it increases slowly. Obviously, no single concentration appears which can be well defined as the onset of inverse micelle formation. Neverthless, inverse micellar droplets of appreciable size begin to form as water concentration increases further. It is apparent that the size

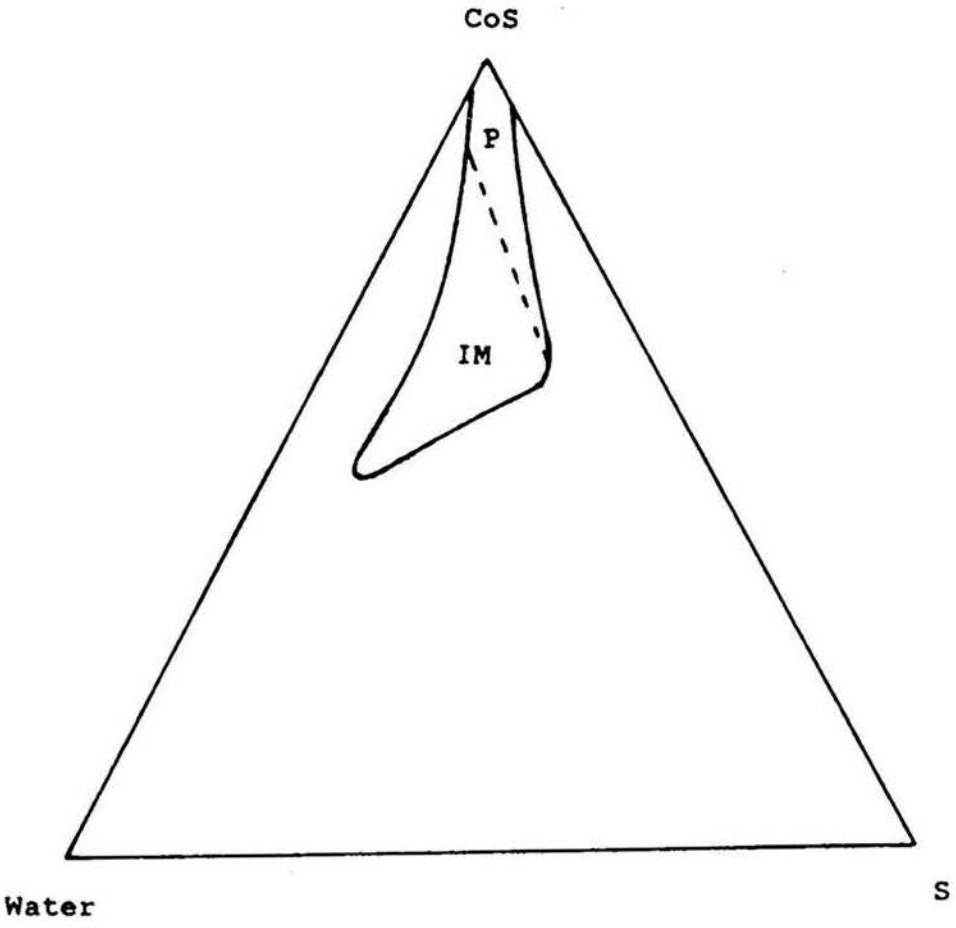

Figure 12. Schematic illustration of L_2 solubility area showing two regions, P and IM, representing premicelles and inverse micelles respectively.

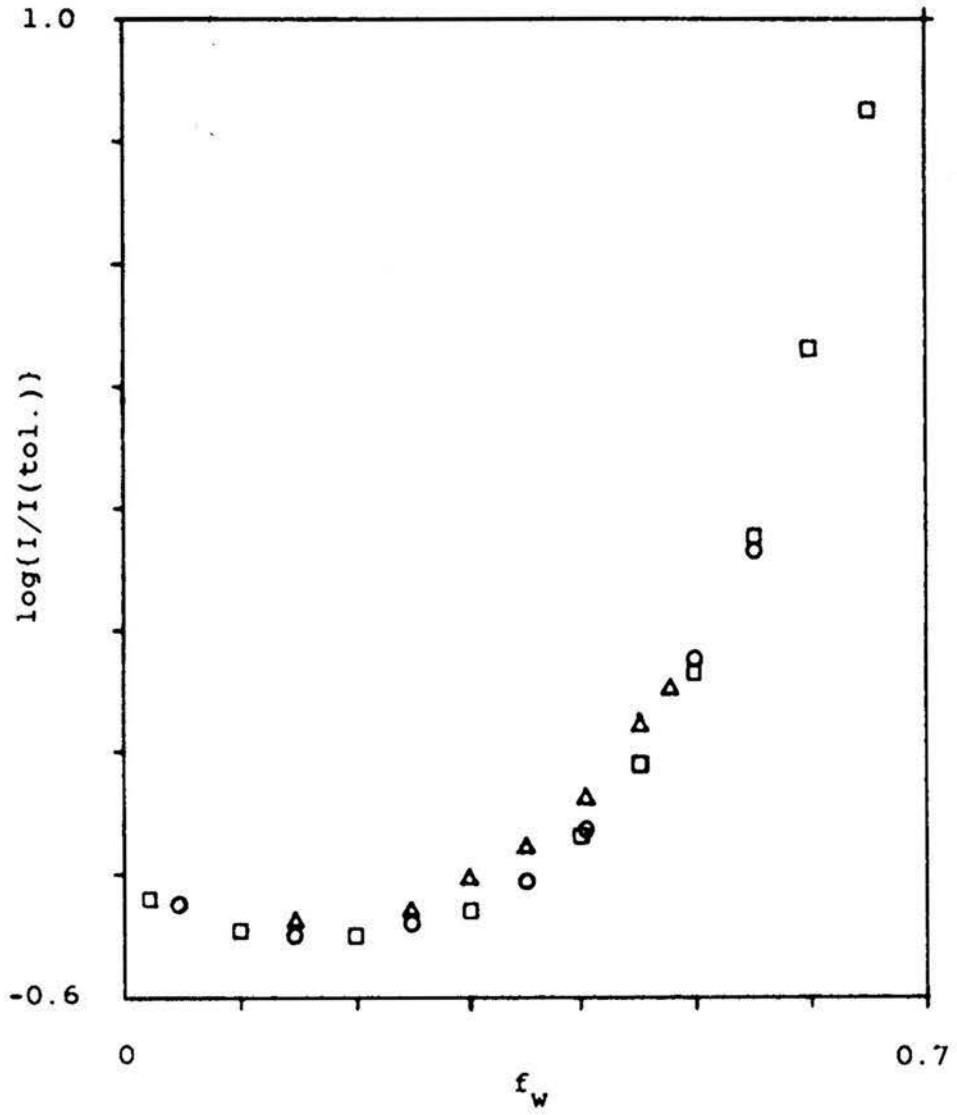

Figure 13. Intensity of scattered light from the cosurfactant solution(L_2) composed of water, SDS, and hexylamine relative to that from pure toluene liquid at 90° as a function of water concentration. The relative intensity is plotted as logarithm. The weight ratio of SDS/Hexylamine: □—5/95, o—10/90, Δ—15/85.

of the inverse micellar droplets changes as water content changes since the ratio of water to surfactant varies. Therefore it would not be suitable to use an extrapolation method to obtain the particle size from such measurements of light scattering.

Inverse micelles are usually thought to have a spherical structure. An inverse micelle contains a water core surrounded by a monolayer of surfactant and cosurfactant molecules whose ionic or polar heads are anchored at the surface of the water core and hydrocarbon tails stick out into the continuous phase of the cosurfactant solution, as pictured in Figure 14. The compositon of the interfacial monolayer is a matter of importance and yet it is difficult to determine. When we are dealing with microemulsions in Article IV of this dissertation, we introduce a technique currently used to dilute a concentrated water-in-oil (W/O) microemulsion. From the dilution line the compositon of the interfacial monolayer can be deduced and hence the composition of the continuous phase can also be known. The ratio of cosurfactant moleoules to surfactant molecules in the monolayer usually ranges from 1:1 to 1:3 for W/O microemulsions(29). This dilution procedure cannot be applied to inverse micellar solutions with no hydrocarbon present. However, We have used a method to do this via conductivity measurements (30).

Having introduced normal micelles, liquid crystals, and inverse micelles, we can now see the application of the

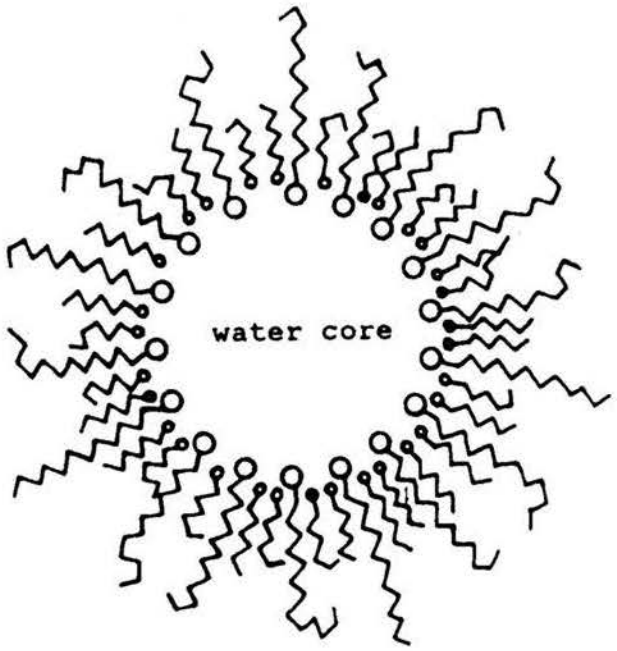

Figure 14. A simplified picture of inverse micelle Structure. Molecules with a long chain are surfactant while those of a short chain are cosurfactant.

packing ratio concept of Eq. 10 to explain this series of phase transitions as the concentration of cosurfactant increases in a three-component system. A cosurfactant mainly acts to increase the volume per surfactant molecule, v, without significantly affecting the parameters a_o and l_c since the neutral cosurfactant molecule is able to pack between the ionic head groups without causing repulsion, as mentioned previously. Therefore as the cosurfactant is added to the normal micellar solution, lamellar liquid crystals form if the packing ratio, $v/a_o l_c$, is in the range between 1/2 and 1. Further addition of cosurfactant will destabilize the liquid crystalline phase and give a more energetically favorable structure, the inverse micelle phase, when the packing ratio is greater than 1(6).

2. Microemulsions

a. Association Structures

A microemulsion is, according to Lindman(11), defined as a system of water, oil, and amphiphiles which is an optically isotropic and thermodynamically stable liquid solution. This definition is rather broad and obviously includes normal and inverse micellar solutions. Friberg(12) suggested that to be entitled to the name microemulsion, the system should contain appreciable amounts of disperse phase, other things being the same. The latter definition is more specific and puts emphasis on association phenomena since the existence of large amounts of disperse phase implies that the system consists of associative structures, so excluding molecularly disperse

systems. It would be more convenient to use this latter definition when investigating physical properties, such as particle size and molecular weight of particles. A molecularly disperse system does not have these macromolecular properties and the concepts of continuous and disperse phase cannot be applied for such systems.

Depending on the phase continuity, there are three possible structures of microemulsions. If the continuous phase is water or aqueous solution, and the disperse phase is oil(hydrocarbon), the microemulsion is called oil-in-water and denoted O/W. In contrast, a water in oil (W/O) microemulsion has a water disperse phase surrounded by an oil continuous phase. When the volume fractions of water and oil are comparable, the system may have a so-called bicontinuous structure (31-33) in which both water and oil components form continuous interpenetrating domains, with neither one surrounding the other(34).

Ninham's packing ratio can certainly be used to predict the phase continuity of a microemulsion(5). However, there are other approaches in terms of interfacial properties, such as wettability of the amphiphile interfacial monolayer which can be considered as an interphase, and interfacial tensions (29,35). As implied above, a microemulsion contains three domains: water-rich, oil-rich, and amphiphile-rich (interphase) domains. If the amphiphile interface is more readily wetted by the oil phase than by water, the oil phase will then be the external or continuous phase and a W/O

microemulsion is formed, whereas the opposite case allows an O/W microemulsion to be formed. The interfacial tension approach is the following. Consider that the interfacial monolayer has a finite thickness. Then there are two interfaces. One is that between the monolayer and oil phase, characterized by an interfacial tension $\gamma_{m/o}$, and the other is between the monolayer and water phase and has an interfacial tension $\gamma_{m/w}$. If $\gamma_{m/o}$ is smaller than $\gamma_{m/w}$, the W/O microemulsion will be the preferred structure (larger surface tension results in larger surface free energy). If $\gamma_{m/o}$ is greater than $\gamma_{m/w}$, a O/W microemulsion will be obtained. This argument is pictured in Figure 15. Thus, to change a W/O microemulsion into an O/W one, $\gamma_{m/o}$ must be increased relative to $\gamma_{m/w}$. This effect can be achieved by using a cosurfactant of shorter chain length to form a more hydrophilic interfacial monolayer. Alternatively, one can use an oil having a larger interfacial tension with respect to water(29).

b. Stability

In this subsection we only give a very brief discussion of some current theoretical treatments of stability of microemulsions. Detailed theories are available in the literature, e.g., papers by Ruckenstein (36-39).

Ordinary dilute (coarse) emulsions are thermodynamically unstable and their (kinetic) stability can be well described by the DLVO theory(40,41). Their stability depends on the relative magnitude of repulsive electrical double layer forces and attractive van der Waals forces

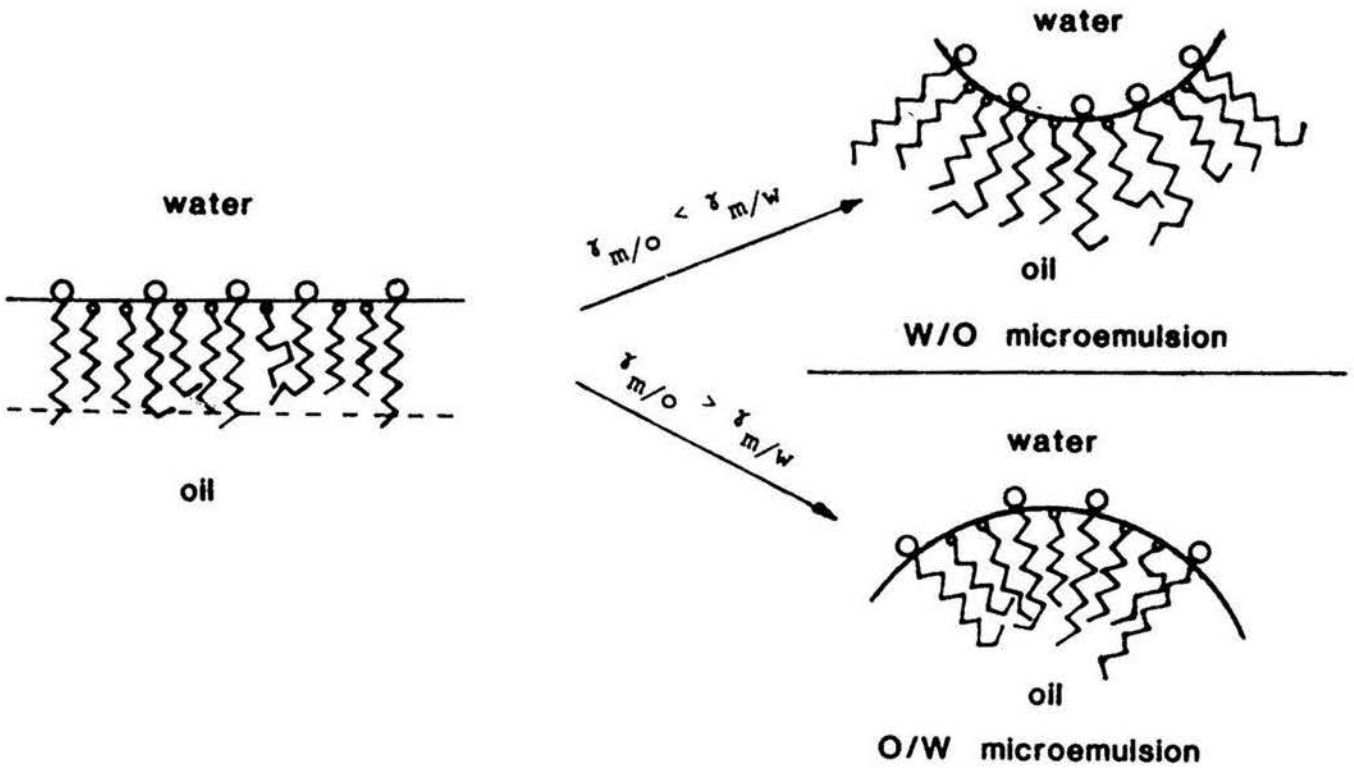

Figure 15. Schematic diagram illustrating the mechanism of the curvature formation of the interfacial film in microemulsions.

between particles. In contrast, microemulsions are spontaneously formed and thermodynamically stable. Their stability cannot be interpreted in terms of those two kinds of forces alone. To explain the stability of microemulsion systems, Schulman and co-workers, who first investigated microemulsions (42), proposed a concept of transient negative interfacial tension between water and oil(43-45). This suggestion can explain the fact that a large interfacial area is produced in a microemulsion system since many small particles are formed. However, it has been subject to criticisms (37,46) because it cannot even account for the finite size of aggregates in the system. As a matter of fact, the spontaneous formation and finite size of droplets of microemulsion can be explained without invoking the negative interfacial tension provided that this tension is small enough ($\sim 10^{-3}$dyne/cm or lower).

Ruckenstein (37), in one of his papers dealing with the thermodynamics of microemulsions, treated a four-component microemulsion system as a two-component, oil and water, system and considered that the surfactant and cosurfactant act only to affect the surface properties of the droplets of one phase in the other. Thus, the free energy of formation of one cm^3 of microemulsion can be written as

$$\Delta G_m = \Delta G_1 + \Delta G_2 + \Delta G_3 \qquad (17)$$

where ΔG_1 is the free energy of formation of interface and is the sum of a positive surface free energy and a negative free

energy of formation of the electrical double layers which form spontaneously. ΔG_2 is due to the attractive van der Waals forces ΔG_2^a and repulsive double layer interactions ΔG_2^r, and in general $\Delta G_2^a << \Delta G_2^r$. ΔG_3 represents the entropic effect and is negative due to formation of a large number of small droplets. Expressions for these different terms have been developed. Figure 16 gives the calculated results of these various contrbutions to ΔG_m as a function of radius of the droplet for an O/W microemulsion for some chosen parameters(38). As can be seen from the figure, the microemulsion is stable since ΔG_m shows a negative minimum at a radius of ~800Å. We also see that the most important contributions to ΔG_m are, in this example, the free energy of formation of the double layer and the free energy of the double layer interactions. The entropic contribution is not important at large radius of droplets and only becomes significant when the droplet radius is smaller than ~250Å.

c. Characterization of Microemulsions

Many methods have been used to characterize microemulsions. Among others, light scattering techniques appear to be very useful in the determination of physical parameters, such as particle size, molecular weight of suspended particles, virial coefficients, interactions between particles, and polydispersity of the system, etc.. We have performed classical time-average light scattering and dynamic light scattering or photon correlation

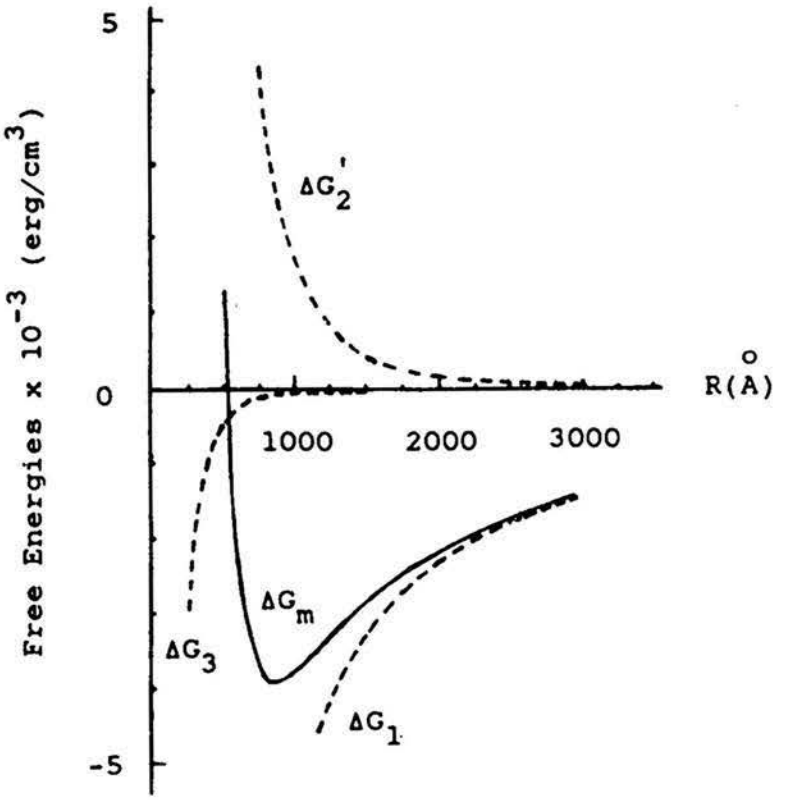

Figure 16. Free energy of formation of an O/W microemulsion, ΔG_m, as a function of radius R of the droplet. Different contributions to ΔG_m are included. Parameters used: surface potential 70 mV; volume fraction of oil 0.3; interfacial tension 10^{-3} dyne/cm; Hamaker constant 10^{-13}erg; Debye length in water $4x10^{-6}$cm; Debye length in oil 10^{-4}cm; temperature 300 K(37).

spectroscopy(PCS) measurements on W/O microemulsion systems composed of aqueous sodium chloride, heptane, hexylamine and sodium dodecyl sulfate(SDS). A fairly detailed discussion about time-average and dynamic light scattering is presented in Article IV of this dissertation.

REFERENCES

1. Hartley, G. S., Aqueous Solutions of Paraffin Chain Salts, Hermann & Cie., Paris, 1936.
2. Tanford, C., The Hydrophobic Effect: Formation of Micelles and Biological Membranes 2nd. Ed., Wiley, New York, 1980.
3. Israelachvili, J. N., in Physics of Amphiphiles: Micelles, Vesicles and Microemulsions (V. Degiorgio and M. Corti, Eds.), Proceedings of the International School of Physics, Italian Physical Society, North-Holland, 1985, Amsterdam.
4. Israelachvili, J. N., Mitchell, D. J., and Ninham, B. W., J. Chem. Soc. Faraday Trans. II 72, 1525(1976).
5. Mitchell, D. J., and Ninham, B. W., J. Chem. Soc. Faraday Trans. II 77, 601(1981).
6. Tanford, C., The Hydrophobic Effect: Formation of Micelles and Biological Membranes, 2nd. Ed., chapter 7. Wiley, New York, 1980.
7. Tanford, C., The Hydrophobic Effect: Formation of Micelles and Biological Membranes, 2nd. Ed., chapter 6. Wiley, New York, 1980.
8. Mazer, N. A., Benedek, G. B., and Carey, M. C., J. Phys. Chem. 80, 1075(1976).
9. Preston, W. C., J. Phys. Colloid Chem. 52, 84(1948).
10. Lindman, B., and Wennerstrom, H., Top. Curr. Chem. 87, 1(1980).

11. Lindman, B.,in Physics of Amphiphiles: Micelles, Vesicles, and Microemulsions (V. Degiorgio and M. Corti, Eds.), Proceedings of the International School of Physics, Italian Physical Society, North-Holland, 1985, Amsterdam.

12 Friberg, S. E., Progr. Colloid & Polymer Sci. 68, 41 (1983).

13. Chu, B., in Dynamic Light Scattering(R. Pecora, Ed.) Plenum, New York, 1985, p. 277.

14. Cazabat, A. M., Langevin, D. Menunier, J., and Pouchelon, A., Adv. Colloid Interface Sci. 16, 175 (1982).

15. Cazabat, A. M., Langevin, D., Menunier, J., and Pouchelon, A., J. Phys. Lett.(Paris) 43, L-89(1982).

16. Huang J. S., and Kim, M. W., Phys. Rev. Lett. 47, 1462(1981).

17. Dorshow, R., de Burraccarrini, F., Bunton, C. A., and Nicoli, D. F.,Phys. Rev. Lett. 47, 1336(1981).

18. Degiorgio, V., in Physics of Amphiphiles: Micelles, Vesicles and Microemulsions (V. Degiorgio and M. Corti, EdS.), Proceedings of the International School of Physics, Italian Physical Society, North-Holland, 1985, Amsterdam, p. 303.

19. Lawrence, A. S. C., Boffey, B., Gingham, G., and Talbot, K., Proc. Int. Congr. Surface Active Substances, 4th, 1964, Vol. II, p673, 1967. Also see ref. 22.

20. Berry, R. S., Rice, S. A., and Ross, J., Physical Chemistry, p.876. Wiley, New York, 1980.

21. Ekwall, P., Mandell, L., and Fontell, K., J. Colloid Interface Sci., 29, 639(1969).

22. Ekwall, P., in Advances in Liquid Crystals(G. H. Brown, Ed.), Vol. 1, p.1. Academic, New York, 1975.

23. Friberg, S., Naturwissenschaften 64, 612(1977).

24. Brown, G. H., Doane, J. W., and Neef, V. D., A Review of the Structure and Physical Properties of Liquid Crystals, CRC Press, 1971.

25. Fontell, K., in Liquid Crystals and Plastic Crystals (G. W. Garry and P. A. Winsor, Eds.), chapter 4. Wiley, New York, 1974.

26. Article III in this dissertation.

27. Friberg, S., in Microemulsions(L. M. Prince, Ed.), chapter 6. Academic, New York, 1977.

28. Sjoblom E., and Friberg, S., J. Colloid Interface Sci. 67, 16(1978).

29. Shah, D. O., Bansal, V. K., Chan, K., and Hsieh, W. C., in Improved Oil Recovery by Surfactant and Polymer Flooding(D. O. Shah, and R. S. Schechter, Eds.),p.293. Academic, New York, 1977.

30. Article II in this dissertation.

31. Clausse, M., Peyrelasse, J., Heil, J., Boned, C., and Lagourette, B., Nature 293, 636(1981).

32. Scriven, L. E., in Micellization, Solubilization, and Microemulsions(K. L. Mittal, Ed.), Vol. 2, p.877. Plenum, New York, 1977.

33. Evans, D. F., Mitchell, D. J., and Ninham, B. W., J. Phys. Chem. 90, 2817(1986).

34. Talmon, Y., J. Chem. Phys. 69, 2984(1978).

35. Prince, L. M., in Microemulsions(L. M. Prince, Ed.), Chapter 5. Academic, New York, 1977

36. Ruckenstein, E., and Chi, J. C., J. Chem. Soc. Faraday Trans. II 71, 1690(1975).

37. Ruckenstein, E., in Micellization, Solubilization, and Microemulsions (K. L. Mittal, Ed.), Vol. 2, p.755. Plenum, New York, 1977.

38. Ruckenstein, E., J. Disp. Sci. & Tech. 2, 1(1981).

39. Ruckenstein, E., J. Colloid Interface Sci. 114, 173 (1986).

40. Derjaguin B. V., and Landau, L. D., Acta Physico-Chemica, 14, 633(1941).

41. Verwey, E. W. J., and Overbeek, J. Th. G., Theory of the Stability of Lyophobic Colloids, Elsevier, New York, Amsterdam, 1948.

42. Hoar T. P., and Schulman, J. H., Nature 152, 102(1943).

43. Stocckenius, W., Schulman, J. H., and Prince, L. M., Kolloid-Z. 169, 170(1960).

44. Schulman J. H., and Friend, J. A., J. Colloid Interface Sci. 4, 497(1949).

45. Prince, L. M., J. Colloid Interface Sci., 23, 165(1967).

46. Shinoda, K., and Friberg, S., Adv. Colloid Interface Sci. 4, 281(1975).

ARTICLE I

MICROEMULSIONS WITH HIGH WATER SOLUBILIZING CAPACITY AT HIGH HYDROCARBON LEVELS AND VERY LOW SURFACTANT CONCENTRATIONS

by

Raymond L. Venable, Kay Lynn Elders,

and

Jiafu Fang

Department of Chemistry

University of Missouri-Rolla

Rolla, Missouri 65401

ABSTRACT

Phase diagrams have been determined showing the extent of the inverse micellar or microemulsion region for systems consisting of water, surfactant, and cosurfactant or mixture of cosurfactant and hydrocarbon with three surfactants and four cosurfactants. The surfactants are sodium dodecyl sulfate, sodium laurate, and tetradecyltrimethylammonium bromide, while the cosurfactants are pentanol, hexanol, pentylamine, and hexylamine. Hexylamine is found to be a very effective cosurfactant giving rise to very good water solubilizing capacity at extremely low surfactant concentrations and very low cosurfactant levels at rather high initial hydrocarbon levels.

INTRODUCTION

Microemulsions have been studied extensively since their introduction by Hoar and Schulman(1). Some fairly extensive reviews and/or overviews are available(2-4) which give the historical background and a fairly up to date presentation of the state of knowledge about microemulsions. Ionic surfactants generally require use of a cosurfactant to form microemulsions and the emphasis has been heavily on medium-chain-length alcohols(5,6) with possibly some use of glycol type compounds or organic acids even occasionally tertiary amines(7,8). Microemulsions typically require 6-10% by weight of surfactant and 8-14% cosurfactant(4). Friberg and Buraczewska(9) have also observed that, as the hydrocarbon level goes above 50% of the components other than water, the ability to solubilize water decreases sharply. This limits the ability to dilute the microemulsion system with the hydrocarbon or to add large amounts of water.

Greatly enhanced water-solubilizing ability is observed at high hydrocarbon levels when quaternary ammonium salts are used in place of the more common anionic surfactants (10,11). These systems still require the usual amounts of surfactant and cosurfactant. However, as recently pointed out(12), use of hexylamine as cosurfactant in place of the more commonly used medium-chain-length alcohols holds promise of greatly reducing the problems associated with solubilization of water at high hydrocarbon levels. The present paper reports a study

of the phase diagrams of some common surfactants using hexylamine, pentylamine, pentanol, and hexanol as cosurfactants in an effort to learn the reason for the great effectiveness of hexylamine under the conditions used in these experiments.

MATERIALS AND METHODS

Materials. The sodium dodecyl sulfate (SDS) was BDH specially pure and was recrystallized twice from absolute ethanol before use. The sodium laurate(SL), pentylamine, hexylamine, and pentanol were purchased from Sigma Chemical Company and used as received. Tetradecyltrimethylammonium bromide (TTMAB) was also purchased from Sigma but was recrystallized by dissolving in a minimal amount of methanol then adding diethyl ether until precipitation occurred. After filtration, the residual ether was removed from the precipitate by evacuation in a desiccator. This process was repeated until a plot of surface tension vs. the logarithm of surfactant concentration showed no minimum. Pentanol and heptane were purchased from Fisher and used as received. The water was double distilled, once from an acidic permanganate solution and once just as a simple distillation from an all-glass system.

Methods. For the titration experiments, dry surfactant was weighed into srew-cap culture tubes, the requisite amount of cosurfactant or hydrocarbon-cosurfactant mixture added, then the water was added dropwise. Samples were stirred vigorously on a vortex mixer after each addition of water. The end point of titration was taken to be the appearance of permanent turbidity or optical birefringence as observed between crossed polarizers. At the end of a titration the samples were stored for several days to be sure that the

turbidity or optical birefringence was indeed permanent. As a further check on the systems with hexylamine as cosurfactant particularly, several series of samples were prepared for long-term storage. In a given series the surfactant-cosurfactant ratio was held constant and varying amount of water added at concentrations below those which gave turbidity or optical birefringence in the titration. These were stored for the periods of time indicated in Table I in each case to see if phase separation occurred. The results of the long-term storage experiments generally agreed with the titration results within 2 or 3%. The long-term storage results are the ones presented where there was a difference. All measurements were carried out at 23±1^{o}C.

RESULTS

The microemulsion regions for the system water-SDS-cosurfactant are shown in Fig. 1 with the four cosurfactants. With hexylamine there is definitely is a normal micellar region and a lamellar liquid crystalline phase, but the magnitude and properties of these regions are beyond the scope of this work and will be reported in a later publication. The existence of these various regions is possible with the other cosurfactants but has not been investigated in this work. The diagrams shown in Fig.1 lie in the base plane of a four-component diagram. Results for the systems with water-SDS-heptane(25%)-cosurfactant(75%) are shown in Fig. 2 while those for heptane(50%)-cosurfactant(50%) appear in Fig. 3 and those for heptane(75%)-cosurfactant(25%) appear in Fig. 4.

The pseudoternary phase diagrams with water-SL-heptane(75%)-hexylamine(25%) as well as the same diagram with TTMAB as the surfactant are shown in Fig. 5. Fig. 6 for heptane(85%)-hexylamine(15%) shows that the ability to solubilize water still drops rather dramatically as hydrocarbon levels rise above 75% even with hexylamine as cosurfactant, particularly for SL and TTMAB. Fig. 7 presents phase diagrams for TTMAB at 0, 25, and 50% heptane. The figure is a bit busy but the results at 50% heptane are shown as an inset so that the shape of the phase diagram in the region of maximum water solubilization is clearly visible.

For systems involving SDS or SL the composition of each system at the point of maximum water solubilization is given in Table I, while the results for TTMAB are given in Table II.

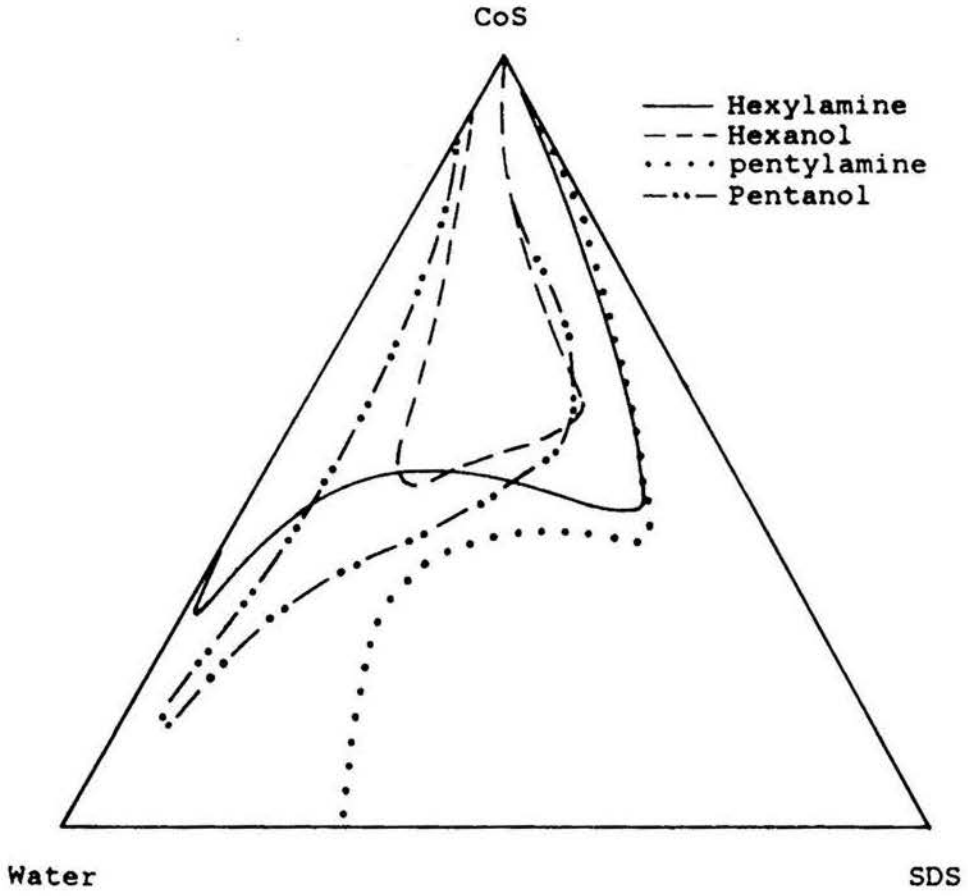

Figure 1. Microemulsion or L_2 region in the system water-SDS-cosurfactant.

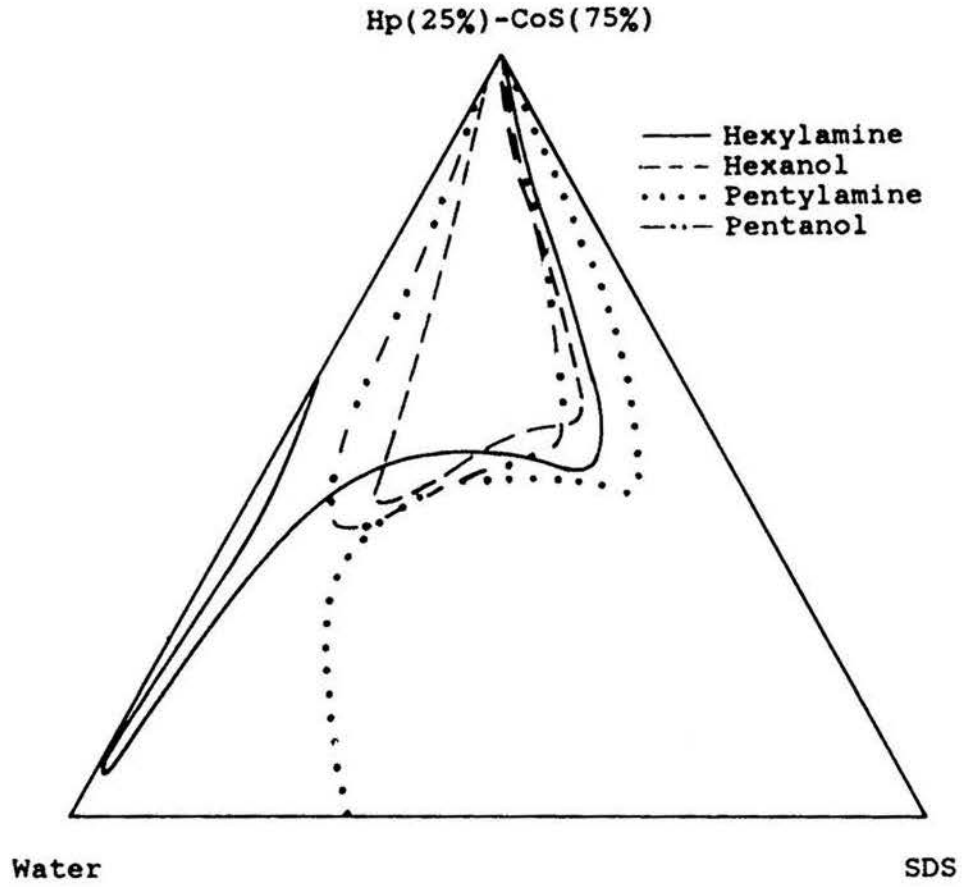

Figure 2. Microemulsion or L_2 region in the system water-SDS-heptane(25%)-cosurfactant(75%).

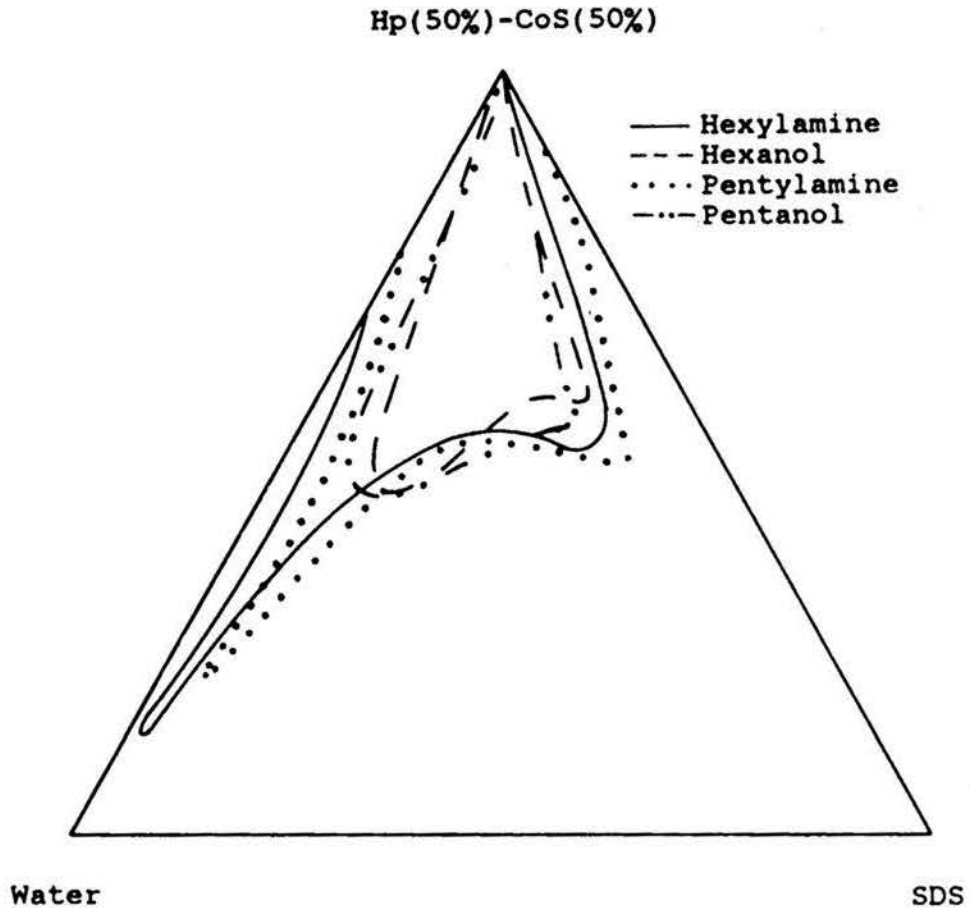

Figure 3. Microemulsion or L_2 region in the system water-SDS-heptane(50%)-cosurfactant(50%).

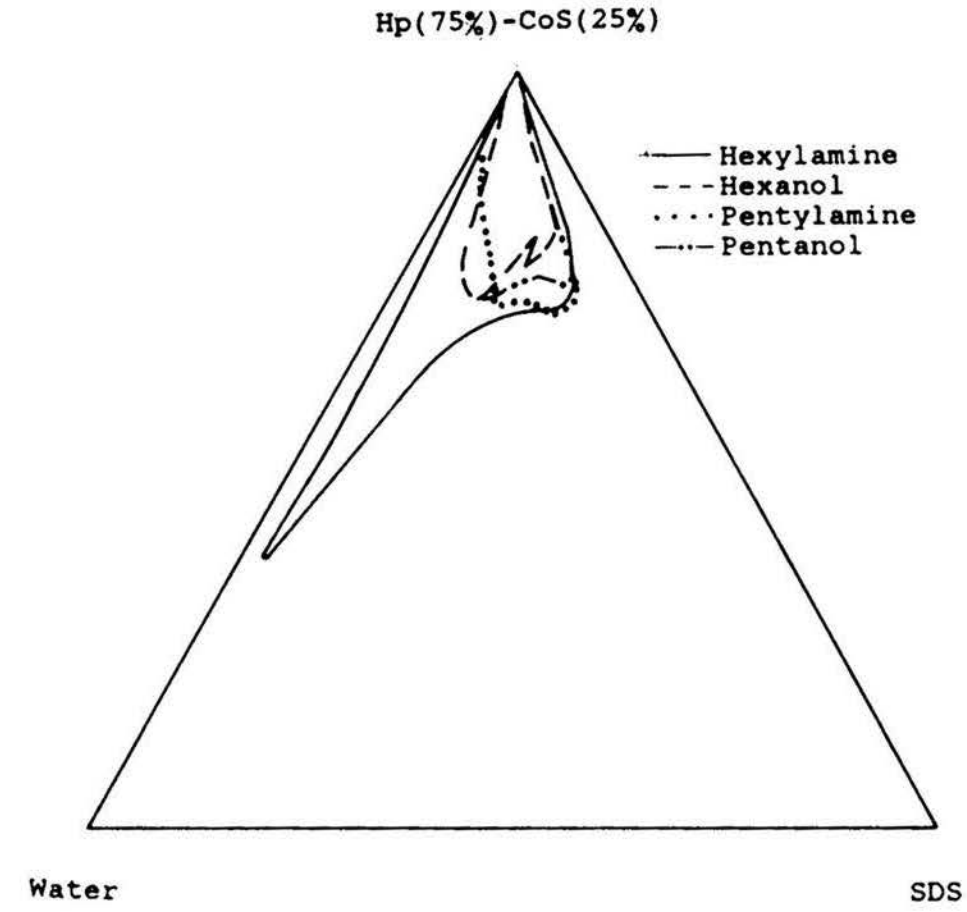

Figure 4. Microemulsion or L_2 region in the system water-SDS-heptane(75%)-cosurfactant(25%).

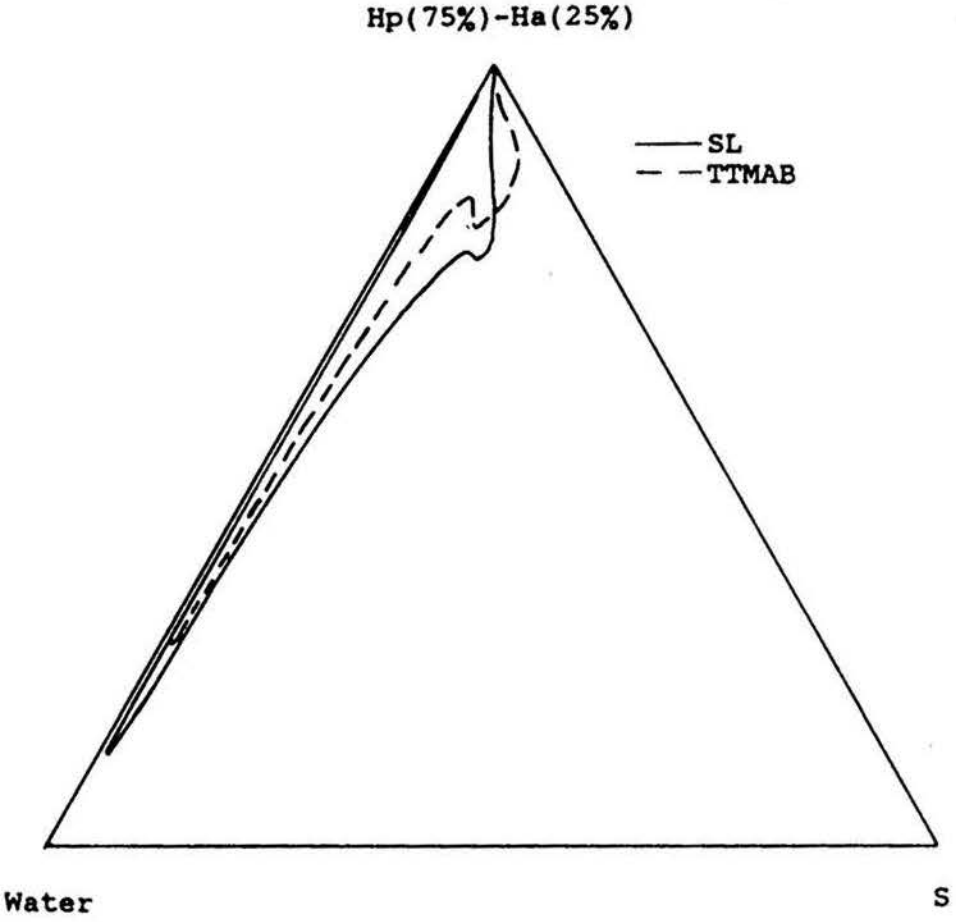

Figure 5. Microemulsion or L_2 region in the system water-surfactant-heptane(75%)-hexylamine(25%).

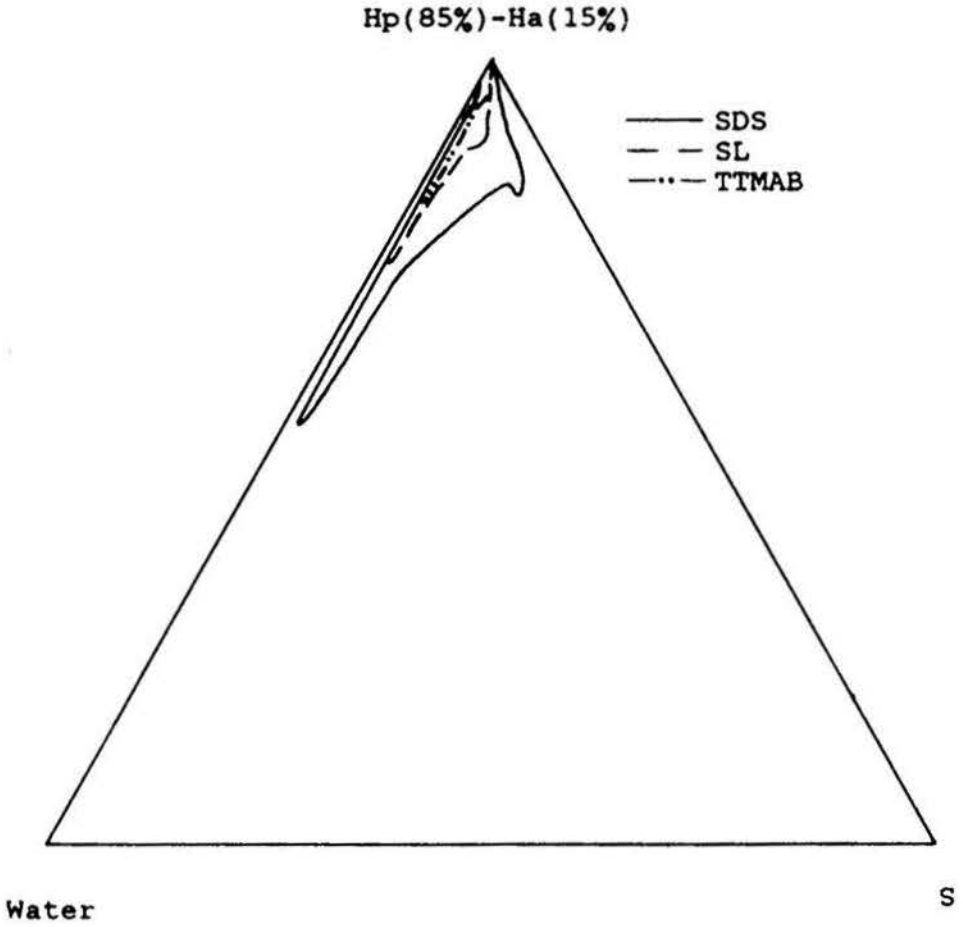

Figure 6. Microemulsion or L_2 region in the system water-surfactant-heptane(85%)-hexylamine(15%).

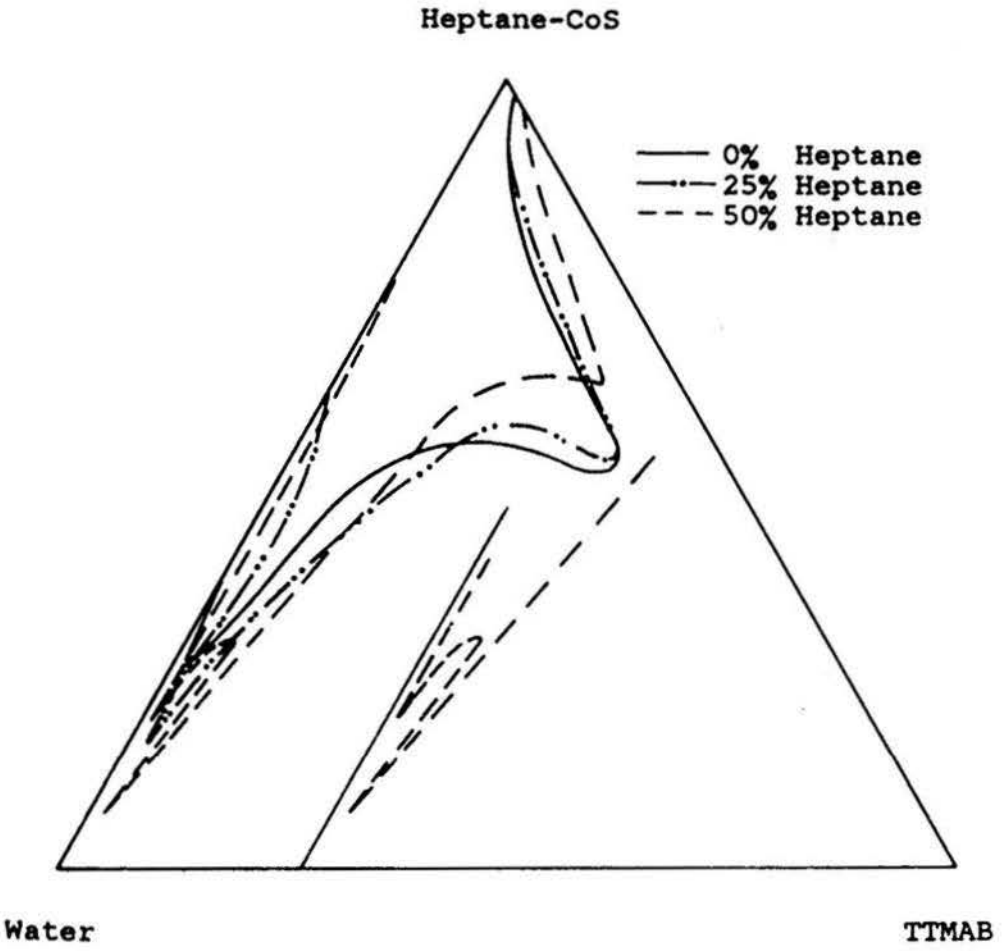

Figure 7. Size and shape of the microemulsion or L_2 region in the system water-TTMAB-heptane-hexylamine as a function of heptane level.

TABLE I

System Composition at Maximum Water Solubilization

Storage time	CoS	Percentage composition				
		Water	SDS	CoS	Heptane	SL
		A. Water-SDS-CoS				
30 days	Ha	67.8	1.0	31.2	—	—
21 days	C_6OH	39.1	15.2	45.7	—	—
Titration	C_5OH	82.1	5.9	12.0	—	—
		B. Water-SDS-Heptane(25%)-CoS(75%)				
20 days	Ha	92.0	0.8	5.4	1.8	—
Titration	C_6OH	43.1	14.8	31.6	10.5	—
Titration	C_5OH	50.1	11.4	28.9	9.6	—
		C. Water-SDS-Heptane(50%)-CoS(50%)				
30 days	Ha	85.0	1.8	6.6	6.6	—
14 days	C_6OH	41.4	13.5	22.6	22.6	—
Titration	C_5OH	43.5	11.3	22.6	22.6	—
Titration	Pa	74.1	5.1	10.4	10.4	—

TABLE I (continued)

		D. Water-SDS-Heptane(75%)-CoS(25%)				
30 days	Ha	60.0	2.8	9.3	27.9	—
Titration	C_6OH	21.2	10.2	17.1	51.4	—
Titration	C_5OH	21.1	8.7	17.6	52.7	—
Titration	Pa	18.3	12.3	17.4	52.1	—
		E. Water-SL-Heptane(75%)-Ha(25%)				
30 days		85.0	—	3.6	10.7	0.7

CoS—Cosurfactant, Ha—Hexylamine, Pa—Pentylamine

C_6OH—Hexanol, C_5OH—Pentanol.

TABLE II

System Composition at Maximum Water Solubilization for TTMAB at the Various Hydrocarbon Levels Studied

Hydrocarbon level(%)	Percentage composition			
	Water	TTMAB	Hexylamine	Heptane
0	72.7	1.4	25.9	0
25	80.5	2.0	13.1	4.4
50*	79.6*	1.2*	9.6*	9.6*
50	91.3	1.7	3.5	3.5
75	73.9	0.7	6.3	19.0

* Data for first tip or "maxima".

DISCUSSION

In the methods section mention was made of checking titration results by long term storage for certain samples as indicated in Table I. Since the solutions which first showed turbidity during a titration were kept for several days to be sure the turbidity was permanent, the water-solubilizing capacity or water solubility limit determined by long-term storage is always less than that determined by titration where there is a difference. The system with heptane(85%)-hexylamine(15%) with SDS is the only system that showed a significant difference between the titration and long-term storage results. In that system titration gave 46% water solubilized at the maximum point, but a considerable degree of phase separation occurred almost immediately. Long-term storage gave only 32% water solubilized at the maximum point.

From Fig. 1 it is obvious that in the systems consisting of water-SDS-cosurfactant, pentanol, pentylamine, and hexylamine are much more effective at solubilizing water than is hexanol. The maximum water solubilization occurs at a lower surfactant concentration with hexylamine than with pentanol. The microemulsion region may connect with the normal micellar region in the pentanol diagram. Pentylamine and water are completely miscible so it is not surprising that the diagram with pentylamine gives one large solubility region connecting with water-SDS axis at approximately 33% SDS in reasonable agreement with the literature (13). Comparison of Figs. 1 and

2 shows that there is no significant change in the size of the microemulsion region when 25% heptane is added to hexanol or to pentylamine. However, there is a significant enhancement of water-solubilizing capacity when 25% heptane is added to hexylamine and a marked reduction in water solubilization with pentanol. This enhancement in water-solubilizing capacity with hexylamine is probably caused by the destabilization of the lamellar liquid crystalline phase due to the presence of heptane. In fact if the water solubilization maximum did not occur at such a low surfactant concentration, the microemulsion region with hexylamine might connect with the normal micellar region.

As shown in Fig. 3 the difference in the size of the microemulsion region with pentanol and with hexanol is not particularly striking at 50% initial hydrocarbon level. Pronounced differences in the associational structures of microemulsions stabilized with pentanol and with hexanol have been reported(5,14), using other surfactants. It is not known if such differences exist with the present systems. As noted in the discussion of Fig. 1, pentanol competes very well with hexylamine in the absence of hydrocarbon, but as shown here in Fig. 3, the amines are far superior to the alcohols at solubilizing water with 50% hydrocarbon in the cosurfactant. Hexylamine is also obviously superior to pentylamine, both in terms of the maximum water solubilizing capacity and in terms of the lower surfactant concentration required.

The reduction in water-solubilizing capacity at hydrocarbon levels above 50% is apparent for all cosurfactants when the results in Fig. 4 are compared with those in Fig. 3. Again there is no really significant difference in the size of the microemulsion region with pentanol and hexanol or for that matter with pentylamine. The great superiority of hexylamine as a cosurfactant for solubilizing water is certainly still obvious. The extremely low surfactant level required is still readily apparent also.

The results shown in Fig. 5 for SL and TTMAB show that hexylamine is tremendously effective at solubilizing water at very low surfactant concentrations with these surfactants as well at 75% initial hydrocarbon level. The decrease in water solubilizing capacity with increasing hydrocarbon level is further illustrated by comparing results for SDS from Fig. 4 with those in Fig. 6 and by comparing the results for SL and TTMAB from Fig. 5 and 6. This comparison shows the change in going from 75 to 85% hydrocarbon. SDS does not lose its effectiveness nearly as badly as do SL and TTMAB, but even so the decrease in water-solubilizing capacity is still very pronounced.

The results shown in Figs. 5 and 6 do, however, point out that the tentative suggestion of the possible importance of something called complementarity of function put forth in a recent paper(12) was premature. That suggestion was based on too few measurements on too few surfactants and does not appear at the present time to be valid.

Reference has already been made to previous work(10,11) showing that, with pentanol as cosurfactant, the quaternary ammonium salts give much larger water solubilization at very high hydrocarbon levels than does the anionic SDS. Comparison of the results summarized in Table I and II for hexylamine as cosurfactant shows that at 50% heptane and 75% heptane TTMAB is indeed somewhat superior to SDS at solubilizing water. The difference is not particularly striking and, as already discussed, at 85% heptane the situation is reversed with SDS being superior to TTMAB.

The effectiveness of hexylamine as a cosurfactant would appear to hold great promise for industrial formulations where amines can be tolerated. Hexylamine does have a pungent odor and all amines tend to be aggressive. These do pose limitations on the uses of hexylamine. However, if the factor or factors responsible for the effectiveness of hexylamine can be uncovered, then other compounds may possibly be found which can be equally effective but have fewer undesirable properties.

The one feature that appears to correlate so far is the solubility of water in the various compounds used as cosurfactants in this study. From Fig. 1 we see that water is sparingly soluble in pentanol (11%) or hexanol (8%) while being quite soluble (62%) in hexylamine. In contrast, as previous mentioned, water and pentylamine are completely miscible. Thus hexylamine is seen to be in an intermediate position between the two extremes as far as ability to

dissolve water is concerned. Neither of the alcohols nor hexylamine is appreciably soluble in water. Hexanol is soluble to the extent of 0.6-0.7% by weight, hexylamine about 1%, and pentanol about 1.5%. Therefore sparing solubility in water may be a necessary condition for a compound to be a good cosurfactant for W/O microemulsion formation at high hydrocarbon levels, but does not seem to to be a sufficient condition. These observations would appear to be in qualitative agreement with the concept of the hydrophile-lipophile balance (HLB) of surfactant systems as put forth by Shinoda et al. (15).

SUMMARY

In all surfactant systems studied so far in our laboratory, hexylamine has been found to give excellent water-solubilizing capacity at high hydrocarbon levels with extremely low surfactant concentrations and very low cosurfactant levels. In general, hexylamine has been far superior to either pentylamine, pentanol, or hexanol in this regard. This superiority of hexylamine is observed with both the aliphatic hydrocarbon heptane and the aromatic hydrocarbon toluene(12). It has been observed with SDS, with the carboxylate salt sodium laurate, and with the quaternary ammonium salt tetradecyltrimethylammonium bromide. Of the possible factors which could be responsible for this behavior, the one that has been found to correlate to date is good solubility of water in the cosurfactant coupled with sparing solubility of the cosurfactant in water.

REFERENCES

1. Hoar, T. P., and Schulman, J. H., Nature (London) 152, 102(1943).
2. Shah, D. O., Bansal, V. K., Chan, K., and Hsieh, W. C., in "Improved Oil Recovery by Surfactant and Polymer Flooding" (D. O. Shah and R. S. Schechter, Eds.), p.297. Academic Press, New York, 1977.
3. Robb, I. D., Ed., "Microemulsions", Plenum, New York, 1982.
4. Friberg, S. E., and Venable, R. L., in "Encylopedia of Emulsion Technology"(P. Becher, Ed.), Vol. 1, p.287. Dekker, New York, 1983.
5. Clausse, M., Peyrelasse, J., Boned, C. A., Heil, J., Nicolar-Morgantini, L., and Zradba, A., in "Surfactants in Solutions" (K. L. Mittal and B. Lindman, Eds.), p.1583. Plenum, New York, 1984.
6. Warnheim, T., Sjoblom, E., Henriksson, U., and Stilbs, P., J. Phys. Chem. 88, 5420(1984).
7. Roux, G., Roberts, D., Perron, G., and Desnoyers, J. E., J. Solution Chem. 9, 629(1980).
8. Desnoyers, J. E., Quirion, F., Hetu, D., and Perron, G., Canad. J. Chem. Eng. 61, 672(1983).
9. Friberg, S. E., and Buraczewska, I., Prog. Colloid Polym. Sci. 63, 1(1979).

10. Venable, R. L., and Weingaertner, D. A., J. Dispersion Sci. Technol. 4, 425(1983).

11. Venable, R. L., J. Amer. Oil Chem. Soc. 62, 128(1985).

12. Venable, R. L., and Viox, D. M., J. Dispersion Sci. Technol. 5, 73(1984).

13. Ekwall, P., in "Advances in Liquid Crystals (G. H. Brown, Ed.), p. 115. Academic Press, New York, 1975.

14. Stilbs, P., Rapacki, K., and Lindman, B., J. Colloid Interface Sci. 95, 583(1983).

15. Shinoda, K., Kunieda, H., Arai, T., and Saijo, H., J. Phys. Chem. 88, 5126(1984).

ARTICLE II

Conductivity Study on the Microemulsion System: SDS Hexylamine-Heptane-Water

by

Jiafu Fang and Raymond L. Venable
Department of Chemistry
University of Missouri-Rolla
Rolla, Missouri 65401

ABSTRACT

Conductivity measurements on the microemulsion system composed of sodium dodecyl sulfate, hexylamine, heptane, and water are interpreted in terms of the percolation and effective medium theories. From this interpretation, the molar ratio of hexylamine to sodium dodecyl sulfate in the microemulsion droplet surface can be deduced. Following that determination it is possible to obtain approximate values for the radius of the water pools and the number and surface area of droplets per unit volume of microemulsions of the system.

INTRODUCTION

The common microemulsion systems containing intermediate chain length alcohols as cosurfactants reach a maximum water solubilization usually about 60% with concentrations of surfactant higher than 15% and of cosurfactant around 25%(1). In a previous study(2), we reported a novel microemulsion system consisting of sodium dodecyl sulfate(SDS), hexylamine, heptane, and water. The system exhibited some unusual properties, such as very high water solubilization at a very low surfactant concentration. The system could reach a maximum water solubilization higher than 90% while the surfactant concentration was as low as about 1.5% and the cosurfactant one less than 7% starting with a hydrocarbon-cosurfactant mixture that was 25% heptane and 75% hexylamine.

Since the discovery of microemulsions, many different techniques have been used to investigate their structures. Among these, conductivity measurement provides a particularly convenient, and useful tool for investigation of structure and phase inversion phenomena in microemulsions(3-5). Our microemulsion system is characterized by a continuous solubility region from high hydrocarbon levels to high water contents. It appears reasonable to expect structure inversions.

It has been shown that for some microemulsion systems conductivity behavior can be described in terms of

percolation and effective medium theories (3,6,7). In the present study we propose a simple model for our systems and find that the conductivity data can be fitted nicely by the effective medium formula. Moreover, the molar ratio of the hexylamine to SDS in the interfacial film can be evaluated using this approach. With this ratio known, we are able to calculate approximately the droplet size and the number of droplets per unit volume of microemulsions based on the assumption that the microemulsion droplets or aggregates are monodisperse.

EXPERIMENTAL

Hexylamine was purchased from Eastman Kodak (Cat.no.117 7559, 99%) and used as received. Haptane was from Fisher(Cat.no. 03008) and used without further purification. Sodium dodecyl sulfate was purchased from BDH and recrystalized twice with absolute ethanol. Water was triple distilled.

Conductivity was measured by using a Kent EIl 5007 conductivity meter operating at 70Hz or 1 kHz and a temperature compensated to 25^{o}C. Each experiment was done while keeping the ratio of SDS to hexylamine constant. Water was added to the sample until the composition of the system is close to the boundary of the microemulsion region where turbidity due to phase separation is observed.

Phase diagrams were determined at 25^{o}C by the titration method, as described elsewhere(2).

RESULTS

Curve a of Fig 1 shows the tertiary phase diagram for the system consisting of SDS, hexylamine(Ha), and water. Curves b, c, and d show pseudotertiary phase diagrams of the systems containing different amounts of heptane(Hp). From these diagrams it is seen that water is soluble in pure hexylamine up to around 63%. However, addition of heptane to hexylamine progressively reduces this water solubility. It is interesting to note that a linear relation exists between the water solubility and weight ratio of heptane to heptane plus hexylamine, when no surfactant is present, as shown by curve (1) in Fig. 2. It is noticeable that the maximum contents of solubilized water in these microemulsion systems are very high even when the oil level is high and the surfactant concentration is very low. Curve (2) in Fig. 2 shows the variation of the maximum water solubilization into the microemulsion with the heptane content as determined from the four phase diagrams of Fig. 1. This water solubilization first increases and reaches a maximum at a hydrocarbon level about 25%, then decreases to about 60% when the ratio of Hp/(Ha+Hp) is equal to 75%.

Figs. 3 to 8 show some typical conductivity data from the present microemulsions. Detailed discussion about these data will be given in the following section.

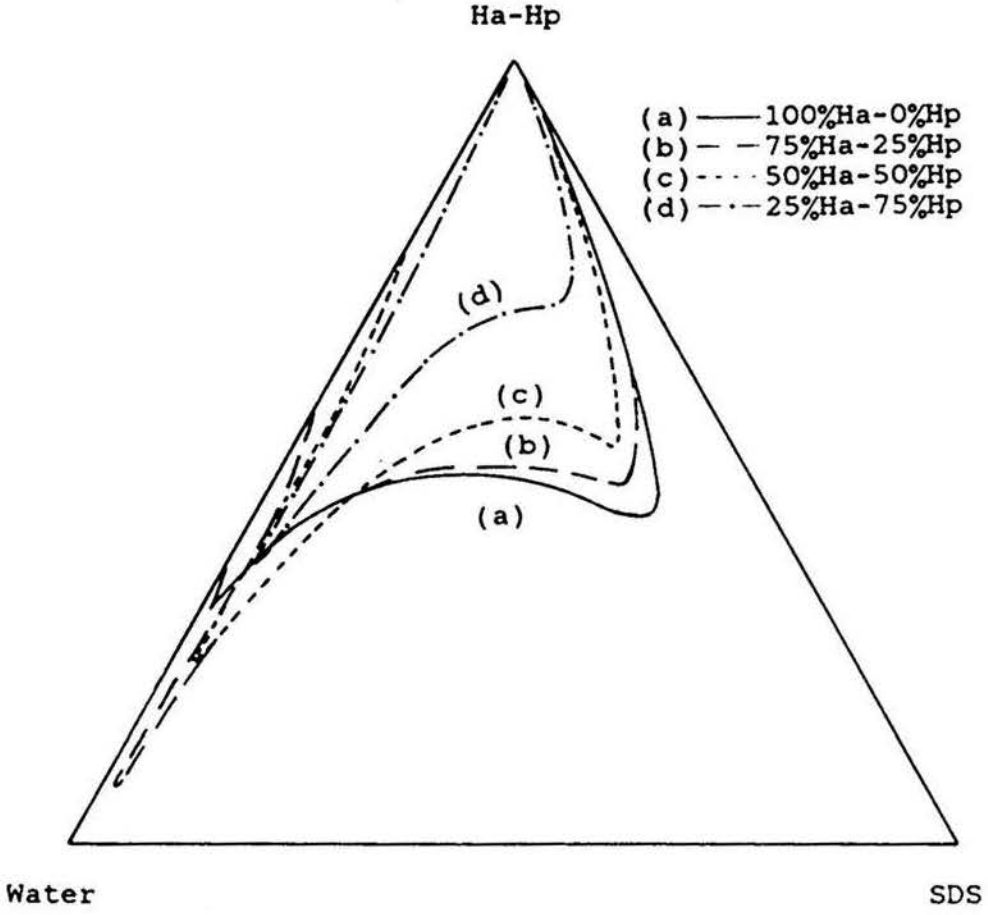

Figure 1. Partial pseudotertiary phase diagrams of the system composed of sodium dodecyl sulfate(SDS), Hexylamine(Ha), heptane(Hp), and water.

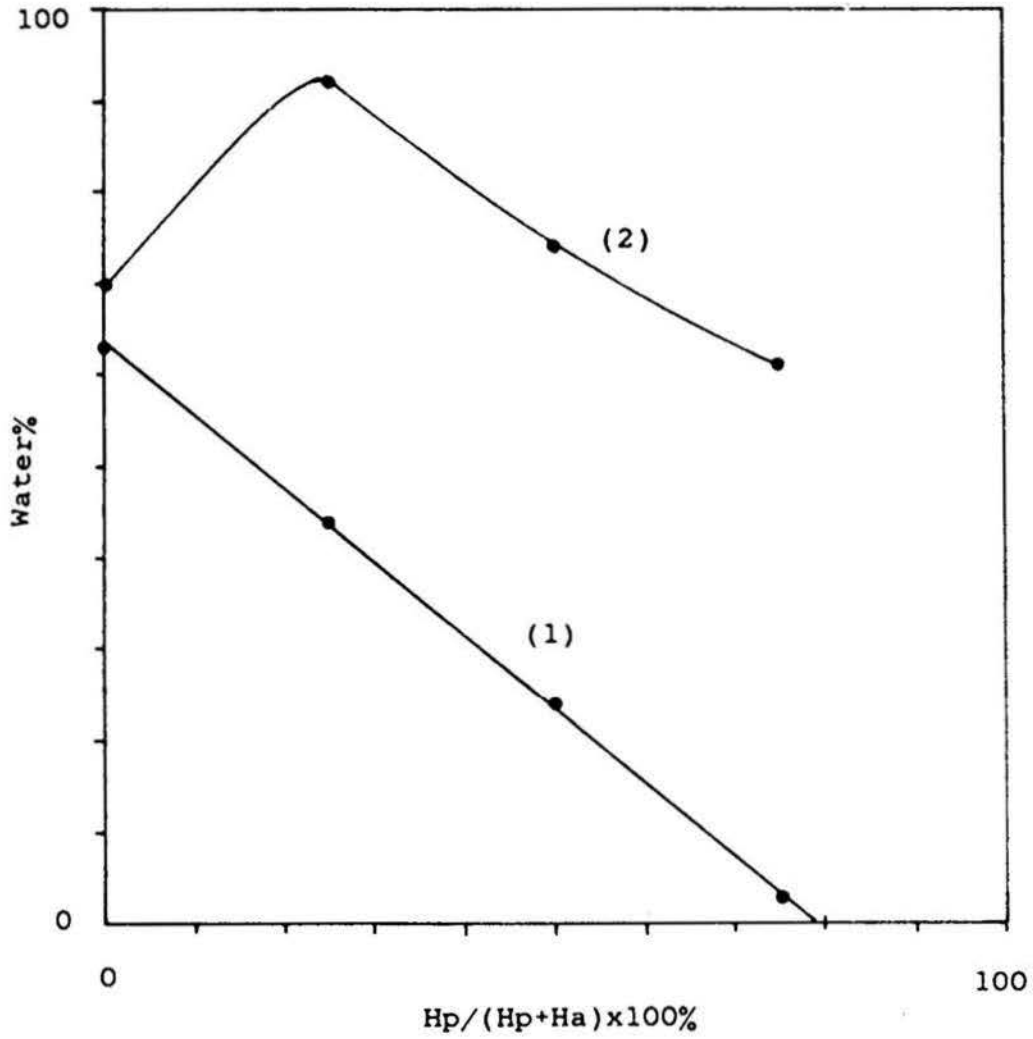

Figure 2. Solubility of water as represented on the phase diagrams of Figure 1. (1) solubility of water in the mixture of hexylamine and heptane with no surfactant present. (2) Maximum water solubilization into the microemulsions.

DISCUSSION

Conductivity behavior of emulsions and microemulsions have been studied by some investigators using various models(3,8,9,). It is expected that microemulsions must have different conductivity properties from emulsions since structures of microemulsions and emulsions are very different. As indicated by some authors(10), oil continuous(W/O) type microemulsions show much more complicated conductivity behavior than O/W type. For the present systems it is believed that the microemulsions are W/O type at low water concentrations. Nevertheless, for our systems we find that the percolation and effective medium theories, which were developed for semiconductor-metal transitions observed in inhomogeneous systems and for transport properties in amorphous solids(11), can be used to explain the conductivity behavior. According to Clausse and co-workers(7), the present microemulsions should belong to the U-type system which is characterized by a phase diagram in which the W/O and O/W areas merge into each other and form a unique domain and the conductivity behavior of such U-type microemulsions can be described by percolation and effective medium theories. Our results agree with such an interpretation as will be shown in the following sections.

It is well known that a microemulsion is a transparent liquid dispersion system of two immiscible liquids(12), such as oil and water, containing amphiphilic molecules as a third

or fourth component. In applying the percolation and effective medium theories to such a system, let us first consider the low water concentration region. When water concentration is low, the microemulsion can be oil continuous. Thus the disperse phase consists of water droplets surrounded by amphiphilic molecules. These droplets behave as the electrical conducting constituents in the system. If the volume fraction , ϕ, of the disperse phase is below a critical value called the percolation threshold, and designated ϕ_p, the conductive droplets are isolated from each other and contribute little to conductance. However, when the volume fraction of the disperse phase reaches and exceeds the percolation threshold, some of these conductive droplets begin to contact each other and form clusters with many conduction paths. Conductivity therefore begins to increase rapidly from an almost zero value to some much higher level. This phenomenon can be seen from Figs. 4 to 8.

Lagourette et al.(3) state that in the vicinity of the percolation threshold the relation of conductivity, σ, to volume fraction, ϕ, can be described by the scaling equation:

$$\sigma \sim (\phi - \phi_p)^t \qquad (1)$$

where t is usually equal to 8/5 (3, 6). Our results are in agreement with this equation, as shown in Fig. 3, where a straight line is found in the range of medium values of ϕ.

For higher concentrations the equation

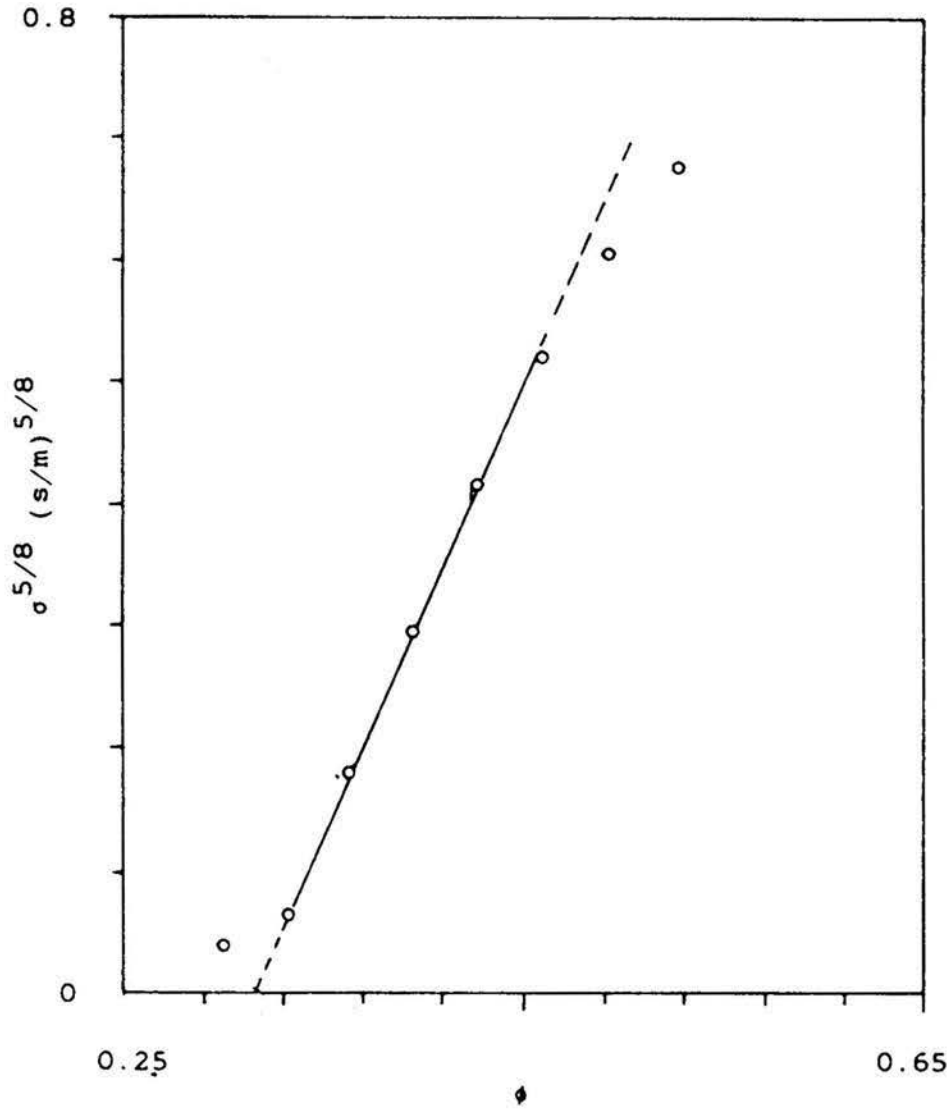

Figure 3. Plot of $\sigma^{5/8}$ vs. volume fraction of water, ϕ (See Eq. 1).

$$\sigma \propto (\phi - \phi_p) \tag{2}$$

fits the conductivity data(3). Figs. 4 to 8 show this relation. The valid range of Eq.(2) overlaps with that of Eq.(1).

From the effective medium theory, the conductivity for a binary composite can be expressed as (3,7,13,14)

$$\frac{\sigma - \sigma_c}{3\sigma} = \frac{\sigma_d - \sigma_c}{\sigma_d + 2\sigma} \phi \tag{3}$$

where σ_c and σ_d are the conductivity of the continuous phase and disperse phase, respectively. For the present systems, σ_d is much larger than σ_c since the continuous phase is oil which shows almost zero conductivity. Thus the above equation can be reduced to

$$\sigma = \frac{3}{2} \sigma_d (\phi - \frac{1}{3}) \tag{4}$$

Obviously, the plot of σ against (ϕ-1/3) should be a straight line passing through the origin and with the slope equal to $3\sigma_d/2$ if the conductivity behavior of the system obeys the equation. Comparing Eq.(4) with Eq.(2), it seems that the percolation threshold is equal to 1/3.

Since the volume fraction ϕ of the disperse phase is not obtained directly from these experiments, it is necessary to calculate it from the weight fractions. To do this, the following assumptions have been made.

(a). All SDS is in the interphase between the water core and oil phase.

(b). The cosurfactant hexylamine distributes among the continuous phase(oil), interphase, and disperse phase. However, since the solubility of hexylamine in water is negligible (less than 1% at 25°C), the amine is considered only present in the interphase and in the oil phase.

(c). The interphase is composed of SDS and hexylamine. Thus the average molar ratio of SDS to hexylamine, γ, in the interphase phase is given by

$$\gamma = N_{Ha}^{int}/N_s$$

where N_{Ha}^{int} is the mole number of hexylamine in the interphase and N_s is the mole number of SDS in the system.

With the above model we can derive a formula to calculate the volume fraction of the disperse phase:

$$\phi = \frac{V_d}{V_t} = \frac{\rho_t}{\rho_d}\left[f_s + f_{Ha}^{int} + f_w\right]$$

$$= \frac{\rho_t}{\rho_d}\left[f_s\left(1 + \gamma\frac{M_{Ha}}{M_s}\right) + f_w\right] \qquad (5)$$

where ρ_t and ρ_d are the densities of the microemulsion system and the disperse phase. The weight fractions of SDS and water in the system are f_s and f_w, respectively, while the weight fraction of hexylamine in the interphase is f_{Ha}^{int}. M_{Ha} and M_s are the molecular weight of hexylamine and SDS. As an approximation, the value of ρ_d can be taken as 1.0 g/ml since

the density of water at 25°C is near 1.0 g/ml, that of SDS is 1.16 g/ml(16), and that of hexylamine is 0.766 g/ml. With this equation, we are able to evaluate the volume fraction of the disperse phase(water core plus interphase) if an appropriate value of the structural parameter γ is chosen. Hence we can plot σ against (ϕ-1/3), as shown in Figs. 4 to 8. From these figures, it is seen that the parameter γ can be determined by fitting the experimental data with the reduced effective medium Eq.(4), that is, by trying different γ values until the straight line passes through the origin. From Eq.(4) the conductivity of the disperse phase, σ_d, can be calculated from the slope of the straight line. Data from systems with the ratio of SDS to (Ha+Hp) equal to 20/80 are plotted in Fig. 9. It is interesting that σ_d shows a linear relation to the ratio by weight between SDS and hexylamine in the system. This result confirms the previous assumption that all SDS is essentially present in the interphase. Since SDS is ionic and largely ionized in contact with water core, the conductivity of disperse phase, σ_d, will increase with increasing concentration of SDS in the system. A similar result was observed by Clausse, et al.(3).

It may be questioned how the parameter γ can remain unchanged while the water content varies over a rather wide range and the ratio of SDS to hexylamine is held constant. This can be interpreted qualitatively. When water concentration increases, the size of water droplets becomes

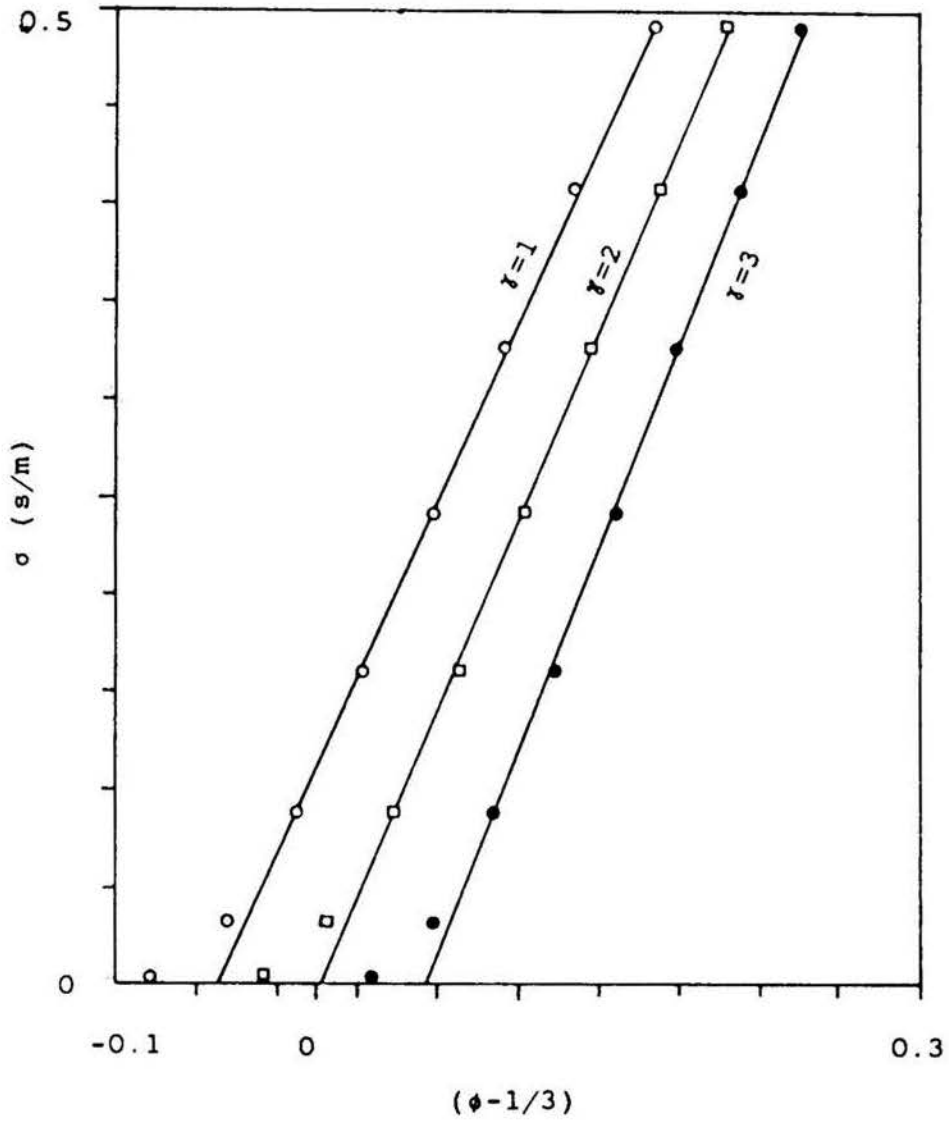

Figure 4. Conductivity, σ, versus (ϕ-1/3) for the system containing SDS, hexylamine(Ha), and water, with the weight ratio SDS/Ha equal to 20/80.

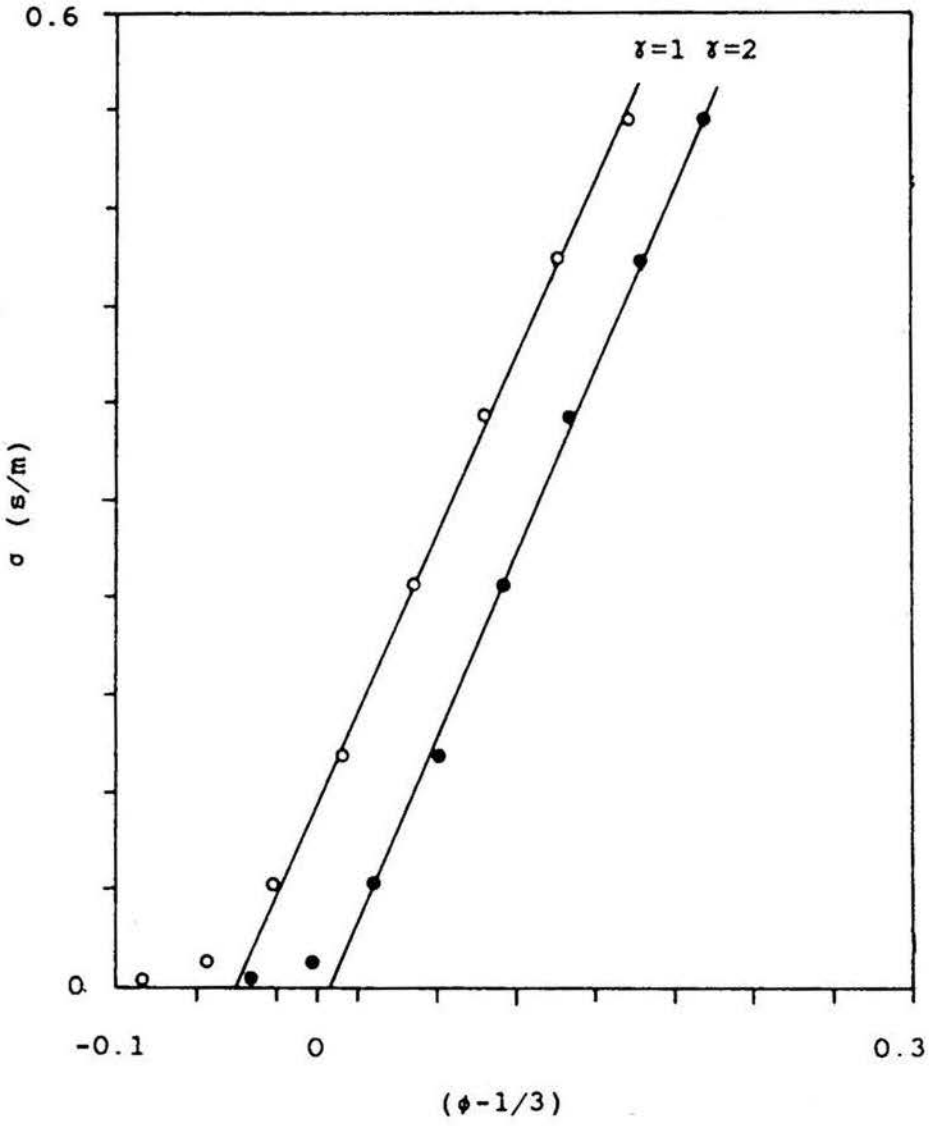

Figure 5. Conductivity, σ, versus (φ-1/3) for the system containing SDS, hexylamine(Ha), heptane(Hp), and water, with the weight ratio Hp/Ha = 25/75 and SDS/(Hp+Ha) = 20/80.

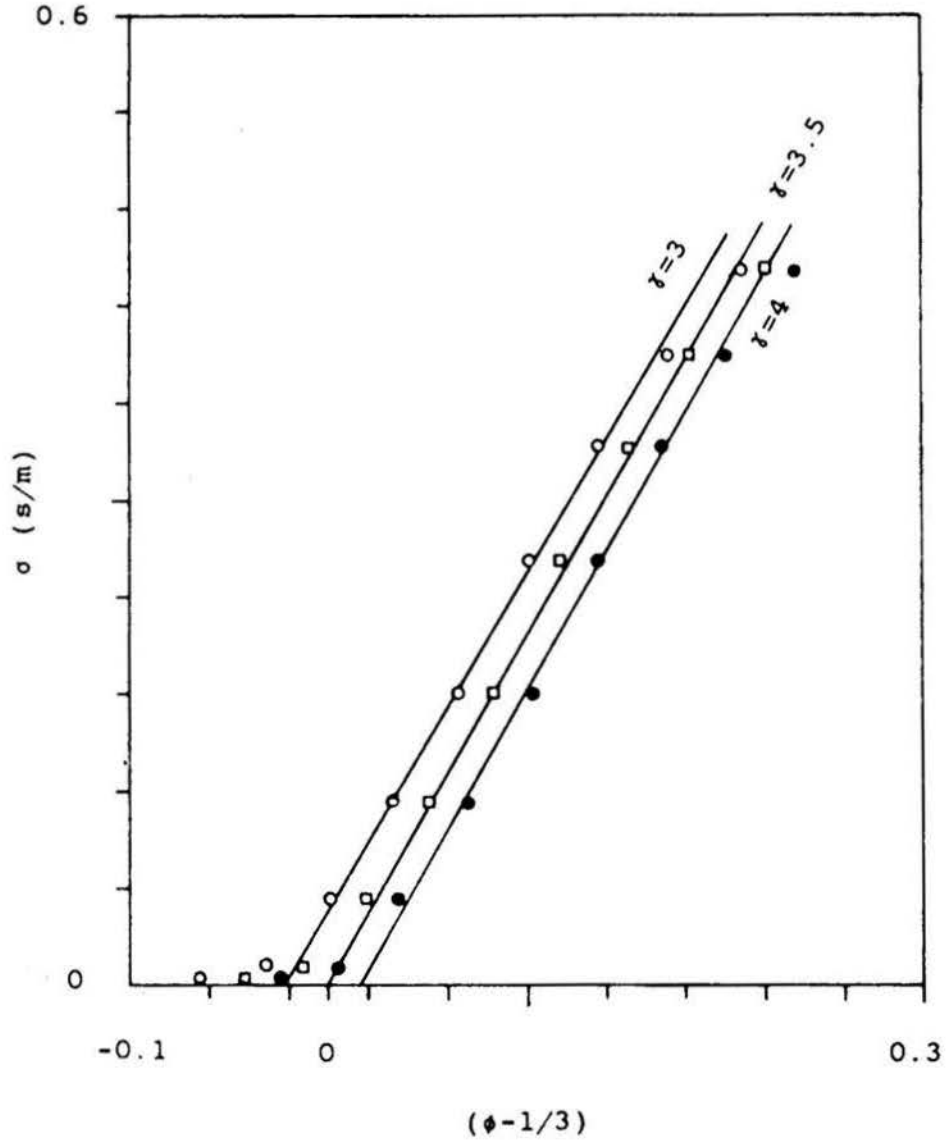

Figure 6. Conductivity, σ, versus (ϕ-1/3) for the system containing SDS, hexylamine(Ha), heptane(Hp), and water, with the weight ratio Hp/Ha = 25/75 and SDS/(Hp+Ha) = 15/85.

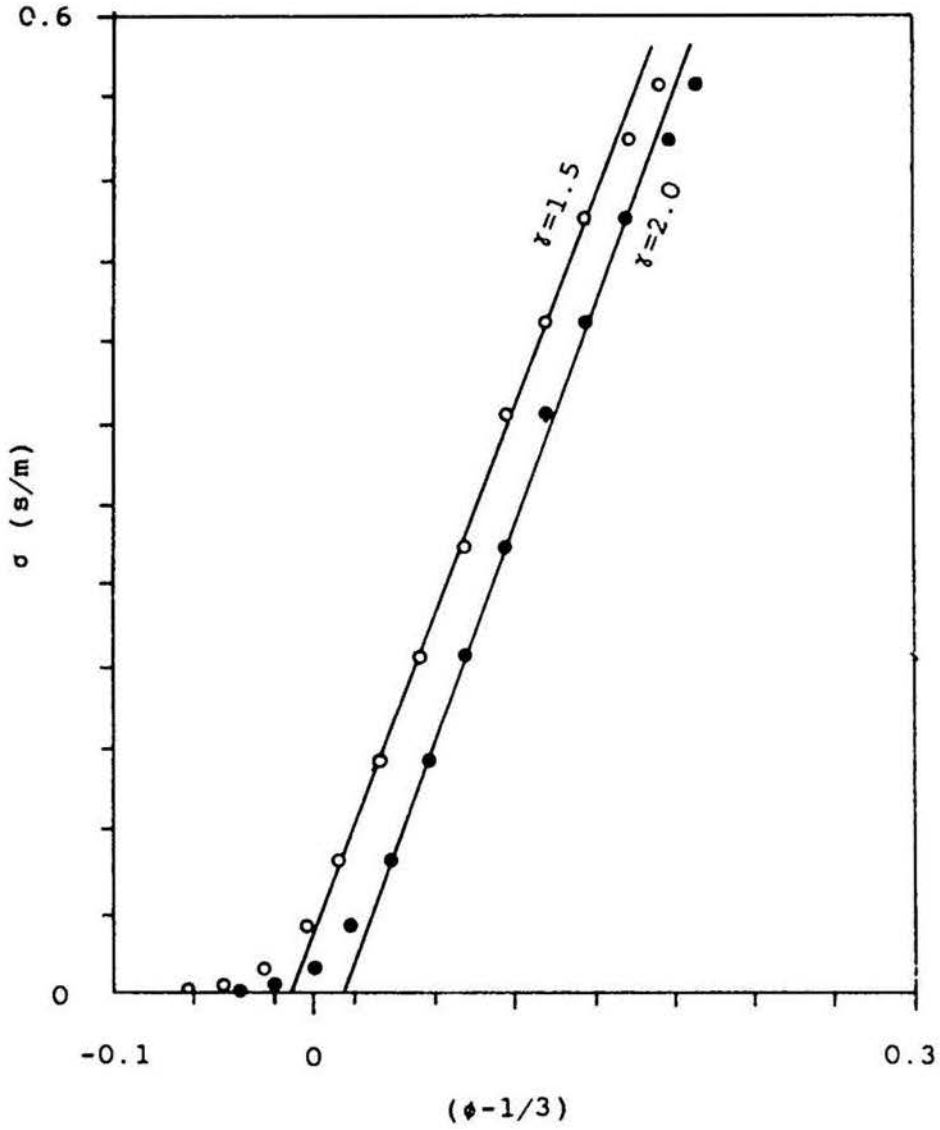

Figure 7. Conductivity, σ, versus (ϕ-1/3) for the system containing SDS, hexylamine(Ha), heptane(Hp), and water, with the weight ratio Hp/Ha = 37.5/62.5 and SDS/(Hp+Ha) = 20/80.

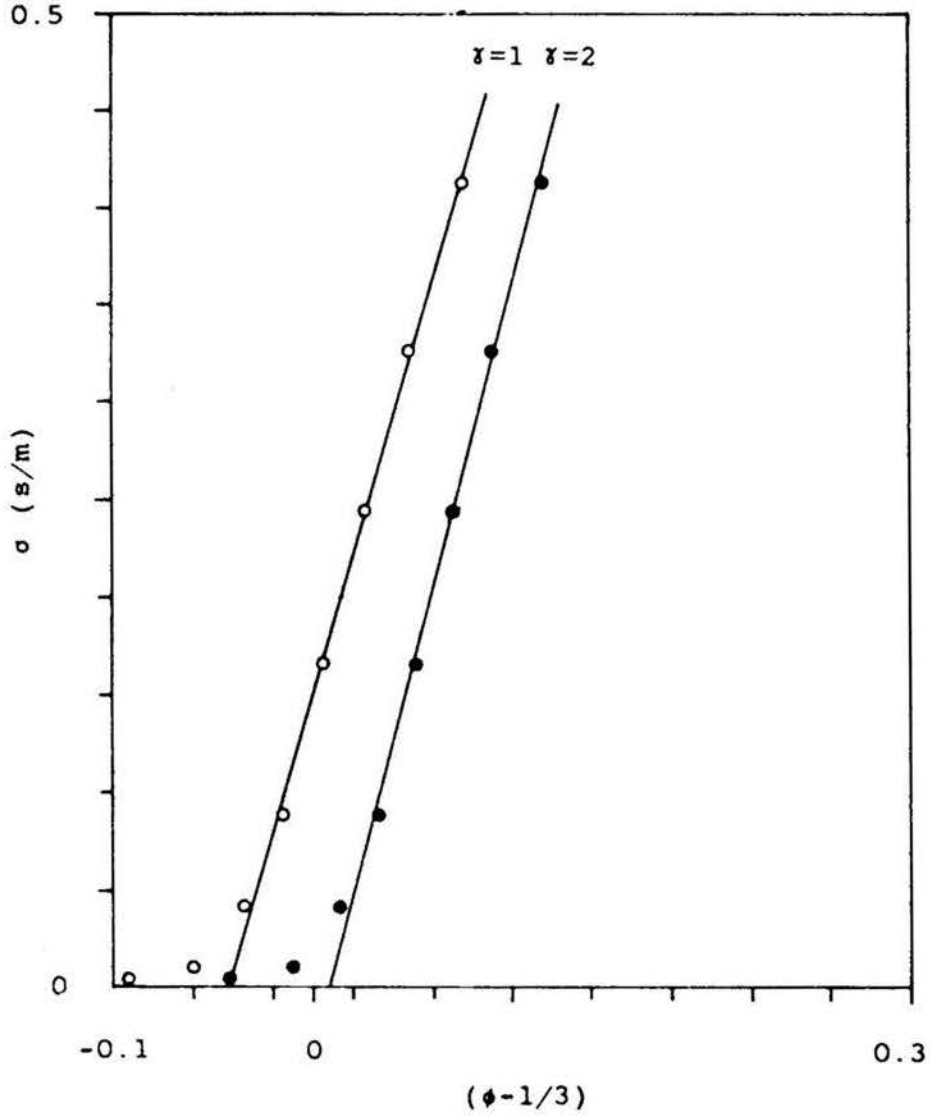

Figure 8. Conductivity, σ, versus (ϕ-1/3) for the system containing SDS, hexylamine(Ha), heptane(Hp), and water, with the weight ratio Hp/Ha = 50/50 and SDS/(Hp+Ha) = 20/80.

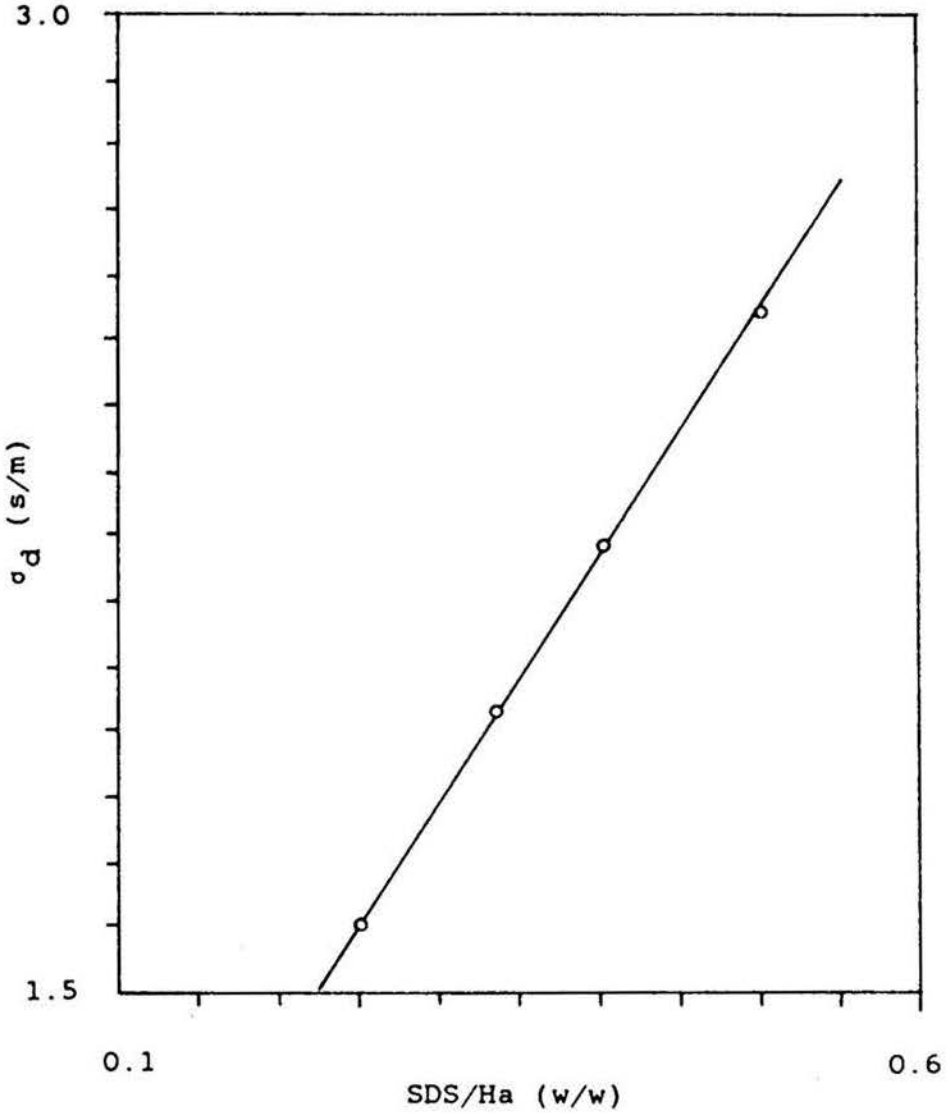

Figure 9. Conductivity of the disperse phase, σ_d, versus the weight ratio SDS/Ha for the microemulsion system with the weight ratio SDS/(Hp+Ha)=20/80.

larger whereas the number of them decreases due to clustering of small droplets so that it is possible to maintain the constant ratio of hexylamine to SDS in the interphase during the addition of water. The constancy of γ is actually in agreement with the result observed by Lagues and coworkers(6) and Shah et al.(16). A quantitative interpretation of this observation will be given later.

It is noted that the parameter γ increases when the ratio of hexylamine to SDS increases. For example, in Figs. 5 and 6, γ increases from about 2.0 to 3.5 when the ratio Ha/SDS changes from 60/20 to 63.75/15 for the systems with Ha/Hp equal to 75/25. This is understandable because, for a given amount of water (assume that the water droplet is spherical), the surface area of water cores is fixed if the system is monodisperse. To cover this area, more hexylamine molecules will be needed if there are not enough SDS molecules available. Since the area of the polar head of the hexylamine molecule is smaller than that of the SDS molecule, γ will increase rapidly with the ratio Ha/SDS. Similar results have been obtained for other systems with different ratios of Ha to (Ha + Hp). The increase in γ with increasing ratio Ha/SDS also explains the increase in σ_d with increasing SDS/Ha since SDS is ionic while hexylamine is largely nonionized and conduction is mainly due to SDS. For a droplet with a given radius, if there are more SDS molecules in the interphase, then there are fewer hexylamine molecules. Therefore the conductivity of the disperse phase, σ_d increases.

We mentioned above that the parameter γ is a constant when water content varies if the ratio SDS/Ha is kept constant and that the reason for this is due to the increase in water droplet size and to the decrease in droplet number. We now interpret this by quantitative calculations.

To evaluate the radius of water droplets, we assume that the microemulsions are monodisperse and the water cores are spherical. Thus the total volume of water droplets is given by

$$V_d = \frac{4}{3}\pi R^3 N_d \tag{6}$$

and the total surface area of these droplets is

$$A_d = 4\pi R^2 N_d \tag{7}$$

where R and N_d are the radius and number of water droplets, respectively. Combining these two equations gives

$$A_d = 3V_d/R = 3W_d/(R\rho_d) \tag{8}$$

On the other hand, A_d can be obtained from consideration of the polar head area of the amphiphilic molecules covering the surface of water cores, assuming that the interphase is a monolayer film. Thus

$$A_d = N_s N_A A_s + N_{Ha}^{int} N_A A_{Ha}$$

$$= N_s N_A (A_s + \gamma A_{Ha}) \tag{9}$$

where N_A is Avogadro's number, A_s and A_{Ha} the areas of the polar heads of an SDS and a hexylamine molecule, respectively.

Combine the last two equations to obtain

$$R = 3W_d/\{N_A\rho_d N_s(A_s + \gamma A_{Ha})\} \tag{10}$$

where

$$W_d = W_s + W_{Ha} + W_w$$

$$= N_s M_s + N_{Ha}^{int} M_{Ha} + W_w$$

$$= N_s(M_s + \gamma M_{Ha}) + W_w$$

Thus

$$R = \frac{3(M_s + \gamma M_{Ha} + W_w/N_s)}{N_A\rho_d(A_s + \gamma A_{Ha})}$$

$$= \frac{3\{M_s + \gamma M_{Ha} + (f_w/f_s)M_s\}}{N_A\rho_d(A_s + \gamma A_{Ha})} \tag{11}$$

where f_w and f_s have been defined in Eq.(5). From conductivity data fitted by the reduced effective medium formula, Eq.(4), the parameter γ can be obtained when the ratio of Ha to SDS is held constant. Then if the following values are taken(17),

$$\rho_d = 1.0 \text{ g/cm}^3$$

$$A_s = 35 \text{ Å}^2$$

$$A_{Ha} = 25 \text{ Å}^2$$

we can calculate the radius of the water droplets for each composition. The results of two sample calculations are shown in Fig. 10 for the system with SDS/(Ha+Hp) =20/80 and the system with SDS/(Ha+Hp) =15/85 while the ratio of hexylamine

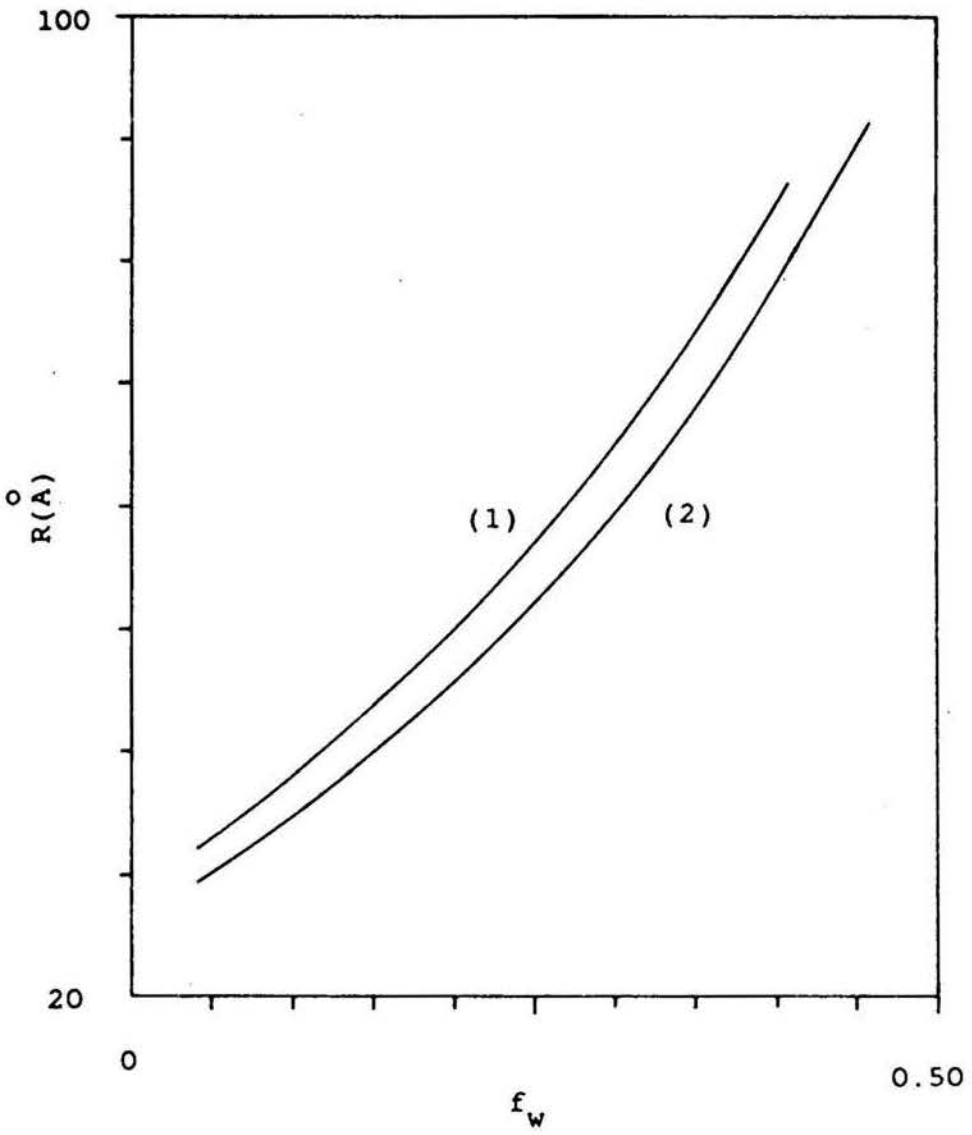

Figure 10. Calculated radius, R, of microemulsion droplets as a function of the weight fraction of water, f_w, for the system with the ratio Hp/Ha=20/80 and the ratio SDS/(Hp+Ha)=20/80 for curve (1) and 15/85 for curve (2).

to heptane is equal to 75/25 for both of the systems. These calculated results of microemulsion droplet sizes are in good agreement with those commonly reported in the literature (10,12). We see that the radius of the droplet is increasing with water weight fraction. Note that this radius increases more rapidly in the high water content range than in the low water content range.

It is easy to show that the number of water droplets per unit volume of microemulsions is given by

$$\tilde{N}_d = N_d/V_t = 3\phi/(4\pi R^3) \qquad (12)$$

Thus the total surface area of droplets per unit volume of microemulsion is

$$\tilde{A}_d = 4\pi R^2 \tilde{N}_d \qquad (13)$$

The calculated results of $\tilde{N}_d$ and $\tilde{A}_d$ for the systems corresponding to Fig. 10 are shown in Figs. 11 and 12. It is seen that $\tilde{N}_d$ decreases with water weight fraction , and $\tilde{A}_d$ decreases with water weight fraction almost linearly. This is because the decrease in $\tilde{N}_d$ outweighs the increase in radius. The general tendency of R and $\tilde{N}_d$ to change with water content is in agreement with the results obtained by Baker and co-workers for a different system using light scattering technique(5).

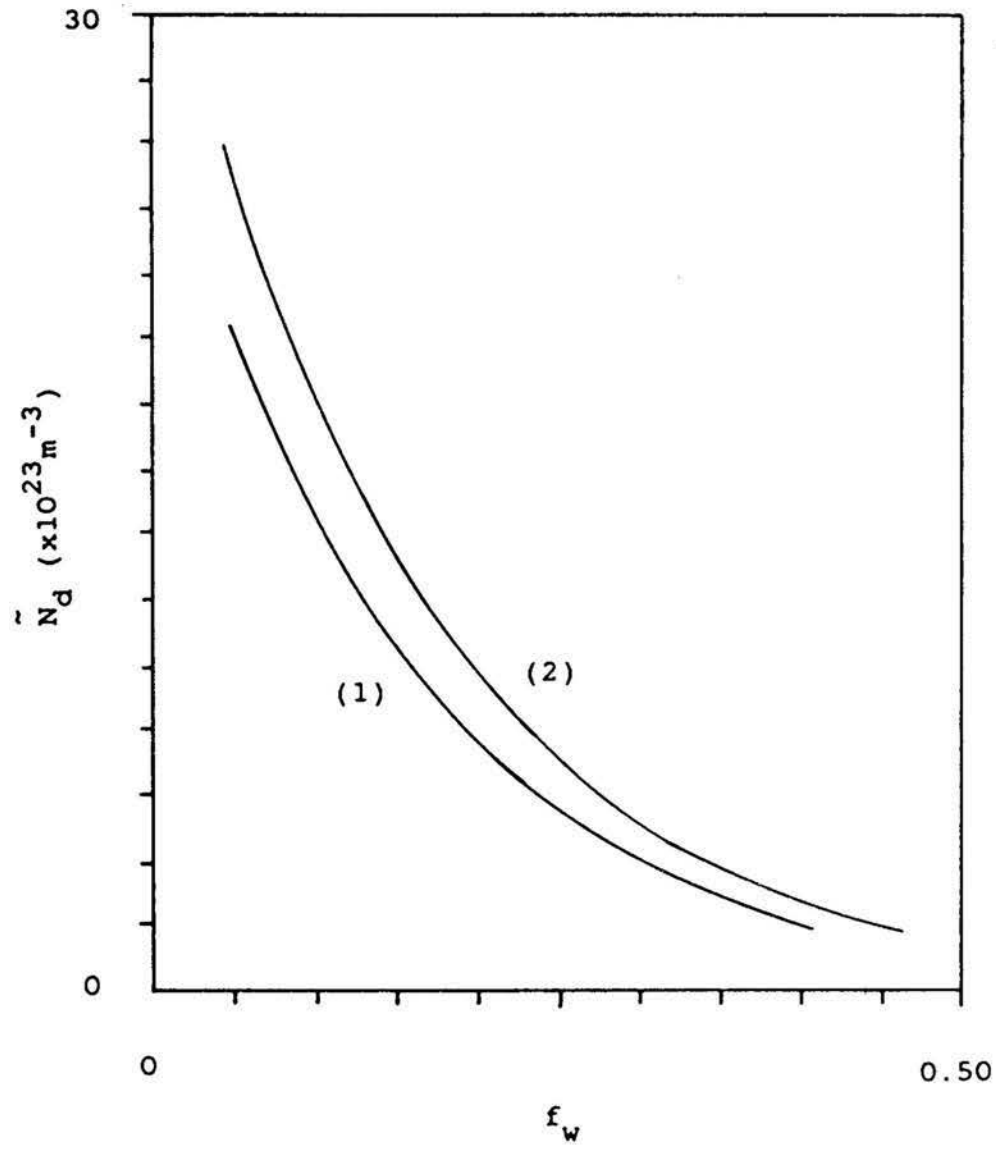

Figure 11. Variation of number of droplets per unit volume of microemulsions, $\tilde{N}_d$, with the weight fraction of water, f_w, for the system with the weight ratio Hp/Ha = 25/75 and SDS/(Hp+Ha) = 20/80 for curve (1) and 15/85 for curve (2).

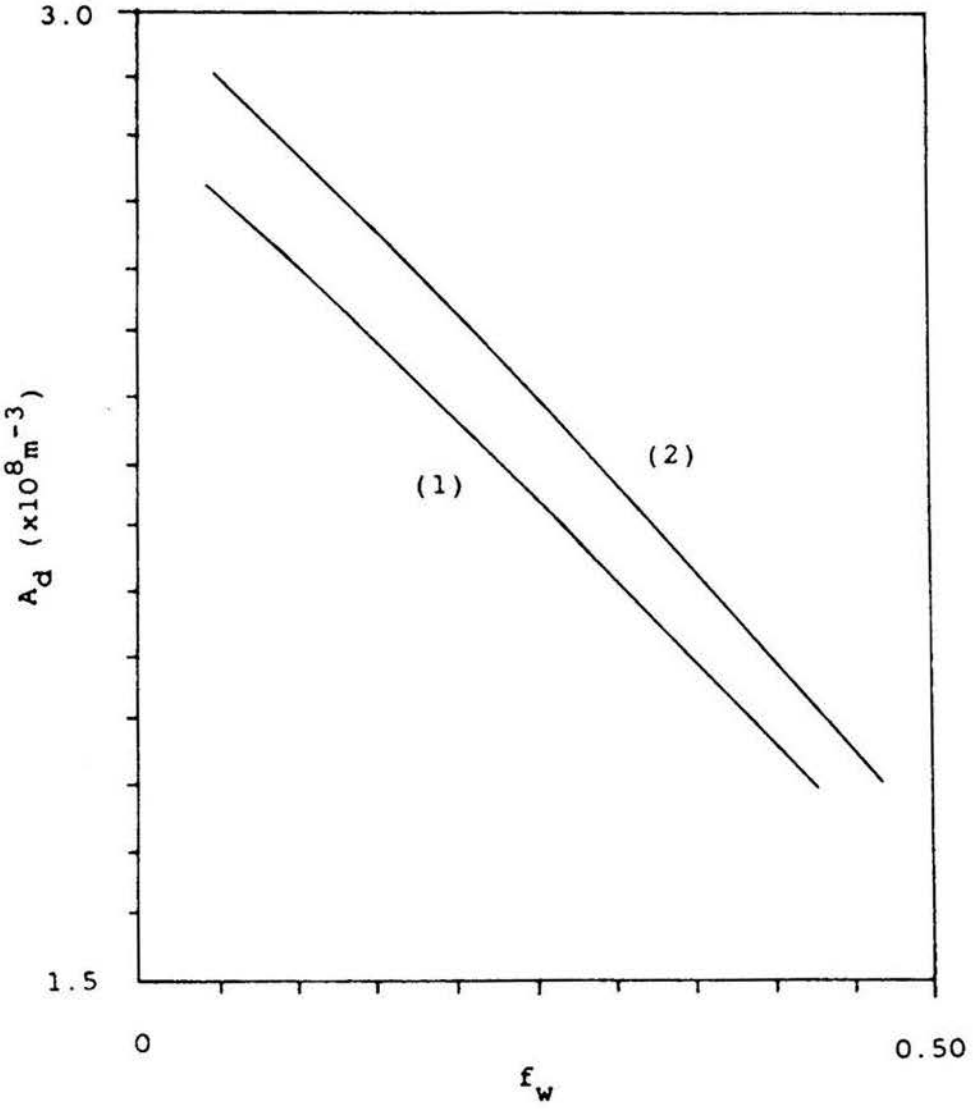

Figure 12. Variation of surface area of droplets per unit volume of microemulsions, $\tilde{A}_d$, with the weight fraction of water, f_w, for the system with the ratio Hp/Ha = 25/75 and SDS/(Hp+Ha) = 20/80 for curve (1) and 15/85 for curve (2).

SUMMARY

For the present microemulsion systems, conductivity behavior can be described by the percolation and effective medium theories. In particular, the important parameter γ of water droplet structure in microemulsions can be found by fitting the experimental data with the effective medium formula. The conductivity of the disperse phase can also be obtained. With the parameter γ known, approximate calculations of water droplet size, the number and surface area of droplets per unit volume of microemulsions are possible.

ACKNOWLEDGEMENTS

The authors are deeply grateful to Dr. Stig Friberg for many helpful discussions during the course of this work. They also want to express their appreciation to the University of Missouri for research support from the Weldon Spring Endowment Fund.

REFERENCES

1. Sjoblom, E., and Friberg, S., J. Colloid Interface Sci. 67, 16(1978).
2. Venable, R. L., Elders, K. L., Fang, Jiafu, J. Colloid Interface Sci. 109, 330(1986).
3. Lagourette, B., Peyrelasse, J., Boned, C., and Clausse, M., Nature 281, 60(1979).
4. Boned, C., Clausse, M., Lagourette, B., Peyrelasse, J., McClean, V. E. R., Sheppard, J., J. Phys. Chem. 84, 1520(1980).
5. Baker, R. C., Florence, A. T., Ottewill, R. H., and Tadros, Th. E., J. Colloid Interface Sci. 100, 332 (1984).
6. Lagues, M., Ober, R., and Taupin, C., J. Phys. Lett. (Paris) 39, L487(1978).
7. Clausse, M., Peyrelasse, J., Boned, C., Heil, J., Nicoles, L., Zradba, A., in "Solution Properties of Surfactants" (K. L. Mittal, Ed.), Plenum, New York, 1983.
8. Hanai, T., Kolloid-Z. 171, 20(1960).
9. Eicke, H.-F., and Denss, A., in "Solution Chemistry of Surfactants"(K. L. Mittal, Ed.), p.699. Plenum, New York, 1979.
10. Foster, K. R., Epstein, B. R., Jenin, P. C., and Mackay, R. A., J. Colloid Interface Sci. 88, 233(1982).

11. Kirkpatrick, S., Phys. Rev. Lett. 27, 1722(1971); Rev. Mod. Phys. 45, 574(1973).

12. Hoar, T. P., Schulman, J. H., Nature 152, 102(1943).

13. Landauer, R. R. J., J. Appl. Phys. 23, 779(1952).

14. Bottcher, C. J. F., Rec. Trav. Chim. 64, 47(1945).

15. Dvolaitzky, M., Guyot, M., Lagues, M., Le Pesant, J. P., Ober, R., Sauterey, C., and Taupin, C., J. Chem. Phys. 69, 3279(1979).

16. Shah, D. O., Bansal, V. K., Chan, K., and Hsieh, W. C., in "Improved Oil Recovery by Surfactant and Polymer Flooding"(Shah, D. O., and Schechter R. S., Eds.), Academic, New York, 1977.

17. Ekwall, P., in "Advances in Liquid Crystals"(G. H. Brown, Ed.), p.1. Academic, New York, 1975.

ARTICLE III

LAMELLAR LIQUID CRYSTAL AND OTHER PHASES IN THE SYSTEM SODIUM DODECYL SULFATE, HEXYLAMINE, WATER, AND HEPTANE

BY

Jiafu Fang and Raymond L. Venable
Department of Chemistry
University of Missouri-Rolla
Rolla, Missouri 65401

ABSTRACT

Phase equilibria have been studied for the system composed of sodium dodecyl sulfate, hexylamine, heptane, and water. Greatest emphasis has been placed on the lamellar liquid crystal region and low angle X-ray diffraction measurements. Equations are developed or modified to allow determination of the degree of penetration of water into the amphiphile double layer as a function of water or amphiphile concentration. It is found that the interfacial area occupied by the polar or ionic head groups of amphiphiles increases with increasing water content.

INTRODUCTION

As mentioned in two previous reports(1,2), the present system composed of sodium dodecyl sulfate(SDS), hexylamine(Ha), water and heptane(Hp), exhibits some novel properties, such as very high water solubilization into the microemulsion at a very low surfactant content. Emphasis in the early work was put on the association structures of the reverse micellar or microemulsion regions. Important structural parameters, such as the molecular ratio between SDS and Ha in the interfacial film of microemulsion droplets, and the size of these droplets, were estimated via conductivity measurements on these microemulsion systems. In the present work, special attention has been paid to the liquid crystal region. Experimental results obtained from low angle X-ray diffraction and phase equilibrium studies are reported.

Although general features of lyotropic lamellar liquid crystal structures are well known(3,4,5), information about the details of the structure, such as conformation of the carbon chains of amphiphile molecules, interactions among these molecules, solubilized hydrocarbon, and solvent, usually water, is not easy to obtain. Solubilized hydrocarbon may have a great deal of influence on the structure of liquid crystals. For example, in Friberg's picneering work (6) about the effect of solubilized hydrocarbons on the structure of lamellar liquid crystals, he and his coworkers pointed out

that addition of certain hydrocarbons to a particular liquid crystal may lead to a change in the angle between the normal to the bilayer interface plane and the molecular axis of the amphiphiles. In the present system, effects of solubilized hydrocarbon on the lamellar structure and the interactions between amphiphile and water molecules will be studied. Particularly, water penetration into the amphiphile bilayer is considered. A modified equation relating the interlayer spacing to water and amphiphile concentrations is derived. Thus it becomes possible to estimate the extent of water penetration at constant ratio of SDS to hexylamine plus heptane. If the measurements of the interlayer spacing are made at constant ratio of SDS to water, an approximate equation, which is also developed in this work, may be used to evaluate the limiting values of the thickness of the bilayer composed of pure SDS or of pure hexyamine.

Experimental

Materials. Hexylamine was purchased from Eastman Kodak (cat. no. 117 7559, 99%) and used as received. Heptane was from Fisher(cat. no.03008) and used without further purification. Sodium dodecyl sulfate(SDS) was purchased from BDH and recrystalized twice with absolute ethanol. Water was triple distilled.

Methods. Unlike the determination of reverse micellar or microemulsion regions, where the titration method is useful(1), determination of liquid crystal phases is more difficult and tedious mainly due to the high viscosities encountered. A quick search for the possible liquid crystal region could be done by titration and centrifugation, followed by microscopic examination between crossed polarizers. Then series of samples were prepared along lines radiating from each corner of the triangular phase diagram in the approximate boundary area of liquid crystal region, followed by centrifugation, long time storage, and careful microscopic examination. Lamellar and hexagonal liquid crystals can readily be distinguished from each other by their different microscopic patterns(3).

The normal micelle or L_1 region was determined in a similar way to that of the microemulsion or L_2 area, but centrifugation was required because of foam formation in this region. In order to locate the extremely narrow isolated, isotropic liquid phase(see Fig. 1), samples were prepared

with very small SDS concentration increments, down to 0.05%. Long time storage was also necessary.

X-ray diffraction patterns were determined using a Kiessig low angle camera from Richard Seifert(7). Ni-filtered Copper Kα radiation was used and the reflection measured by a Tennelec position sensitive detection system (Model PSD-100). A small amount of a liquid crystal sample was sucked into a thin wall glass capillary. Then the capillary with the two ends sealed was mounted on the sample holder for determination of the diffraction pattern. Bragg's law was used to calculate the interlayer spacing:

$$\lambda = 2d \sin\theta \qquad (1)$$

where $\lambda = 1.542$ Å and θ is the diffraction angle. For the camera used in this experiment, θ is calculated using the the following equation:

$$\tan(2\theta) = \frac{Z_c D_c}{2(PL+x)} \qquad (2)$$

where D_c (cm) is the measured distance between the two symmetric diffraction maxima, PL (mm) the path length from the sample to the detector, x (mm) the correction factor for the path length, and Z_c the conversion factor from the detector to the recorder. Z_c can be callibrated by measuring the powder diffraction pattern with a sample of known d-spacing.

Some comments about the preparation of liquid crystal samples for X-ray diffraction is in order. A liquid crystal sample was prepared by weighing the desired amounts of SDS,

hexylamine (or the mixture of hexylamine and heptane), and water into a test tube with a screw cap. The sample was then mixed on a vibromixer, followed by centrifuging with a microcentrifuge so that any solid SDS powder or liquid droplets sticking on the wall of the test tube collected on the bottom. Such procedure was repeated several times until the sample appeared homogeneous. A final centrifugation step was done with a high speed centrifuge so that all bubbles were driven out of the liquid crystal sample. Then the sample was thermostated for several hours to reach equilibrium in a water bath at 25^{o}C. If the sample was too thick to be mixed well on the vibromixer, a specially constructed glass tube was used. The tube with one end previously sealed had a constriction in the middle. SDS powder was first weighed into the tube, which was driven through the constriction into the bottom using a thin stick. Then two liquids were weighed into the tube. The open end of the tube was sealed with parafilm and the tube placed in a microcentrifuge with this end up so that all components were collected on the bottom after centrifugation, leaving the upper portion of the tube clean. Then the tube was quickly sealed with a flame. In this way no component would be decomposed or lost during sealing. Centrifugation of the sample back and forth through the constriction at a high speed causes thorough mixing and the liquid crystal sample becomes homogeneous.

RESULTS

Phase Equilibria. Fig. 1 gives the phase diagram for the system containing SDS, hexylamine, and water. The magnitude of the lamellar liquid crystal region is quite large. No other liquid crystal phase has been found in the system. It is interesting to note that there exists an extremely narrow isolated, optically isotropic liquid phase spanning from about 78% to 95% water, with an SDS content below 1.0%. This region is so narrow that it will appear only as a line in the lower left hand portion of the phase diagram. A solubility test of the oil soluble dye Sudan 4 in the three-phase area composed of the three isotropic liquid layers showed that the middle phase represented by the narrow isolated liuid phase, is probally an O/W type microemulsion (8), because the dye was very sparingly soluble in this layer. No further study of this phase has been attempted.

Low Angle X-Ray Diffraction Results. For most cases only the first diffraction line was observed although sometimes a much weaker second line was obtained. X-ray diffraction data for such systems are typically presented as plots of the d-spacing vs. the water weight fraction over the fraction of all other components(9-15). Results for the lamellar liquid crystalline region from Fig. 1, which contains no heptane (System A) are shown in Fig. 2. In Fig. 3 results are shown for System B where 5% heptane has been added to the hexylamine while Fig. 4 shows the results obtained with 10% heptane added to the hexylamine (System C).

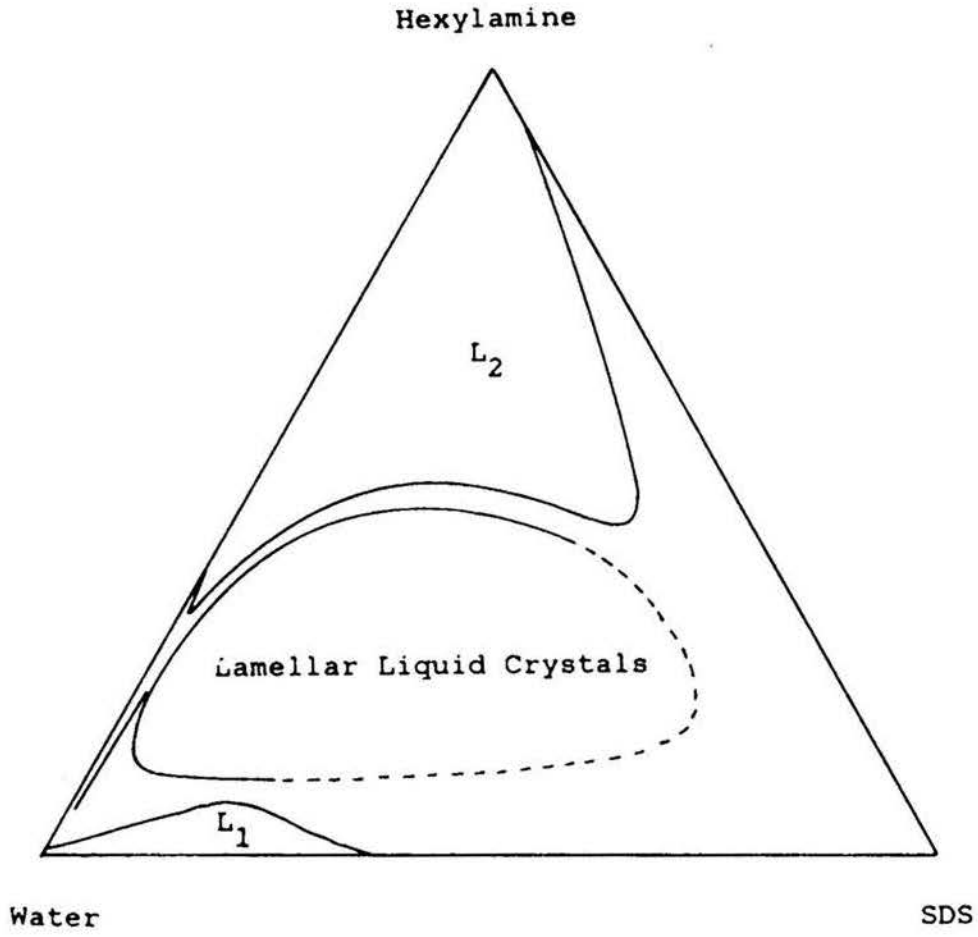

Figure 1. Phase diagram for the water-SDS-hexylamine showing the L_1 and L_2 phases, a lamellar liquid crystalline phase and a very small isotropic liquid phase.

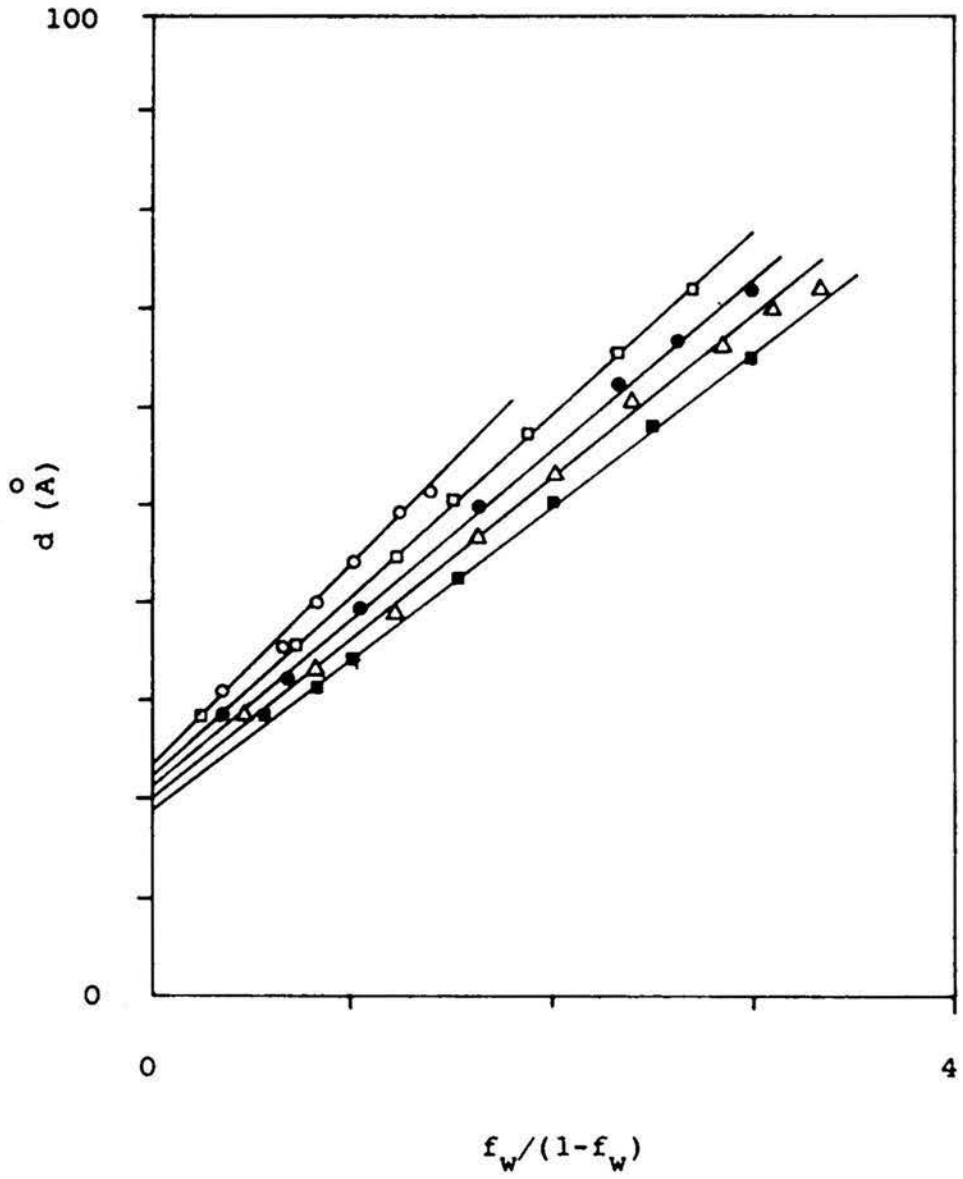

Figure 2. Interlayer spacing, d, vs the ratio of water weight fraction to the fraction of all other components, $f_w/(1-f_w)$, for System A(No heptane present). at weight ratios of SDS/Ha: O—70/30, □—60/40, ●—50/50, Δ—40/60, ■—30/70.

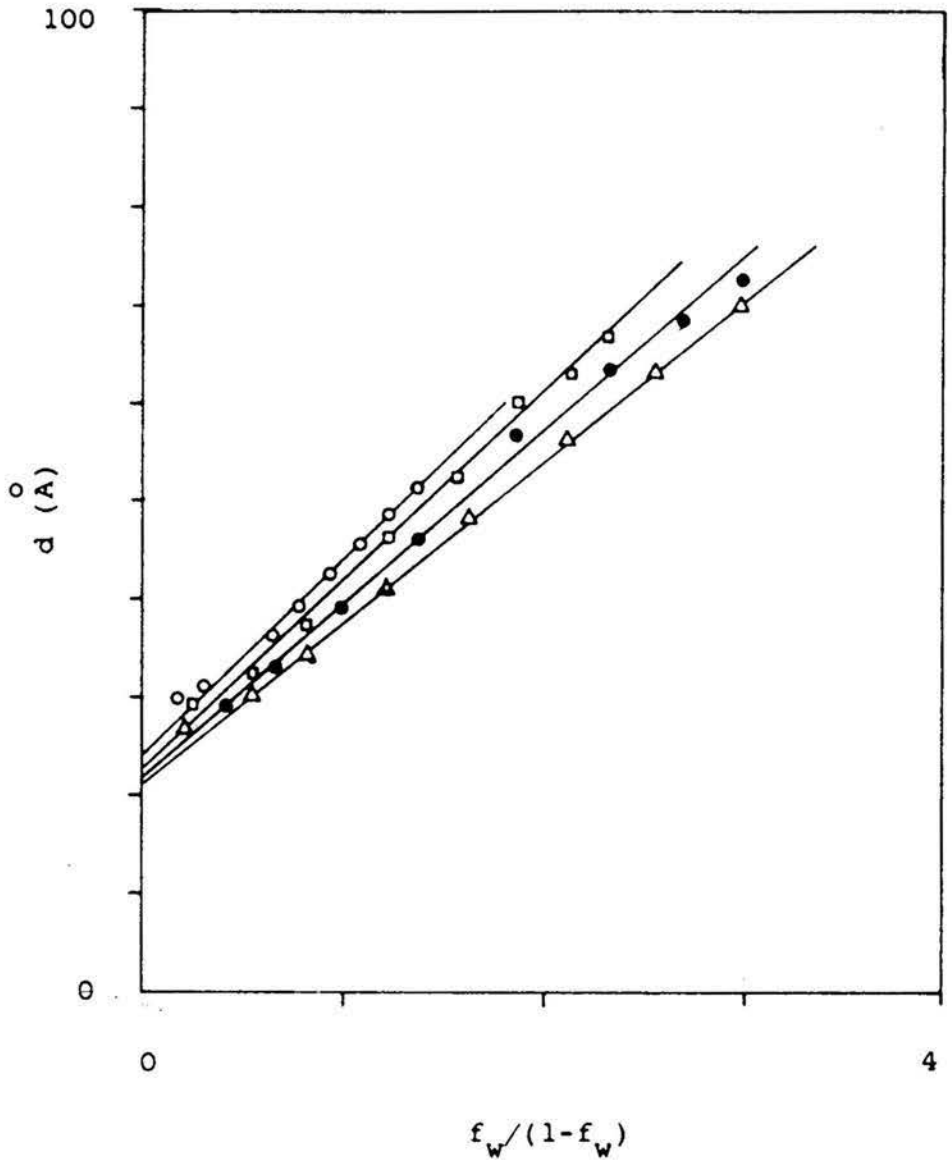

Figure 3. Interlayer spacing, d, vs the ratio of water weight fraction to the fraction of all other components, $f_w/(1-f_w)$, for System B(Hp/Ha= 5/95) at weight ratios of SDS/(Hp+Ha): O—70/30, ▫—60/40, ●—50/50, Δ—40/60.

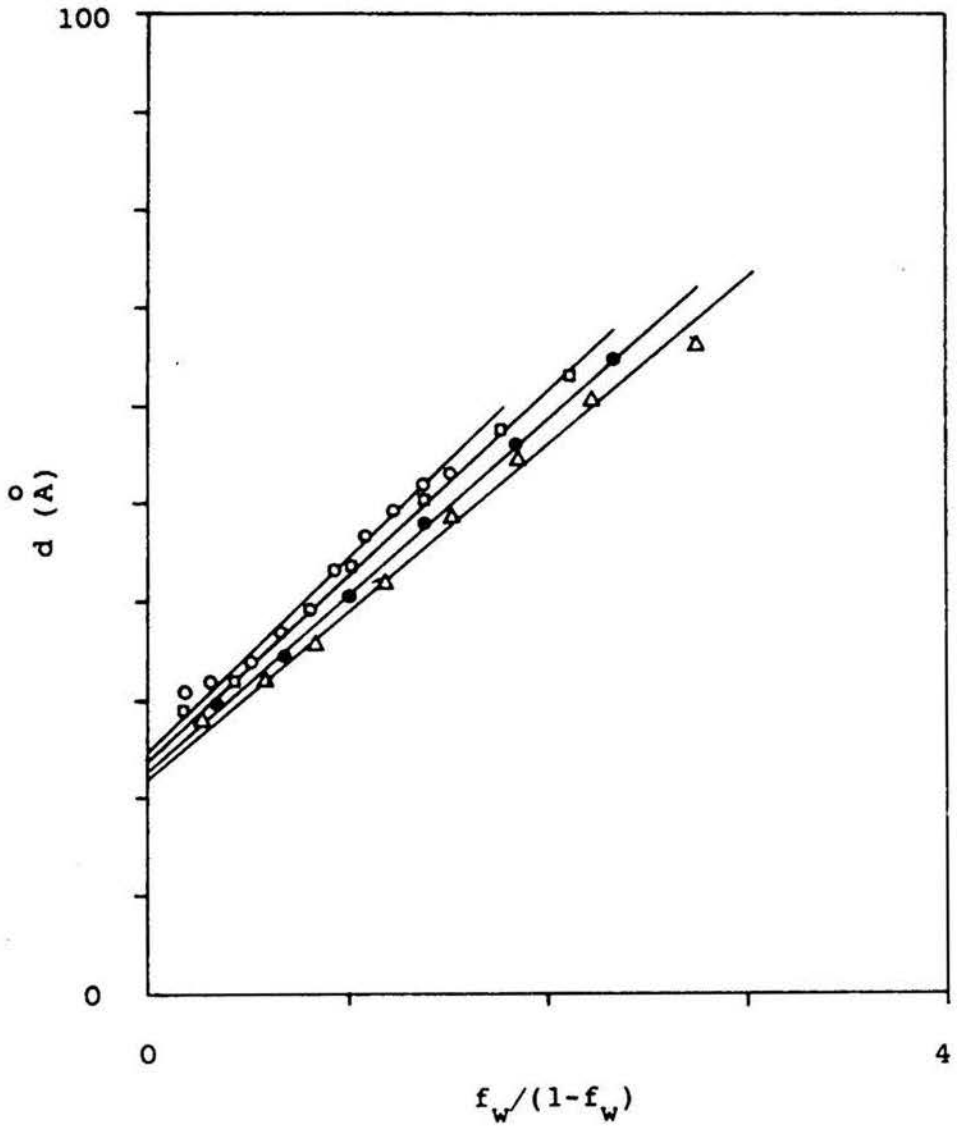

Figure 4. Interlayer spacing, d, vs the ratio of water weight fraction to the fraction of all other components, $f_w/(1-f_w)$, for System C(Hp/Ha= 10/90) at weight ratios of SDS/(Hp+Ha): O—70/30, □—60/40, ●—50/50, Δ—40/60.

DISCUSSION

It is well known (10-17) that the structure of lamellar liquid crystals of amphiphile-water systems consists of indefinitely expandable, parallel double layers of amphiphiles (plus solubilized hydrocarbon, if any) with layers of water intercalated between the amphiphile bilayers at regularly repeating distances. As a first approximation, one may assume no mutual penetration between the amphiphile bilayer and aqueous layer. All amphiphile molecules take such a position that their hydrocarbon chains lie in the interior of the double layer while the polar or ionic groups are anchored at the interface between the bilayer and aqueous layer and interact with water molecules. If hydrocarbon is dissolved into the liquid crystal, it must go to the interior of the amphiphile double layers. With the above picture of the lamellar liquid crystal structure, it is easy to derive an equation relating the interlayer spacing, d, to the concentrations of the constituents (9,16):

$$d = d_o/\phi_o \tag{3}$$

where d_o is the thickness of the amphiphile bilayer, and ϕ_o the sum of the volume fractions of the substances forming the double layer. The quantity ϕ_o is given by

$$\phi_o = \frac{n_s V_s + n_{Ha} V_{Ha} + n_{Hp} V_{Hp}}{n_s V_s + n_{Ha} V_{Ha} + n_{Hp} V_{Hp} + n_w V_w}$$

$$= \frac{n_o V_o}{n_o V_o + n_w V_w} \tag{4}$$

where V_i is the partial molar volume and n_i is the number of moles of component i and n_o is the total number of moles and V_o the mean partial molar volume of the organic components. The quantity ϕ_o may also be written as

$$\phi_o = 1/(1 + \frac{\upsilon_w}{\upsilon_o} \frac{f_w}{1-f_w}) \tag{5}$$

where f_w is the weight fraction of water in the system, υ_w is the partial specific volume of water and υ_o the mean specific volume of the constituents of the amphiphile bilayer of the organic components and is given by

$$\upsilon_o = V_o/M_o.$$

M_o is the corresponding average molecular weight of the constituents of the amphiphile bilayer given by

$$M_o = \frac{n_s}{n_s + n_{Ha}} M_s + \frac{n_{Ha}}{n_s + n_{Ha}} M_{Ha} \tag{6}$$

Substitution of Eq. (4) into Eq. (3) gives

$$d = d_o + d_o \frac{\upsilon_w}{\upsilon_o} \frac{f_w}{1-f_w} \tag{7}$$

If the X-ray diffraction measurements are made on systems obtained by adding water to the system at a constant ratio of

hexylamine to SDS, and if there is no penetration of the water into the amphiphile bilayer, or vice versa, then d_o, v_w, and v_o all remain constant. A plot of d versus $f_w/(1-f_w)$ should be a straight line whose slope is $d_o(v_w/v_o)$ and intercept at zero water concentration is d_o. Figs. 2, 3, and 4 gives such plots.

However, penetration of water into the amphiphile bilayer may not be neglected for the present system. One possible reason for this may be the fact that water is much more soluble in hexylamine than in medium chain length alcohols(16). There may also exist an appreciable solubility of SDS in the water layer. To show whether the mutual penetration between the amphiphile double layer and water layer exists, we need to examine Fig. 2, 3, and 4 closely. Before doing this, it is necessary to show that the volume of the system is additive so that the data treatment can be made much simpler.

If the volume is additive, we have

$$v = 1/\rho = \Sigma\ f_i v_i^o = \Sigma\ f_i/\rho_i^o \qquad (8)$$

where v_i^o is the specific volume of component i, v is the specific volume of the system, f_i is the weight fraction of i, and ρ and ρ_i^o are the densities of the sample and pure component i, respectively. Thus, based on the assumption that volumes are additive, ρ can be calculated and compared with the experimental values if the density of each component in the system is known. The calculated density should not deviate

much from the experimental one. This comparison is made on some microemulsion systems instead of liquid crystals because the high viscosity of the liquid crystalline phase makes density measurements very difficult. Fig. 5 shows the variation of the ratio between the experimental and calculated densities, ρ_e/ρ_c, with the water weight fraction for some microemulsion systems. It is seen from Fig. 5 that the discrepancy first increases when f_w is small, then reaches some small and almost constant value. The effect of heptane is to decrease the discrepancy between ρ_e and ρ_c. As shown in Fig. 6, it seems that the effect of increasing the ratio SDS/Ha (w/w) is also to reduce this discrepancy. The small positive density deviation means that there is a contractive volume effect upon formation of the microemulsion. The statement that the volumes in the microemulsion region are additive is justified. We extend this conclusion to the liquid crystal region with confidence since Fig. 6 shows that increasing the ratio SDS/Ha (w/w) lowers the deviation, and the liquid crystal region appears at higher ratios of SDS/Ha than does the microemulsion region.

Thus in Eq.(7), v_w/v_o can be replaced by

$$\frac{v_w}{v_o} = \frac{1/\Sigma f_i'/\rho_i}{\rho_w} \qquad (9)$$

where f_i' is the weight fraction of component i in the mixture constituting the amphiphile double layer (SDS, Ha, and Hp).

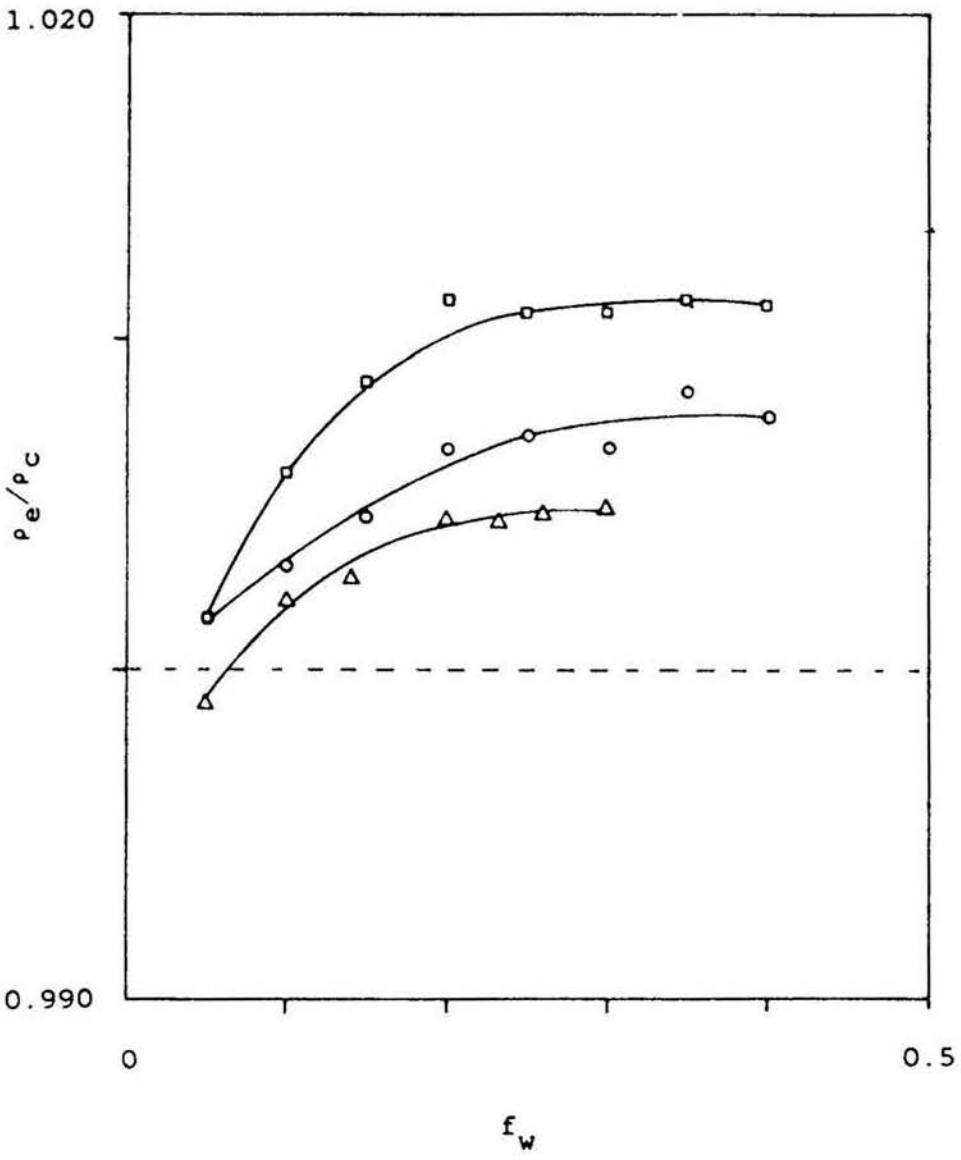

Figure 5. Ratio of experimental to calculated density, ρ_e/ρ_c, vs water weight fraction, f_w, in the microemulsion or L_2 region for systems with the weight ratio SDS/(Hp+Ha)=20/80 and the ratio Hp/Ha: □—0/100, O—25/75, Δ—50/50.

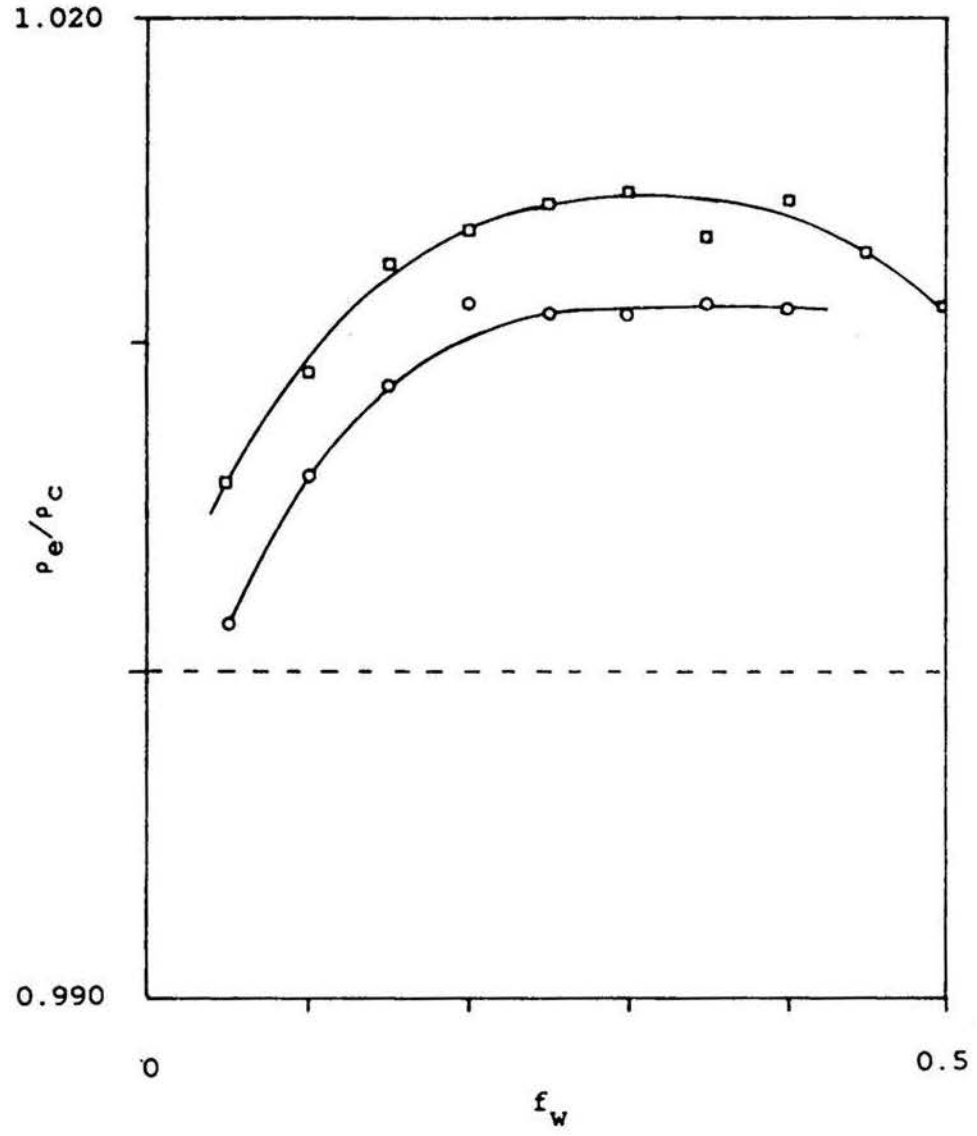

Figure 6. Ratio of experimental to calculated density, ρ_e/ρ_c, vs water weight fraction, f_w, in the microemulsion or L_2 region for systems with the weight ratio SDS/Ha: ▫—10/90, O—20/80 while Hp/Ha = 0.

TABLE I

Comparison of (v_w/v_o) between Experimental and Calculated Values, and Values of the Proportionality Constant b of Eq. (11).

System A: Hp/Ha = 0					
SDS/Ha	30/70	40/60	50/50	60/40	70/30
$(v_w/v_o)_e$	0.803	0.750	0.749	0.772	0.795
$(v_w/v_o)_c$	0.853	0.887	0.923	0.963	1.006
b	0.060	0.184	0.230	0.245	0.250

System B: Hp/Ha = 5/95				
SDS/(Ha+Hp)	40/60	50/50	60/40	70/30
$(v_w/v_o)_e$	0.744	0.737	0.764	0.748
$(v_w/v_o)_c$	0.881	0.915	0.958	1.003
b	0.187	0.240	0.280	0.316

TABLE I (continued)

	System C: Hp/Ha = 10/90			
SDS/(Ha+Hp)	40/60	50/50	60/40	70/30
$(v_w/v_o)_e$	0.719	0.772	0.733	0.707
$(v_w/v_o)_c$	0.877	0.915	0.950	1.000
b	0.121	0.181	0.290	0.266

If mutual penetration between the amphiphile bilayer and water layer in the liquid crystal were negligible, the ratio v_w/v_o obtained from the slope of a plot of d vs. $f_w/(1-f_w)$ should be close to the value calculated based on the assumption of no penetration and should increase with increasing the ratio of SDS/(Ha+Hp). This should be so because SDS has the highest density, 1.16 g/cm^3(18), of any of the components of the system, and the specific volume of the bilayer, v_o, should become smaller when the SDS content increases. Table I compares the experimental with calculated values of v_w/v_o, and two important facts are seen. First, the calculated value is always greater than the experimental one. Second, there is no obvious tendency for v_w/v_o to increase with increasing the ratio of SDS/(Ha+Hp), and in some cases it even decreases. Such results may be expected if water penetration into the amphiphile bilayer occurs.

Considering water penetration into the bilayer and assuming a negligible solubility of the amphiphiles in the aqueous layer, Eq. (7) can be modified as follows. Because of the penetration of water, the actual volume fraction of the amphiphile bilayer, designated ϕ_b, must include a factor representing the penetration. Thus

$$\phi_b = \phi_o(1 + x) \qquad (10)$$

where ϕ_o is the volume fraction of the bilayer without water penetration and x a factor giving the effect of this penetration. When there is no water penetration, x must be

equal to zero, so $\phi_b = \phi_o$. As a first approximation, we further assume that the water penetration into the bilayer is proportional to the water content in the liquid crystal, that is,

$$x = bf_w \tag{11}$$

where b is a proportionality constant. Thus

$$\phi_b = \phi_o(1 + bf_w)$$

which upon substitution of Eq. (5) becomes

$$\phi_b = (1 + bf_w)/(1 + \frac{v_w}{v_o} \frac{f_w}{1-f_w}) \tag{12}$$

Substitue Eq. (12) into Eq. (3) to obtain

$$d = d_o\left[(1 + \frac{v_w}{v_o} \frac{f_w}{1-f_w})/(1 + bf_w)\right] \tag{13}$$

Therefore a straight line passing through the origin and with a slope equal to d_o should be observed if d is plotted against the quantity in the brackets and the parameter b is chosen properly. Figs. 7, 8, and 9 show such plots for the three series of liquid crystals corresponding to Fig. 2, 3, and 4. It is seen that for the present systems, the straight line has an intercept on the d axis greater than zero if b is chosen to be zero. This means that water penetration into the bilayer has occurred, that is, a positive value of b must be chosen to give a zero intercept of the straight line. On the other hand,

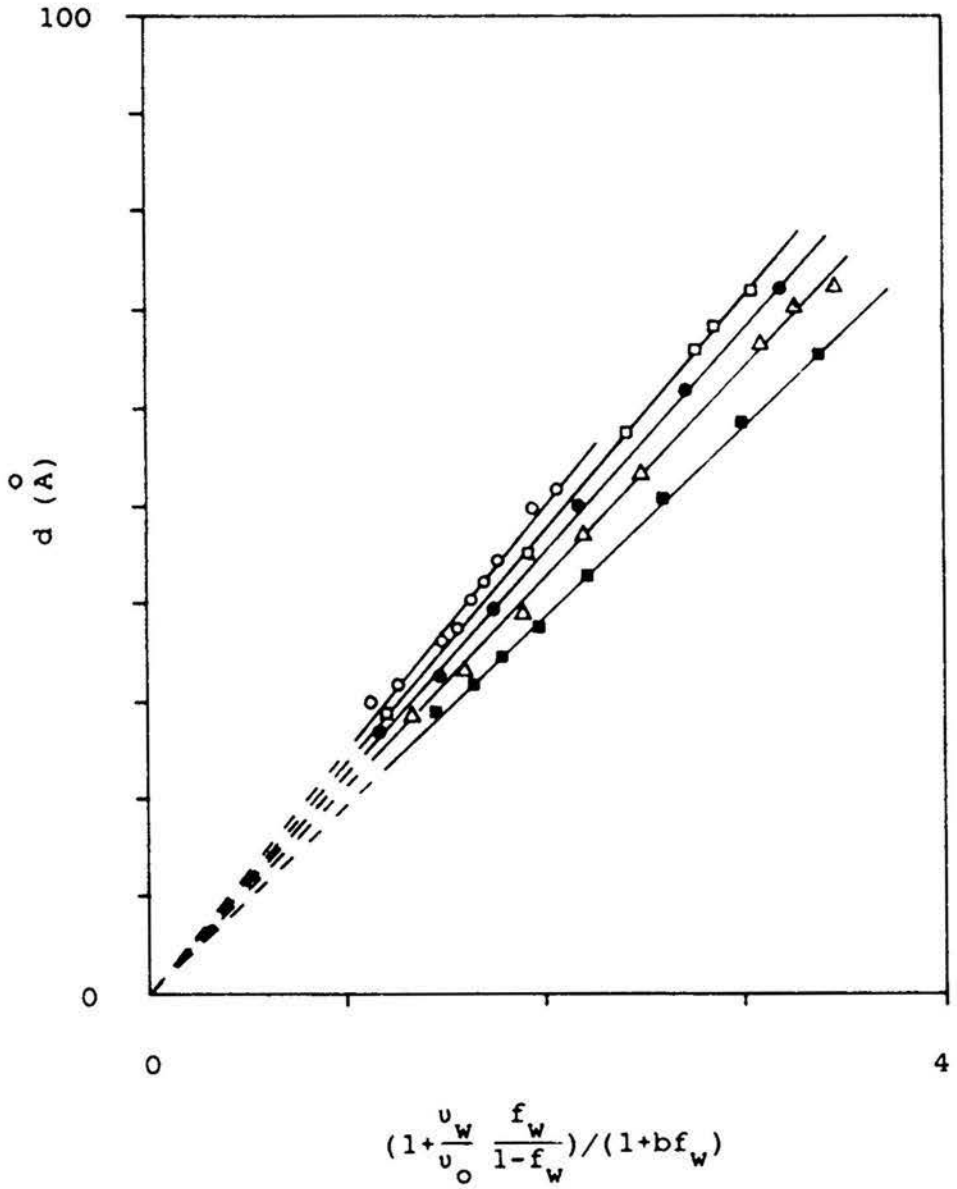

Figure 7. Interlayer spacing, d, plotted according to Eq. 13 for System A with the ratio of SDS/Ha: O—70/30, □—60/40, ●—50/50, Δ—40/60, ■—30/70.

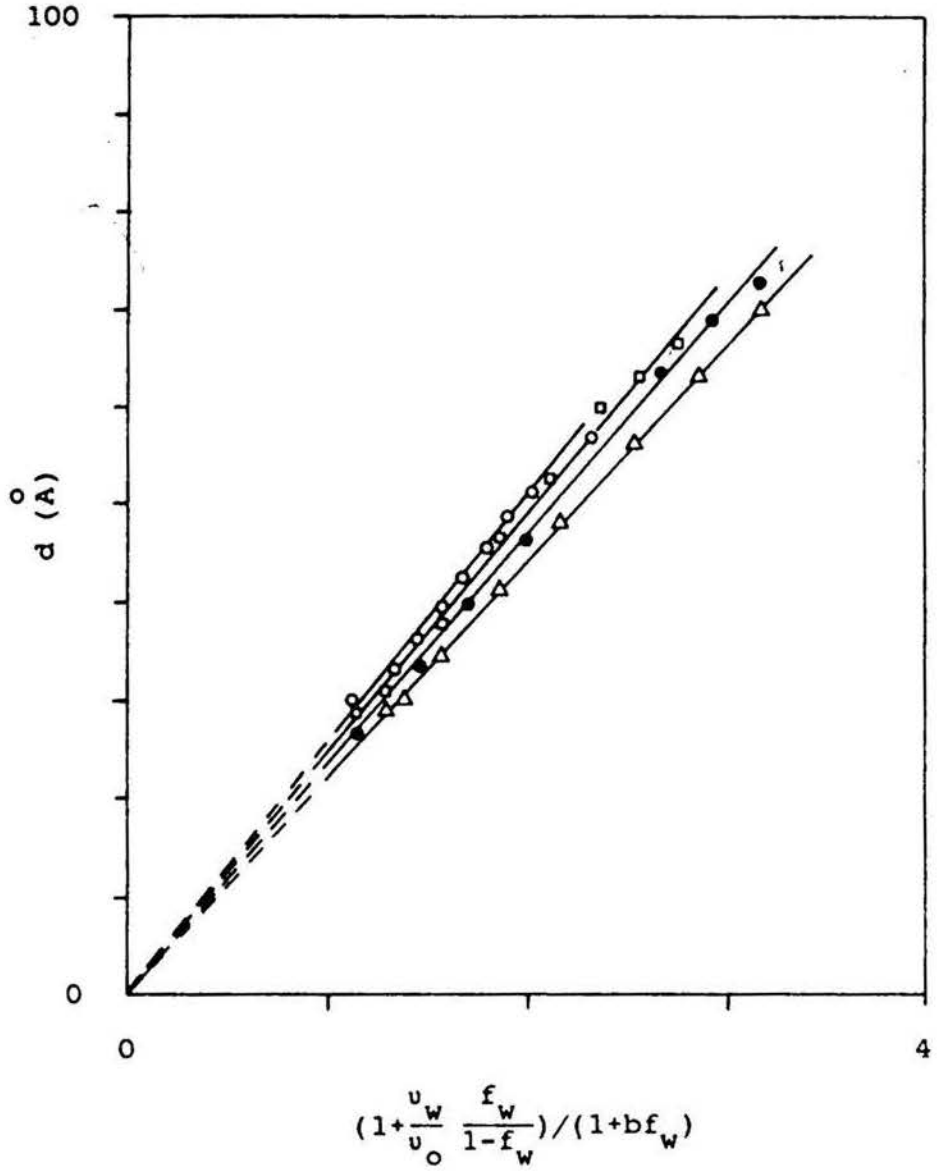

Figure 8. Interlayer spacing, d, plotted according to Eq. 13 for System B with the ratio of SDS/(Hp+Ha): O—70/30, □—60/40, ●—50/50, Δ—40/60.

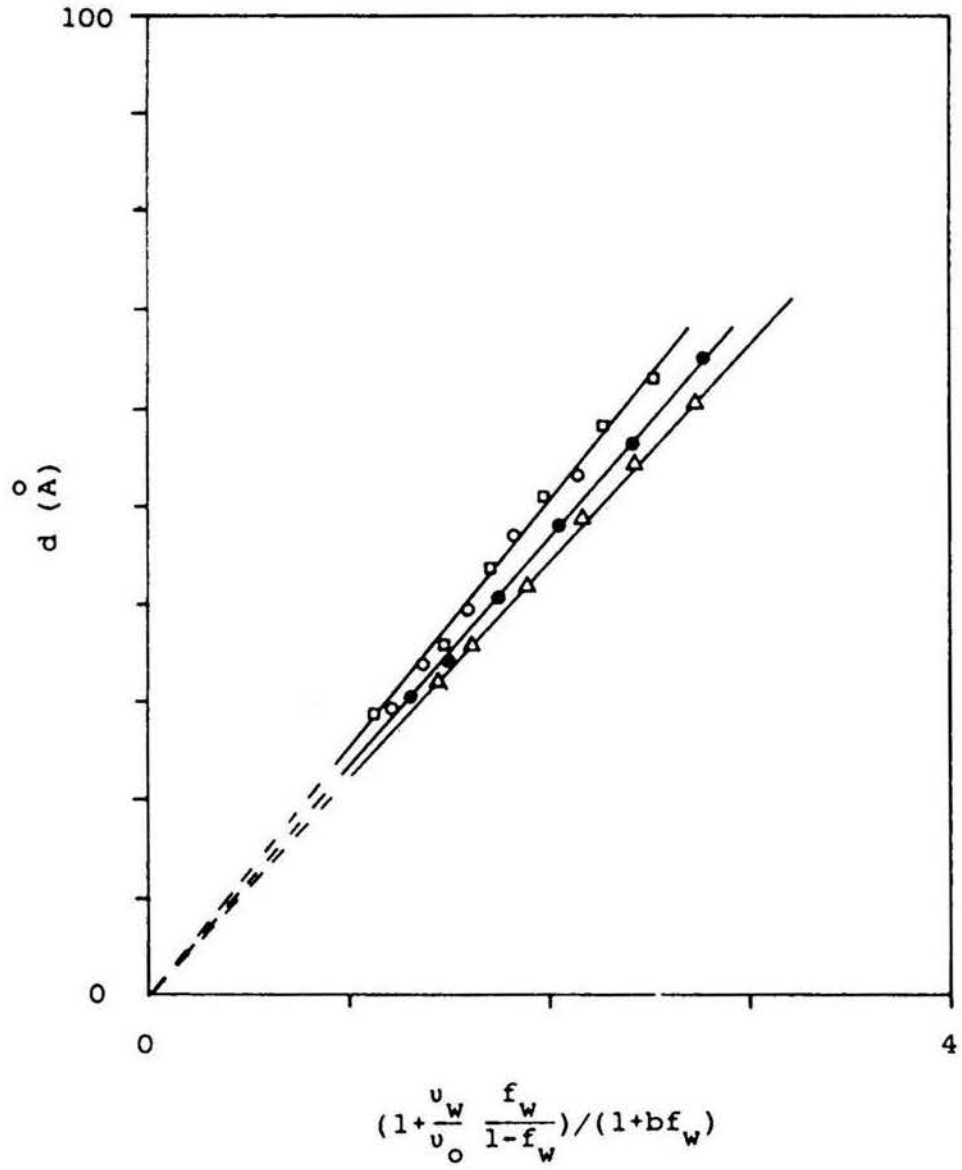

Figure 9. Interlayer spacing, d, plotted according to Eq. 13 for System C with the ratio of SDS/(Hp+Ha): O—70/30, □—60/40, ●—50/50, Δ—40/60.

if the dissolution of the amphiphiles into the aqueous layer surpassed the water penetration into the bilayer, a negative value of b would be chosen. The values for the three series of systems are given in the last line for each system in Table I. Fig. 10 shows the thickness of the bilayer at zero water concentration, d_o, versus the molar ratio hexylamine to SDS. These b and d_o values are obtained from Figs. 7, 8, and 9 using the linear least squares method.

From Table I it is seen that, when the molar ratio of SDS to hexylamine is low, the value of b is small. This value increases rapidly with this ratio at first and then more slowly. This is particularly obvious for the tertiary system A, which contains no hydrocarbon. When the liquid crystal contains a small amount of heptane (System B), the water penetration into the bilayer seems to be enhanced because a larger value of b must be used in order to make the straight line in Fig .7, 8, and 9 pass through the origin. This means that the presence of a small amount of heptane enhances the interactions between water and amphiphile molecules for these systems. A related result has been observed in the microemulsion region, where the addition of a small amount of heptane to the reverse micellar region at a SDS concentration increases the water solubilization into the microemulsion drastically (2). It may be expected, however, that because of the hydrophobic nature of hydrocarbon, further increase in content of heptane will eventually lead to weakening the interactions between water and amphiphile molecules so that

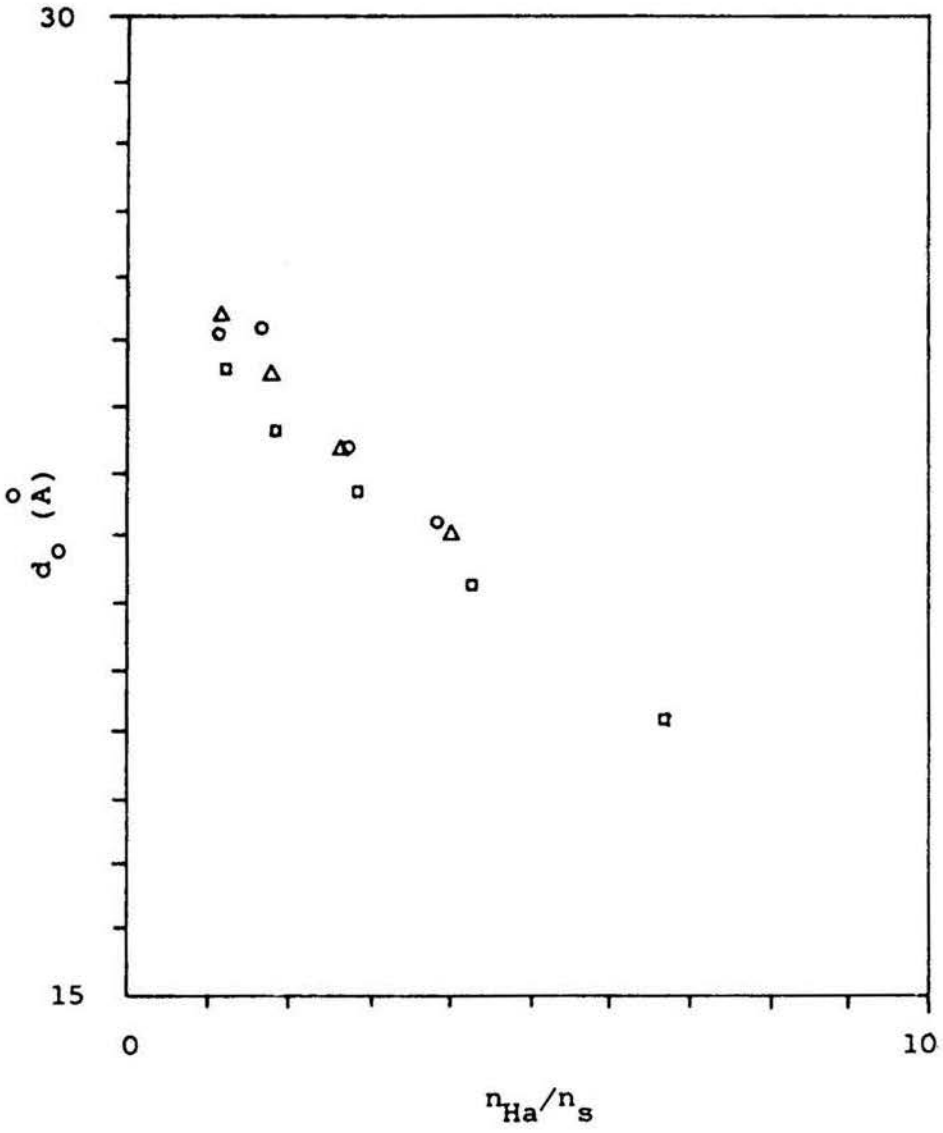

Figure 10. Bilayer thickness, d_o, as a function of the molar ratio of hexylamine to SDS, n_{Ha}/n_s, for: □—System A, Δ—System B, O—System C.

the water penetration into the amphiphile double layer decreases (7). This begins to be observed for System C in which the weight ratio Ha/Hp is 10/90.

It is obvious from Table I that, for all three series of systems, increase in SDS concentration causes an increase in water penetration into the bilayer. Since SDS is an ionic surfactant, its interactions with water should be expected to be stronger than those of the polar, but neutral, hexylamine molecule. We will also see this effect in a later section dealing with the average interfacial area per polar group of amphiphilic molecules.

Fig. 10 shows the plot of the interlayer spacing at zero water concentration, d_o, versus the molar ratio hexylamine to SDS. The effect of this ratio is pronounced as d_o decreases almost linearly with increase in the ratio. Since the hexylamine molecules are shorter than SDS molecules, there is more space available for the tails of SDS molecule to move around and assume less extended configurations as the molar ratio of hexylamine to SDS increases. Therefore the thickness of the bilayer on average will decrease.

Fig. 10 also shows the effect of solubilized hydrocarbon on the interlayer spacing at zero water concentration. A solubilized hydrocarbon molecule can either locate in the center of the bilayer and move around since it is in a liquid state and highly disordered (7,15,19-23), or penetrate into the array of hydrocarbon chains of the amphiphiles. For the former case, an increase in interlayer spacing would be

expected. For the latter, little or no increase in interlayer spacing would occur. From Fig. 10 we see that a small amount of solubilized heptane in the liquid crystal causes an increase in interlayer spacing at zero water concentration. That is, there certainly exist non-penetrating heptane molecules.

Measuring the interlayer spacing at constant ratios between SDS and hexylamine plus heptane makes data treatment easy because the thickness of the bilayer is constant during the addition of water to the system. We also did the measurements keeping the weight ratio of SDS to water constant and varying the concentration of hexylamine. Although such measurements make data treatment more complicated because the thickness of the bilayer is no longer constant, we can look further into the effect of hexylamine content on the bilayer structure. According to the above analysis, one may expect a decrease in interlayer spacing upon the addition of more hexylamine to the liquid crystal. This is seen from Fig. 11, in which the effect of water concentration is also obvious. However, the more important thing in making measurements under this condition is to extract some new information from the experimental results. By proposing a linear relation of the thickness d_o of the amphiphile bilayer to the volume fraction of hexylamine in the bilayer, we will show that it is possible to estimate the thickness of the bilayer of pure SDS or of pure hexylamine.

For the ideal case, we may assume that neither water penetration into the bilayer nor dissolution of the

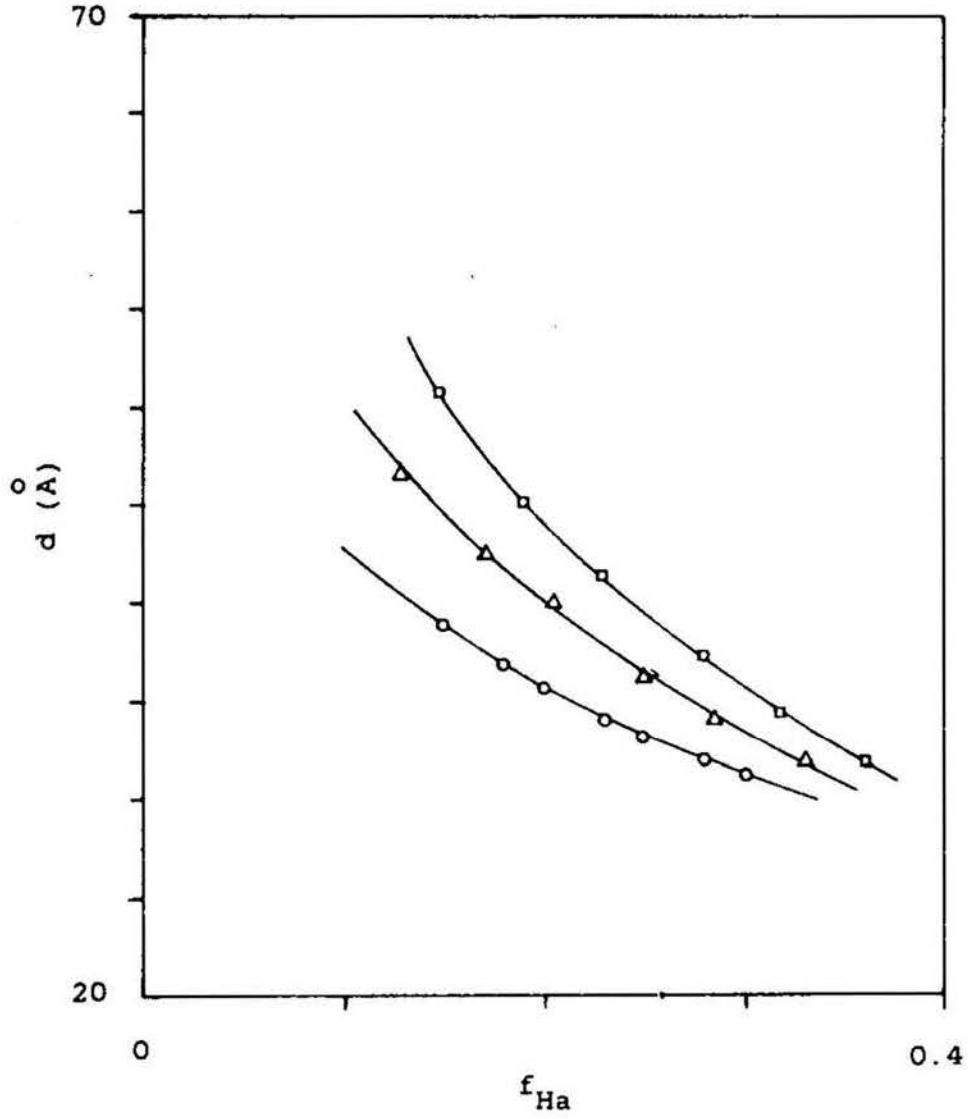

Figure 11. Interlayer spacing, d, vs weight fraction of hexylamine, f_{Ha}, for System A for the weight ratio of SDS/H_2O: □—30/70, Δ—40/60, O—50/50.

amphiphiles into the aqueous layer is appreciable. Under the condition of constant ratio between SDS and water, variation of hexylamine concentration and therefore the molar ratio n_s/n_{Ha} in the system, will cause the thickness of the amphiphile bilayer ,d_o, to change. In order to relate this variation of d_o to the concentration of SDS and hexylamine, let us first consider the limiting cases. If there were no hexylamine present, the thickness of the bilayer would be equal to twice the length of the SDS molecules, which may take any particular conformations. We designate this thickness as d_s^o. On the other hand, if the volume fraction of SDS in the double layer was equal to zero, the bilayer thickness, d_{Ha}^o, would be twice the length of hexylamine molecules. Their conformations would be associated with the condition at which the extrapolation is made. The following equation satisfies these limiting conditions:

$$d_o = d_s^o \phi_s' + d_{Ha}^o \phi_{Ha}' \tag{14}$$

where ϕ_s' and ϕ_{Ha}' are the volume fraction of SDS and hexylamine in the double layer only. Therefore

$$\phi_s' + \phi_{Ha}' = 1 \tag{15}$$

and

$$d_o = d_s^o - (d_s^o - d_{Ha}^o)\phi_{Ha}' \tag{16}$$

Substitution of this equation into $d = d_o/\phi_o$ gives

$$d\phi_o = d_s^o - (d_s^o - d_{Ha}^o)\phi'_{Ha} \qquad (17)$$

For the ideal case where no mutual penetration occurs between the bilayer and aqueous layer, ϕ_o is given by Eq.(4). With the assumption that the volume of the liquid crystal system is additive, ϕ_o and ϕ'_{Ha} can be calculated readily. Eq.(17) should give a straight line if $d\phi_o$ is plotted versus ϕ'_{Ha}. Thus the value of d_s^o may be obtained by determining the intercept after extrapolating to zero hexylamine concentration. The slope of such a plot gives $-(d_s^o-d_{Ha}^o)$. Therefore, d_{Ha}^o can be obtained either by combination of the intercept with the slope or by extrapolation to $\phi'_{Ha}=0$. These results are presented in Fig. 12, where a linear relation does exist if ϕ'_{Ha} is not taken close to the boundary of the liquid crystal region. From Eq.(17) it is expected that the straight line should be independent of the ratio between SDS and water. However, some deviation from this is seen in Fig. 12. The line at the weight ratio SDS/H_2O equal to 40/60 is very close to that at SDS/H_2O = 50/50, but the line with SDS/H_2O = 30/70 is obviously lower than the other two. This deviation might result from the nonideality of the liquid crystal system due to a different extent of water penetration at different ratios between SDS and water.

Information about the mean interfacial area per polar group of amphiphile molecules can be derived from the measurement of the interlayer spacing of the liquid crystal if some appropriate approximations are made. Here again we

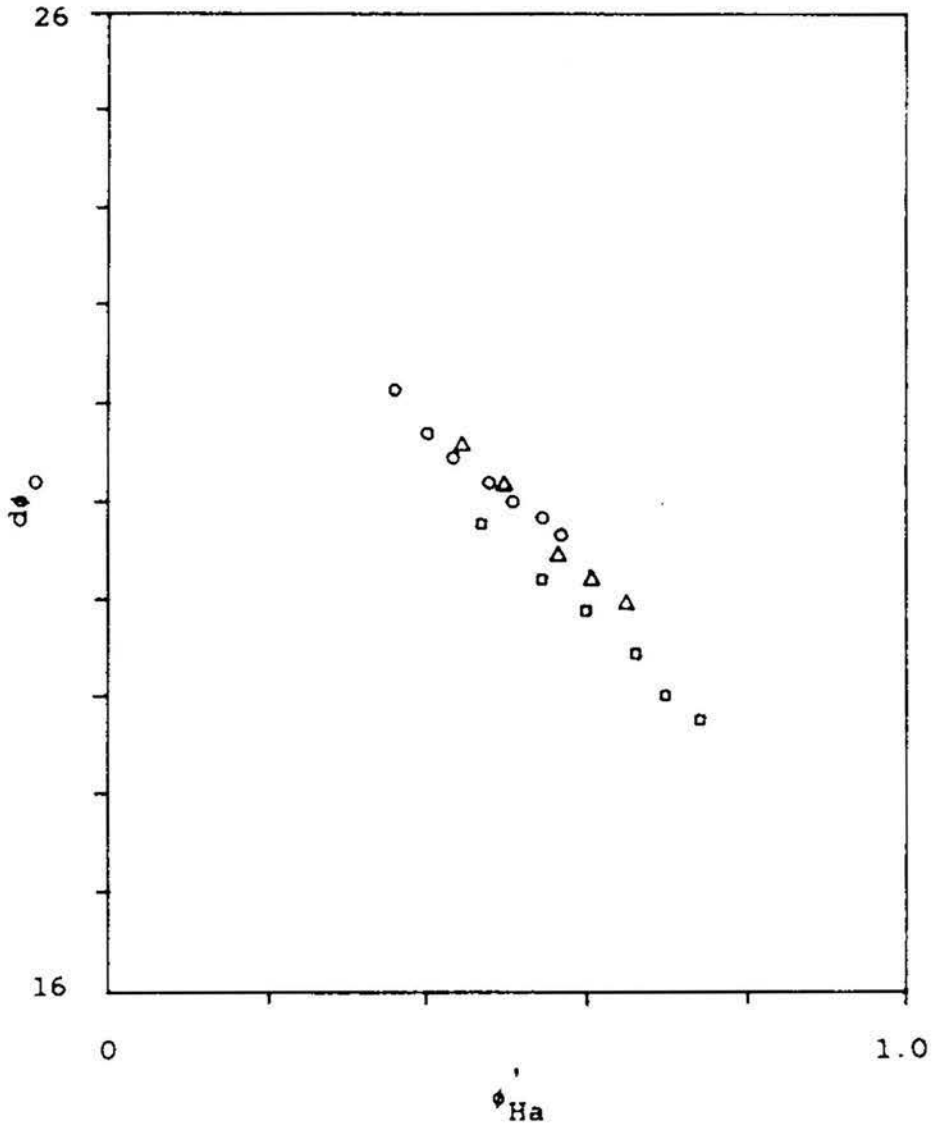

Figure 12. Plots of $d\phi_o$ vs ϕ'_{Ha}, according to Eq. 17 for System A at the weight ratio of SDS/H_2O: □—30/70, Δ—40/60, O—50/50.

assume that no penetration occurs between the aqueous layer and the amphiphile bilayer and all hydrocarbon is incorporated within the interior of the bilayer. With these assumptions it is easy to derive an equation to calculate the average area per polar group for the lamellar liquid crystal(16,17).

$$S = \frac{2M_o(\upsilon_o + R_H\upsilon_H + R_w\upsilon_w)}{N_A d} \qquad (18)$$

where M_o is given by Eq. (6), and

$$R_H = f_{Hp}/(f_{Ha} + f_s)$$

$$R_w = f_w/(f_{Ha} + f_s)$$

and υ_i is the specific volume of component i, N_A Avogadro's number, and d the measured interlayer spacing. The average interfacial area per polar group of amphiphile molecules versus the molar ratio between water and the sum of SDS plus hexylamine for the three series of systems are presented in Figs. 13, 14, and 15. In these figures the curves were calculated from computer fitted graphs of log(d) vs. log(ϕ_o). From these figures, some conclusions can be drawn.. First, the mean interfacial area per polar group of the amphiphiles increases with the molar ratio of water to the amphiphiles. This feature is in agreement with the one generally expected (3,15). Second, the higher the ratio of SDS to water, the larger the average interfacial area per polar group. This is reasonable because interactions between SDS and water are

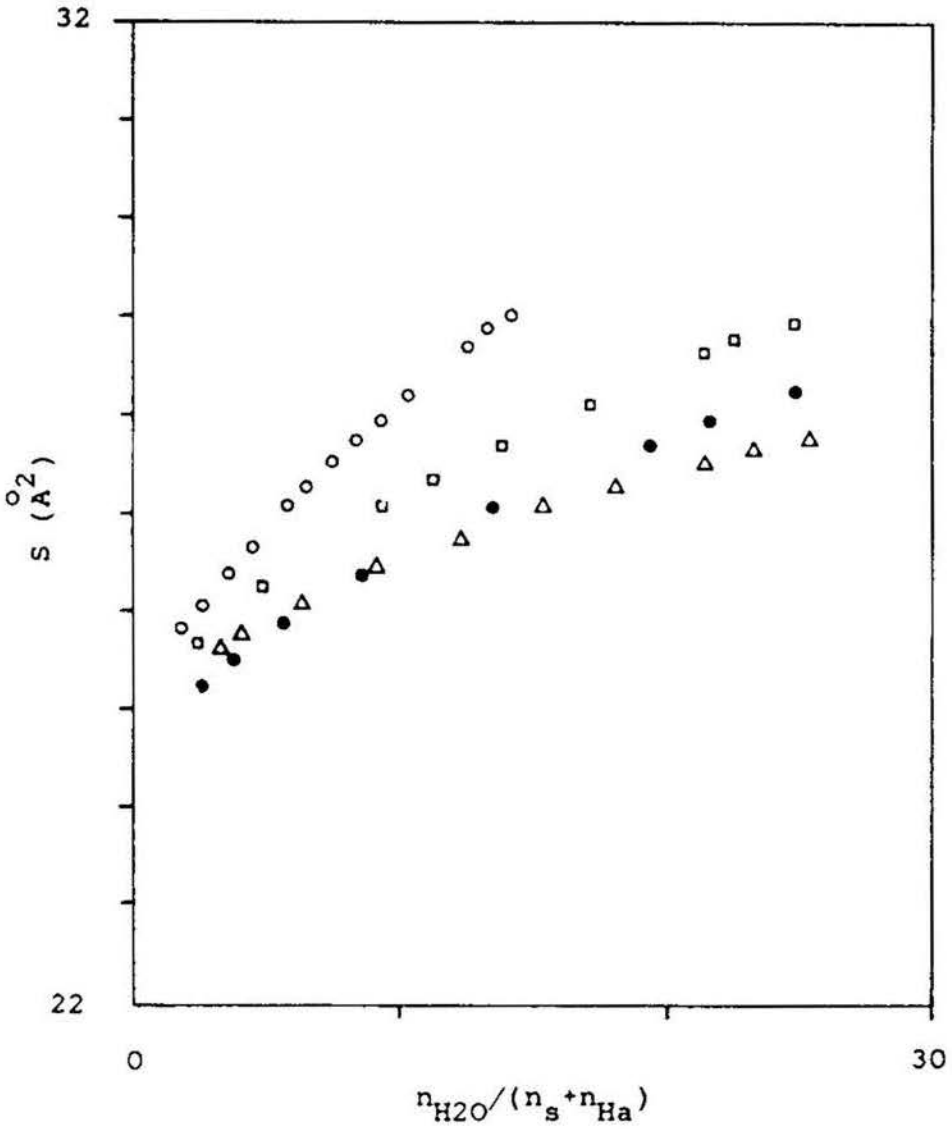

Figure 13. Calculated mean surface area per amphiphile molecule, S, vs $n_{H_2O}/(n_s+n_{Ha})$ for System A at the weight ratio of SDS/Ha: O—70/30, □—60/40, ●—50/50, Δ—40/60.

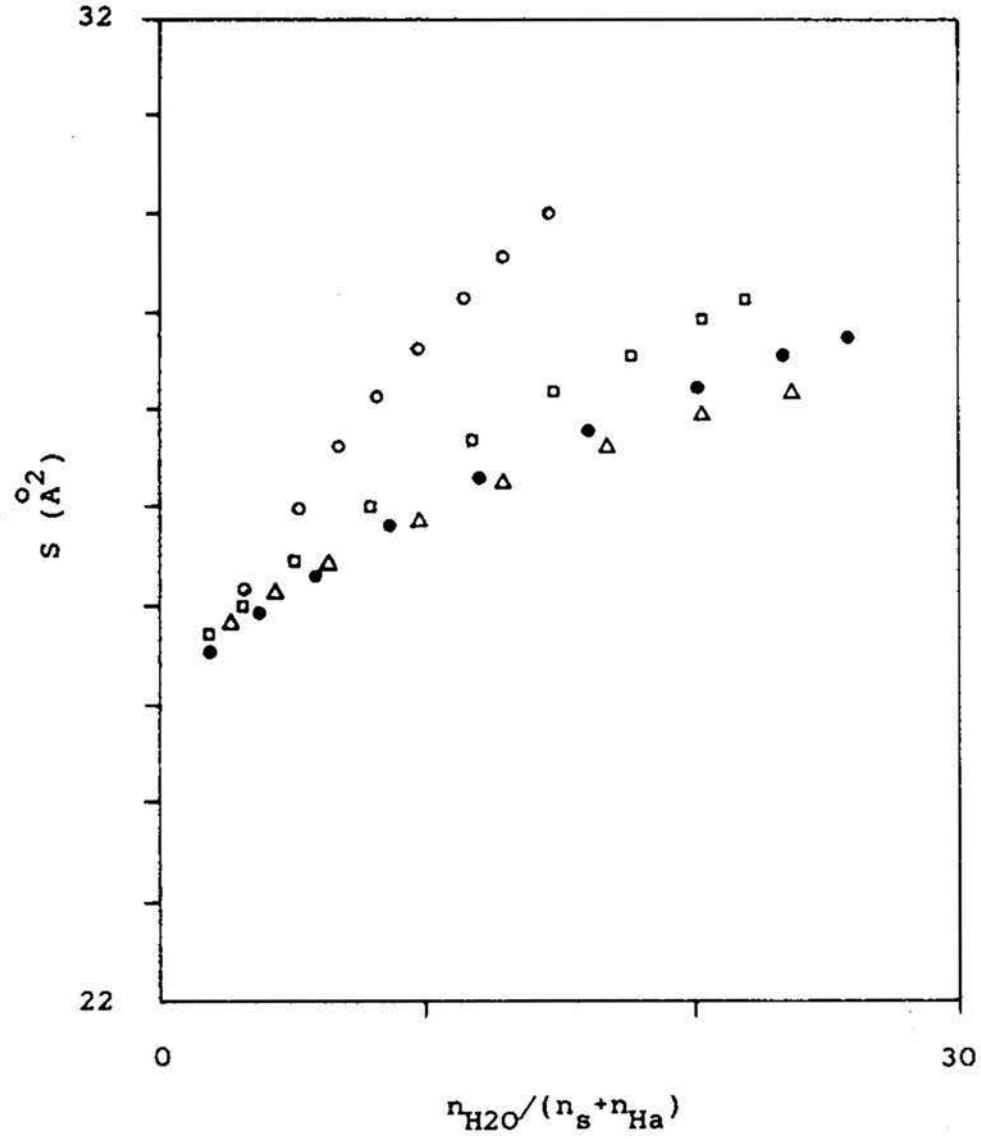

Figure 14. Calculated mean surface area per amphiphile molecule, S, vs $n_{H_2O}/(n_s+n_{Ha})$ for System B at the weight ratio of SDS/Ha: O—70/30, □—60/40, ●—50/50, Δ—40/60.

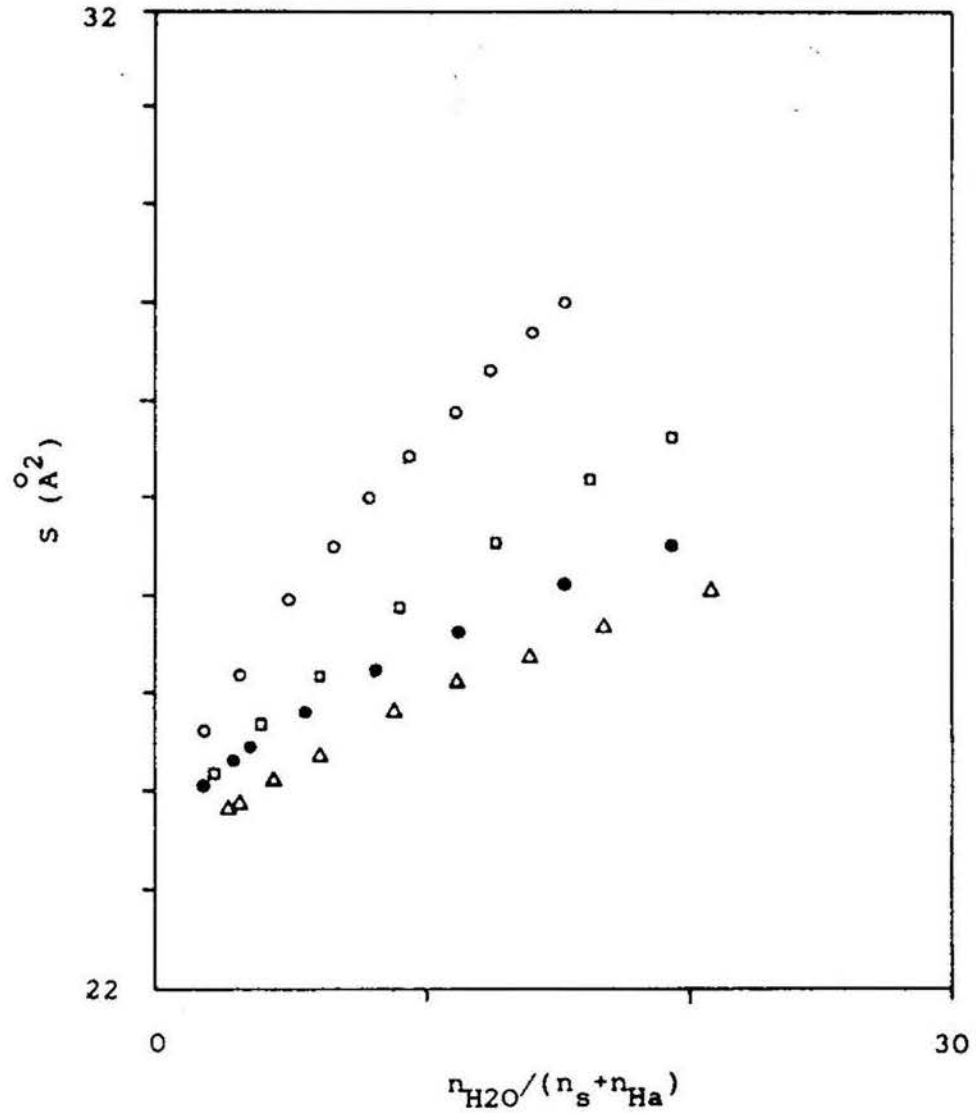

Figure 15. Calculated mean surface area per amphiphile molecule, S, vs $n_{H_2O}/(n_s+n_{Ha})$ for System C at the weight ratio of SDS/Ha: O—70/30, □—60/40, ●—50/50, Δ—40/60.

stronger than those between hexylamine and water. Increasing the hydrocarbon concentration eventually leads to decreasing the interfacial area. This result is best seen by comparing Fig. 14 with Fig. 15, since the difference between Figs. 13 and 14 are indistinguishable within the limits of experimental error. This effect of solubilized hydrocarbon on the interfacial area per polar group may be attributed to the hydrophobic nature of hydrocarbon which weakens the interactions of the polar group of amphiphilc molecules with water(6) so that the interfacial area decreases as hydrocarbon content increases.

SUMMARY

Phase equilibria have been investigated for the systems composed of SDS, hexylamine, water, and heptane. Emphasis has been on the study of the lamellar liquid crystal region by means of low angle X-ray diffraction. It is possible to evaluate water penetration into the amphiphile double layer of the lamellar liquid crystals using a modified equation relating the measured interlayer spacing to the water concentration or amphiphile content. Measurements of X-ray diffraction at a constant weight ratio between SDS and water are made more informative by means of the approximation that the thickness of the amphiphile bilayer is linearly proportional to the volume fraction of SDS in the bilayer. The average interfacial area per polar group of amphiphilic molecules is also calculated and the results show that this area becomes larger as water concentration increases.

ACKNOWLEDGEMENTS

The authors are deeply grateful to Dr. Stig Friberg for many helpful discussions during the course of this work. They also want to express their appreciation to the University of Missouri for research support from the Weldon Spring Endowment Fund.

REFERENCES

1. Venable, R. L., Elders, K., and Fang, Jiafu, J. Colloid Interface Sdi. 109, 330(1986).
2. Fang, Jiafu, and Venable, R. L., J. Colloid Interface Sci., in press.
3. Ekwall, P., in "Advances in Liquid Crystals"(G. H. Brown, Ed.), Vol. I, p.1. Academic Press, New York, 1975.
4. Friberg, S. E., Mol. Cryst. Lig. Cryst. 40, 49(1977).
5. Brown, G. H., Doane, J. W., and Neef, W. D., "A Review of the Structures and Physical Properties of Liquid Crystals", p.65. CRC Press, Boca Raton, FL., 1971.
6. Friberg, S. E., Moucharafieh, N., and Larsen, D. W., Mol. Cryst. Lig. Cryst. 53, 189(1979).
7. Friberg, S. E., Progr. Colloid Polym. Sci. 68, 41(1983).
8. Friberg, S. E., Venable, R. L., Kim, M., and Neogi, P., ColloidS & Surfaces 15, 285(1985).
9. Fontell, K., in "Liquid Crystals and Plastic Crystals" (G. W. Gray and P. A. Winsor, Eds.), Vol.2, p.80. Wiley, 1974.
10. Husson, F., Mustacchi, H., and Luzzati, V., Acta Crystallogr. 13, 668(1960).
11. Luzzati, V., Mustacchi, H., Skoulios, A., and Husson, F., Acta Crystallogr. 13, 660(1960).
12. Luzzati, V., and Husson, F., J. Cell Biol. 12, 207 (1962).

13. Fontell, K., Ewkall, P., Mandell, L., and Danielsson, I., Acta Chem. Scan. 16, 2294(1962).

14. Luzzati, V., in "Biological Menbranes"(D. Chapman, Ed.), Academic Press, London and New York, 1968.

15. Park D., Rogers, J., Toft, R. W., and Winsor, P. A., J. Colloid Interface Sci. 32, 81(1970).

16. Francois, J., Gilg, B., Spegt, P.A., and Skoulios, A. E., J. Colloid Interface Sci. 21, 293(1966).

17. Ekwall, p., Mandell, L., and Fontell, K., J. Colloid Interface Sci. 29, 639(1969).

18. Dvolaitzky, M., Guyot, M., Lagues, M., Le Pesant, J. P., Ober, R., Sautezey, C., and Taupin, C., J. Chem. Phys. 69, 3279(1979).

19. Charvolin, J., Manneville, P., and Deloche, B., Chem. Phys. Lett. 23, 345(1973).

20. Chen, D. M., Reeves, L. W., Tracey, A. S., and Tracey, M. M., J. Am. Chem. Soc. 96, 5349(1974).

21. Reeves, L. W., and Tracey, A. S., J. Am. Chem. Soc. 96, 5729(1975).

22. Boden, N., Jackson, P., Levine, Y. K., and Ward, A. J. I., Chem. Phys. Lett. 37, 100(1976).

23. Radley, K., Reeves, L. W., and Tracey, A. S., J. Am. Chem. Soc. 80, 174(1976).

ARTICLE IV

LIGHT SCATTERING STUDY OF MICROEMULSIONS COMPOSED OF SODIUM DODECYL SULFATE, HEXYLAMINE, HEPTANE, AND AQUEOUS SODIUM CHLORIDE SOLUTION

by

Jiafu Fang and Raymond L. Venable
Department of Chemistry
University of Missouri-Rolla
Rolla, Missouri 65401

ABSTRACT

Time-average and dynamic light scattering measurements were used to determine molecular weights, diffusion coefficients, and particle size or radii along with virial coefficients. The results are generally consistent with the hard sphere model of microemulsion droplets. Increasing the ratio of water to surfactant results in a larger droplet with each ionic surfactant molecule occupying a larger area in the interface. Negative second virial coefficients and positive third virial coefficients were observed.

INTRODUCTION

Since their introduction in 1943 by Hoar and Schulman,[1] microemulsions as they are called, have attracted much interest. Literature about microemulsions has been growing at a very fast rate in the last decade or so.[2] This is not surprising because of their potential technological importance.[3]

As pointed out by Shinoda and Friberg,[4] microemulsions can be viewed as colloidal dispersions consisting of apparently homogeneous systems of low viscosity, containing hydrocarbon (oil), water, surfactant, and in many cases cosurfactant if an ionic surfactant is used. A microemulsion may have an oil-in-water (O/W), or water-in-oil (W/O),[5] or bicontinuous structure,[6,7] depending on the nature and composition of the system. Whatever the structure of the microemulsion is, most surfactant molecules and most cosurfactant molecules are adsorbed as a monolayer at the interface between water and oil regions.

Following the first investigation of interaction problems of microemulsion systems by Vrij and coworkers,[8,9] many contributions to the same topic have appeared in the literature.[10-14] Like other organic media, W/O microemulsions have negligible interactions due to electrical forces,[15] thus providing a simpler model system than water continuous or O/W systems. Vrij and coworkers interpreted their data on the intensity of scattered light from a W/O microemulsion

composed of potassium oleate, hexanol, benzene and water using a two-term osmotic pressure expression. One is due to the hard sphere interactions and the other is a minor contribution treated as an attractive perturbation to allow deviation from the hard sphere behavior for the system.[8] Dynamic light scattering has also been used to investigate micellar or microemulsion systems, especially W/O microemulsions.[16-27]

In this paper we will present scattered light intensity data and diffusion coefficient measurements for a pseudo quarternary W/O microemulsion system composed of sodium dodecyl sulfate (SDS), hexylamine, heptane, and an aqueous sodium chloride solution. Hexylamine has been chosen as a cosurfactant because it exhibits some properties different from commonly used medium chain length alcohols.[28,29] Using a correct dilution procedure we were able to dilute a concentrated microemulsion without changing the particle size, thus making it possible to interpret our light scattering data. We have determined the particle size and the molecular weight for two series of microemulsions. Virial coefficients for both the osmotic pressure and diffusion coefficient have also been determined. Combination of intensity and diffusion coefficient measurements has allowed us to explain their dependence on the volume fraction of particles.

THEORETICAL BACKGROUND

A. MEASUREMENTS OF INTENSITY OF SCATTERED LIGHT

Light scattering by a colloidal dispersion of particles that are small with respect to the wavelength of the incident light is the result of fluctuations of particle concentration caused by Brownian motion. The concentration fluctuation is determined by the osmotic compressibility. The excess reduced intensity of scattered light (or excess Rayleigh ratio) of the solution, $I(\phi)$, over that of the solvent (continuous phase in the case of microemulsions) at a scattering angle of 90° relative to the direction of the incident beam is given by

$$I(\phi) = \frac{2\pi^2 n_o^2 (dn/d\phi)^2}{\lambda_o^4 N_A} \frac{RT\phi}{(d\Pi/d\phi)} \qquad (1)$$

This is a modification of an equation given by Debye.[30] In this equation n_o is the refractive index of the medium, $(dn/d\phi)$ the specific refractive index increment, λ_o the wavelength of the incident light in a vacuum, R the gas constant, T the absolute temperature, N_A Avogadro's number, ϕ the volume fraction of particles (disperse phase), and Π the osmotic pressure. Eq. 1 applies when unpolarized incident light is used. If a vertically polarized incident beam is used,[31] the factor of 2 in Eq. 1 must be replaced by a factor of 4. Note that Eq. 1 has been written in terms of the volume fraction of the particles. Concentration expressed in terms of grams per cubic centimeter, which is more commonly used in

light scattering experiments, can also be used without changing the form of the equation, if the composition of particles in the microemulsion does not change during dilution.

To apply Eq. 1, it is necessary to find the osmotic compressibility. The most straightforward way to estimate this quantity is to express the osmotic pressure as a power series in terms of volume fraction of particles:[32]

$$\Pi = \frac{RT}{V_m} \phi(1 + B_2\phi + B_3\phi^2 + \ldots) \qquad (2)$$

where V_m is the molar volume of the particle and B_2 and B_3 are the second and third virial coefficients. B_2 is directly related to the interaction potential, U(r), between two particles as given by Mcquarrie[33]

$$B_2 = \frac{2\pi}{v_m}\int_0^\infty \{1 - \exp(-U(r)/kT)r^2dr \qquad (3)$$

where r is the distance between the centers of two particles and v_m the volume of the droplet. The third virial coefficient has a much more complicated expression involving interaction potentials among three particles.[33] The interactions among three particles may be negligible when the concentration of particles in the solution is low, but may not be ignored in concentrated W/O microemulsions.[10]

Eqs. 1 and 2 can be combined to give

$$\frac{\phi}{I} = \frac{1}{K_\phi V_m}(1 + 2B_2\phi + 3B_3\phi^2 + \ldots) \qquad (4)$$

where

$$K_{\phi} = 4\pi^2 n_o^2 (dn/d\phi)^2 / \lambda_o^4 N_A \qquad (5)$$

Eq. 4 may be normalized such that $(\phi/I)_{\phi=0} = 1$. Then it becomes

$$\frac{\phi}{I} = 1 + 2B_2\phi + 3B_3\phi^2 + \ldots \qquad (6)$$

Another theoretical approach to estimating the osmotic compressibility is to use modern theories of fluids. In microemulsion systems, it is expected that the major contribution to the osmotic pressure is due to the hard sphere interactions. A minor contribution is due to the long range London-van der Waals attractive forces between the aqueous cores of droplets[8] or to the interpenetration of hydrocarbon tails of surfactant molecules when two particles approach each other.[8,9,11,13] This attractive interaction is frequently treated as a perturbation to the hard sphere model. Therefore the osmotic pressure can be written as a sum of contributions from hard sphere interactions and attractive interactions.

$$\Pi = \Pi_{hs} + \Pi_a \qquad (7)$$

The hard sphere interaction contribution to the osmotic pressure, Π_{hs}, is best described by an equation of state given by Carnahan and Starling[34]

$$\Pi_{hs} = \frac{RT}{V_{hs}} \phi_{hs}(1+\phi_{hs}+\phi_{hs}^2-\phi_{hs}^3) / (1-\phi_{hs})^3 \qquad (8)$$

In Eq. 8, ϕ_{hs} is the volume fraction and V_{hs} the molar volume of the hard spheres. The attractive interaction contribution to the osmotic pressure is given by[13]

$$\Pi_a = \frac{kT}{v_m} B_a \phi^2 \tag{9}$$

where B_a is given by

$$B_a = \frac{2\pi}{kTv_m}\int_0^\infty g(r)U_a(r)r^2dr \tag{10}$$

Here $U_a(r)$ is the attractive potential between two particles and $g(r)$ the radial distribution function. If $g(r)$ is taken as

$$g(r) = \begin{cases} 0, & \text{for } r \leq 2R_{hs} \\ 1, & \text{for } r \geq 2R_{hs} \end{cases} \tag{11}$$

then Eq. 10 becomes

$$B_a = \frac{2\pi}{kTv_m}\int_{2R_{hs}}^\infty U_a(r)r^2dr \tag{12}$$

Combination of Eqs. 1, 7, 8, and 9 yields

$$I(\phi) = K_\phi V_m \phi / \left[\frac{(1+2x\phi)^2 - x^3\phi^3(4-x\phi)}{(1-x\phi)^4} + 2B_a\phi\right] \tag{13}$$

where $x = (\phi_{hs}/\phi) = (R_{hs}/R_m)^3$.

B. DYNAMIC LIGHT SCATTERING

Dynamic light scattering technique[35-39] allows one to accurately and quickly determine the diffusion coefficient of particles suspended in a continuous medium.[40,41] The time autocorrelation function of the scattered light intensity is given by

$$G_2(t) = \langle I_s(0) I_s(t) \rangle \tag{14}$$

where t is the decay time, I_s the scattered light intensity, and the angle brackets mean ensemble average. Since the number of particles in the scattering volume is usually large, the scattered light commonly shows Gaussian statistics. For such a case the normalized intensity autocorrelation function satisfies the following equation[36,42]

$$g_2(t) = \frac{G_2(t)}{\langle I_s \rangle^2} = 1 + C|g_1(t)|^2$$

where C is a constant for a given experiment. The quantity $g_1(t)$ is the modulus of the normalized autocorrelation function of the scattered electric field. For a monodisperse system of N identical particles which are small compared to the wavelength of the incident light, $g_1(t)$ can be expressed as a single exponential[36]

$$g_1(t) = \exp(-Dq^2 t) \tag{16}$$

Therefore $g_2(t)$ becomes

$$g_2(t) = 1 + C \exp(-2Dq^2 t) \tag{17}$$

Here q is the scattering wave vector, and is given by

$$q = \frac{4\pi n_o}{\lambda_o} \sin(\theta/2) \tag{18}$$

where θ is the angle at which the scattered light is measured. D is the translational diffusion coefficient of the particle and is related to osmotic compressibility by[13]

$$D = \frac{v_m}{f} (\partial\Pi/\partial\phi) \tag{19}$$

where f is the friction coefficient between the particle and the continuous medium. The friction coefficient f can be written as a power series of the volume fraction

$$f = f_o(1 + \beta\phi + \gamma\phi^2 + \ldots) \tag{20}$$

where f_o is give by Stoke's law as

$$f_o = 6\pi\eta_o R_H \tag{21}$$

Here η_o is the viscosity of the continuous phase, R_H the hydrodynamic radius of the particle. In the low volume fraction range the diffusion coefficient satisfies the following equation[43]

$$D = D_o(1 + k_d\phi) \tag{22}$$

where k_d is the second virial coefficient for the diffusion coefficient and can be shown to relate to the second virial coefficient of osmotic pressure, B_2, and to that of the friction coefficient. At very low concentrations, terms above the first order of ϕ in Eqs. 2 and 20 can be neglected. Then it is easy to verify from Eq. 19 that

$$D = D_o(1 + (2B_2 - \beta)\phi) \tag{23}$$

Comparison of this equation with Eq. 22 gives

$$k_d = 2B_2 - \beta \tag{24}$$

which can further be written as[44,45]

$$k_d \approx 1.45 - 0.56\alpha \tag{25}$$

where α is a parameter related to the interaction potential between particles.[44]

The diffusion coefficient at zero concentration, D_o, is given by the Stokes-Einstein law[46,47]

$$D_o = \frac{kT}{f_o} = \frac{kT}{6\pi\eta_o R_H} \tag{26}$$

Therefore it is possible to calculate the hydrodynamic radius of the particle from D_o.

Polydispersity causes a dispersion of the diffusion coefficient. The correlation function $g_1(t)$ is no longer exponential and it can be expressed in terms of moments[48,49] of the distribution of the decay rates $\Gamma = Dq^2$

$$g_1(t) = \exp(-\langle\Gamma\rangle t)\left[1 + \frac{\mu_2}{2!}t^2 - \frac{\mu_3}{3!}t^3 + \ldots\right] \tag{27}$$

where μ_i is the ith monment of the decay rates Γ and is given by[49]

$$\mu_2 = (\Gamma - \langle\Gamma\rangle)^2 \tag{28}$$

$$\mu_3 = (\Gamma - \langle\Gamma\rangle)^3$$

The average diffusion coefficient is expressed as

$$\langle D_z \rangle = \frac{\langle\Gamma\rangle}{q^2} = \frac{\Sigma\ N_i M_i^2 D_i}{\Sigma\ N_i M_i^2} \tag{29}$$

the so-called Z-average diffusion coefficient, where N_i is the number of particles of species i having molecular weight M_i and diffusion coefficient D_i. The index of polydispersity can be defined as the normalized Z-average variance of the distribution of D's

$$\frac{\mu_2}{\langle\Gamma\rangle^2} = \frac{\langle D_z \rangle^2 - \langle D_z \rangle^2}{\langle D_z \rangle^2} \tag{30}$$

which provides information similar to that obtained from the more common indices of polydispersity M_w/M_N and M_z/M_N.[50]

EXPERIMENTAL

A. MATERIALS

Sodium dodecyl sulfate was purchased from BDH and recrystalized twice from absolute ethanol. Hexylamine was obtained from Eastman Kodak (Cat. no. 117 7559, 99%) and used without further purification. Heptane was from Aldrich (Cat. no. 15487-3, 99+%, spectrophotometric grade) and used as received. Water was triple distilled.

B. METHODS

1. Light Scattering. Both dynamic light scattering and time average intensity measurements were performed on a Brookhaven Instruments Corporation BI200SM goniometer system. The light source is a 5 mW He-Ne laser used at a wavelength of 632.8 nm. The intensity and autocorrelation function were recorded with a 9865A photomultiplier connected to a 128 channel digital correlator. Sample cells with a diameter of 12 mm were borosilicate glass with a refractive index of 1.460 at the experimental wavelength. The sample cell containing the scattering solution and covered with a Teflon cap was placed in a toluene bath. Toluene has a refractive index of 1.490 and was used as the index matching liquid, which is essential to reduce error caused by reflection. A Zimm plot program was used when making intensity measurements. This program allowed automatic discard of any point if the relative error was greater than about 0.5% in five repetitive measurements of intensity.

2. Refractive Index Indices of refraction for microemulsions were measured using an Abbe refractometer. It was found that the refractive index varied linearly with concentration of the disperse phase (droplets) along the dilution line, which will be described in detail later.

3. Viscosity Viscosity measurements of the continuous phase were carried out by means of an Ubbelohde viscometer.

4. Density Densities of solutions were determined with a Mettler/PAAR DMA 40 digital density meter. It was found that the measured density of a microemulsion is very close to that calculated by assuming that the mixture is ideal. The difference between the calculated and measured density is usually 1.0% or less.[29]

All measurements were performed at 25°C.

C. SAMPLE PREPARATION

The importance of sample preparation for light scattering experiments cannot be overemphasized. Besides the common difficulties, such as dust removal, encountered in light scattering experiments on macromolecular solutions,[51] light scattering experiments on microemulsions generally suffer severely from the difficulty in diluting a concentrated microemulsion without changing the particle size of the disperse phase. Presence of a cosurfactant makes it impossible to dilute a concentrated W/O microemulsion using only the pure hydocarbon as the diluent without causing a modification of the structure and composition and thus the

size of the particles. This is brought about because cosurfactant molecules potentially distribute between the aqueous core, continuous oil phase, and the interfacial phase.[52] Often, the solubility of common cosurfactants in the aqueous phase is low and may be neglected. In such cases the cosurfactant effectively distributes between the continuous and interfacial phases. In some cases, the solubility of water into the continuous phase may not be negligible.[10] In order to make light scattering measurements more meaningful, it is important to find a proper dilution procedure so that the scattering data can be correctly interpreted and comparison made between experiments and theories.

So far the most commonly used dilution procedure is the one proposed first by Schulman[52,53] and improved later by Graciaa.[54] This method has been subject to some restrictions[55] and criticisms.[56] Recently, some other new methods have been proposed using fluorescence emission[57] and dialysis techniques.[58] However, these new dilution techniques have not been widely adopted.

In the present work we have used Schulman's procedure. First, a concentrated W/O microemulsion must be prepared which will be diluted with its continuous phase. This original microemulsion must be saturated, i.e., must be on the demixing line or very close to it.[58,59] To prepare this original microemulsion, we fixed the molar ratio of water to SDS. The amount of heptane added to this mixture depended on the required concentration of the disperse phase. To this ternary

turbid mixture hexylamine was added dropwise with gentle shaking until the mixture suddenly became transparent and a concentrated W/O microemulsion resulted. In order to determine the composition of the continuous phase of this microemulsion, a known amount of the hydrocarbon was added to it. The microemulsion broke down and became turbid. This mixture was titrated with hexylamine until a clear solution appeared again. This procedure was repeated several times. The total amount of hexylamine was plotted versus the total amount of heptane. If the plot was a straight line, the composition of the continuous phase was considered to have been determined correctly.[55] The ratio of the amount of hexylamine in the continuous phase to that of heptane is equal to the slope of the straight line. If the plot is not a straight line, then the solubility of water in the continuous phase cannot be neglected and a mixture of the cosurfactant with a small amount of water must be used instead of pure cosurfactant. Various ratios of water in this mixture should be tried until a straight line results. In our experiments we used 1m aqueous NaCl solution instead of pure water. It was expected that addition of salt would reduce the solubility of water into the continuous phase as well as that of hexylamine into the aqueous cores via the "salting-out" effect.[60] Moreover, we found that use of brine made it easier to observe the end-point of the titration. Two series of microemulsions were prepared for this study. One has the molar ratio of water to SDS equal to 70 (denoted Series A) and the other equal to 50

(Series B). Dilution results are presented in Fig. 1. The weight ratio of hexylamine in the continuous phase to heptane (denoted Ha(c)/Hp) was 0.040 for Series A, and Ha(c)/Hp = 0.046 for Series B, as can be seen from the slopes of the dilution lines in Fig. 1.

The validity of the above dilution procedure for W/O microemulsions has been justified by small angle neutron scattering and ultracentrifugation techniques,[61] although light scattering itself can also be used for this purpose.[10]

Once the composition of the continuous phase has been determined, the concentration of the disperse phase (droplets) can be calculated assuming that all oil is present in the continuous phase. The volume fraction of droplets is defined as

$$\phi = \frac{V_s + V_{aq} + V_{Ha(d)}}{V_s + V_{aq} + V_{Ha} + V_{Hp}} \qquad (31)$$

where V_s is the volume of SDS which is calculated from its mass and the known density of 1.16 g/cm^3, V_{aq} the volume of the aqueous solution. $V_{Ha(d)}$ is the volume of hexylamine in the disperse phase while V_{Ha} is the total volume of hexylamine in the system. V_{Hp} is the volume of heptane.

Removal of dust from microemulsions often causes some special difficulties compared to normal nonaqueous polymer solutions. A small change in composition may cause structural changes in the droplets. For our systems we found that filtration was better than high speed centrifugation.

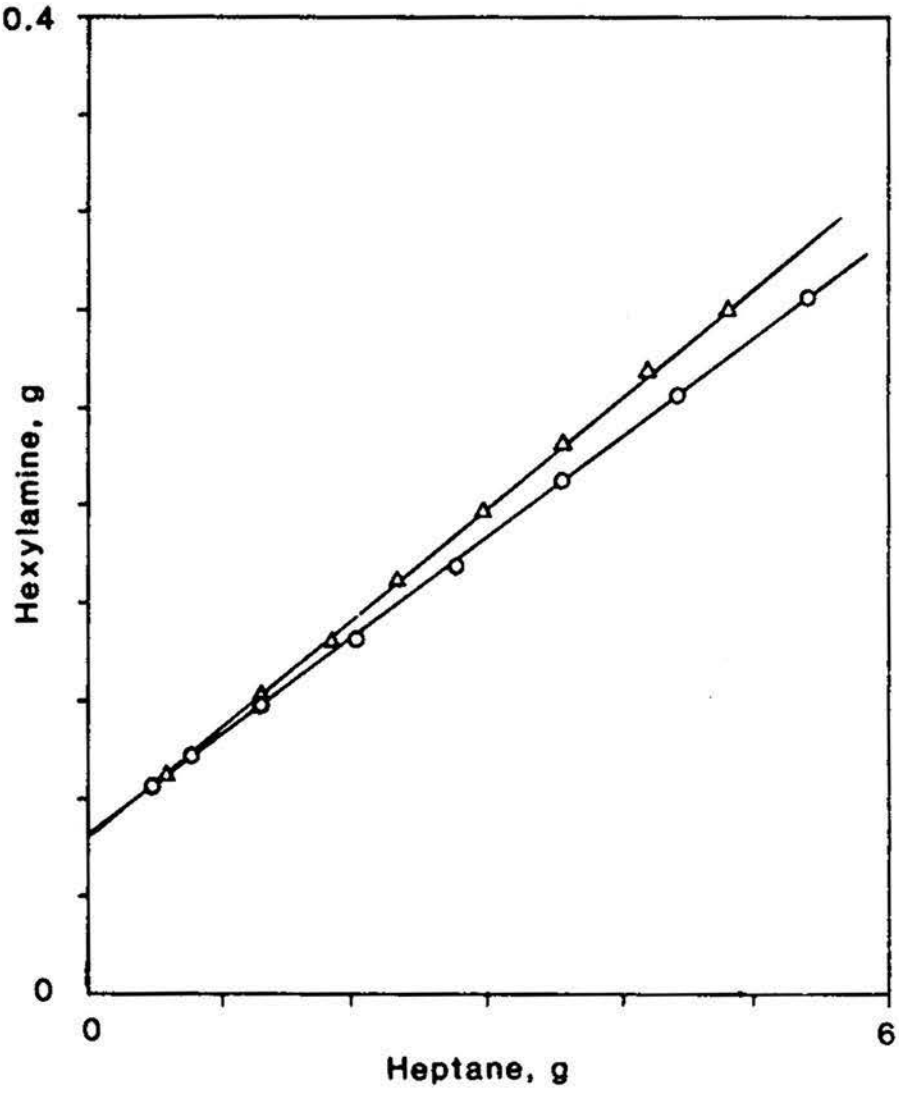

Figure 1. Dilution lines for 0.100 g SDS and 1.0 m NaCl aqueous solution. Molar ratio of water to SDS, n_w/n_s: O—70.2(Series A); Δ—50(Series B).

Reproducible results could be obtained with filtration if enough care was taken. However, if ultracentrifugation was the final step in a dust removal procedure, it was often difficult to obtain reproducible results. Perhaps centrifugation caused a concentration gradient to build up. In any case a long time was required for the solution to regain its homogeneity. In our experiments we used 0.20μ Teflon membranes (Gelman Science, Ann Arbor, Michigan). We found that the best results were obtained when a closed circulation filtration system was used.

RESULTS

A. DYNAMIC LIGHT SCATTERING

Some typical autocorrelation functions of scattered light intensity from microemulsion Series A are presented in Figs. 2, 3, and 4. It is seen that these correlation functions decay exponentially and smoothly with time. As mentioned before, the scattered light intensity autocorrelation function for a monodisperse microemulsion system can be fitted with a single exponential. This takes the following form in our experiments

$$G_2(t) = B\,(1 + C\exp(-2\Gamma m\Delta t)) \tag{32}$$

B is the base line which is the uncorrelated and flat portion of the curve for long time regimes, m is the channel number, and Δt is the sample time. Γ is the decay rate or linewidth containing interesting information and is given by

$$\Gamma = Dq^2 \tag{33}$$

Thus measurements of Γ enable one to calculate the diffusion coefficient, D, of the particle. Eq. 32 can also be written in a linear form

$$\ln\{G_2(t)/B - 1\} = \ln C - 2\Gamma t \tag{34}$$

where $t = m\Delta t$ is the decay time. Therefore if the system is fairly monodisperse, the plot of $\ln\{G_2(t)/B-1\}$ versus t should be a straight line with a slope equal to -2Γ. Figs. 2b,

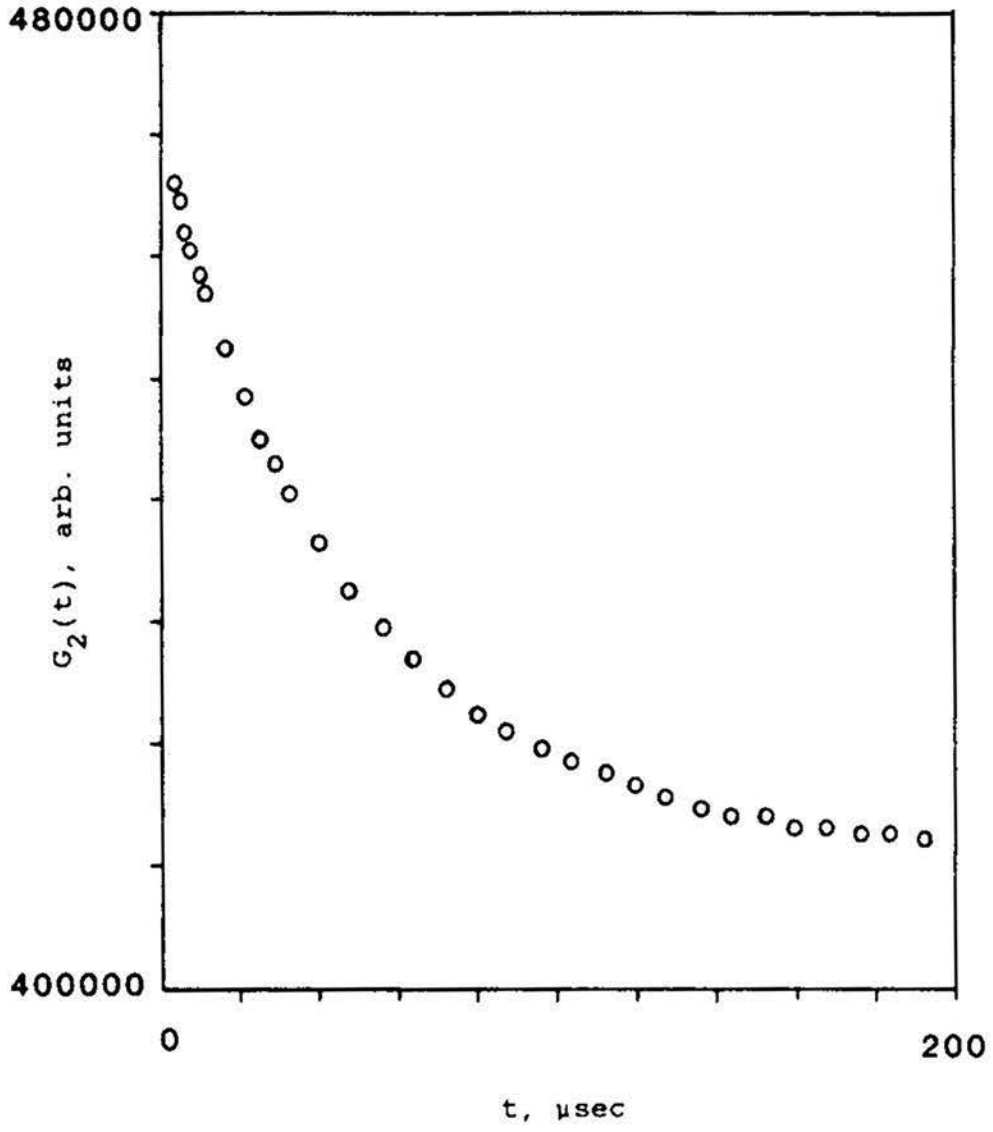

Figure 2a. Autocorrelation function of scattered light intensity from a microemulsion: ϕ=0.116, Series A.

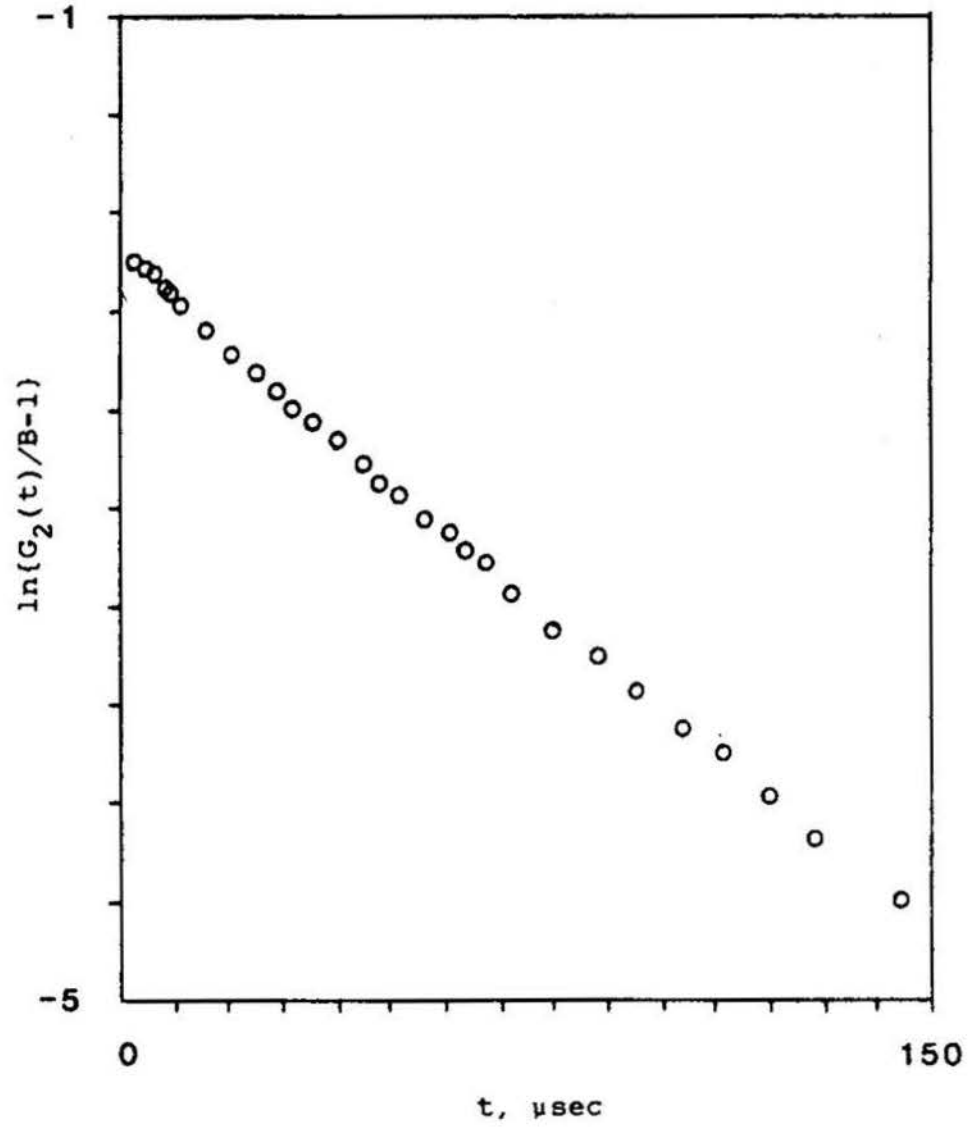

Figure 2b. Plot of $\ln\{G_2(t)/B-1\}$ vs. decay time, t.
Data from Figure 2a.

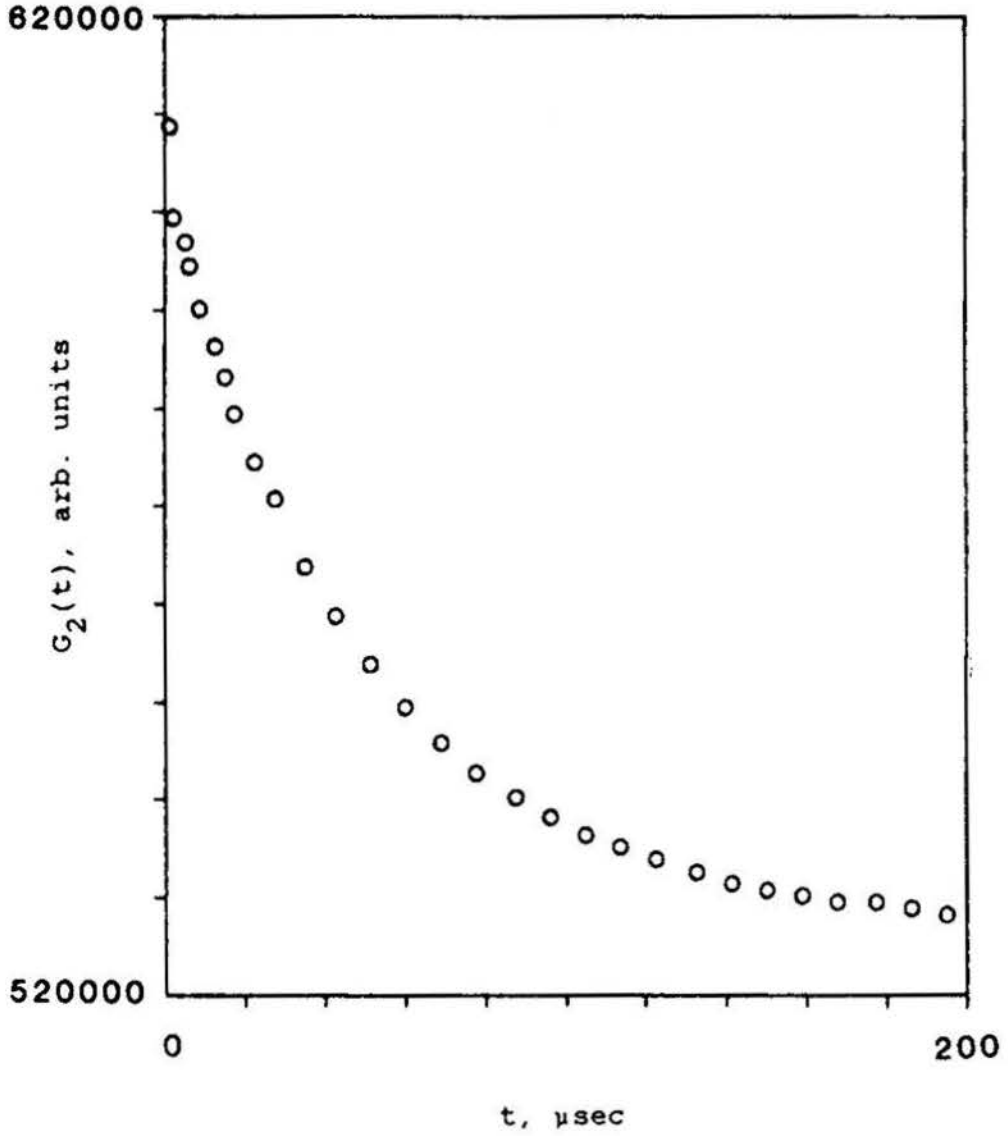

Figure 3a. Autocorrelation function of scattered light intensity from a microemulsion: ϕ=0.076, Series A.

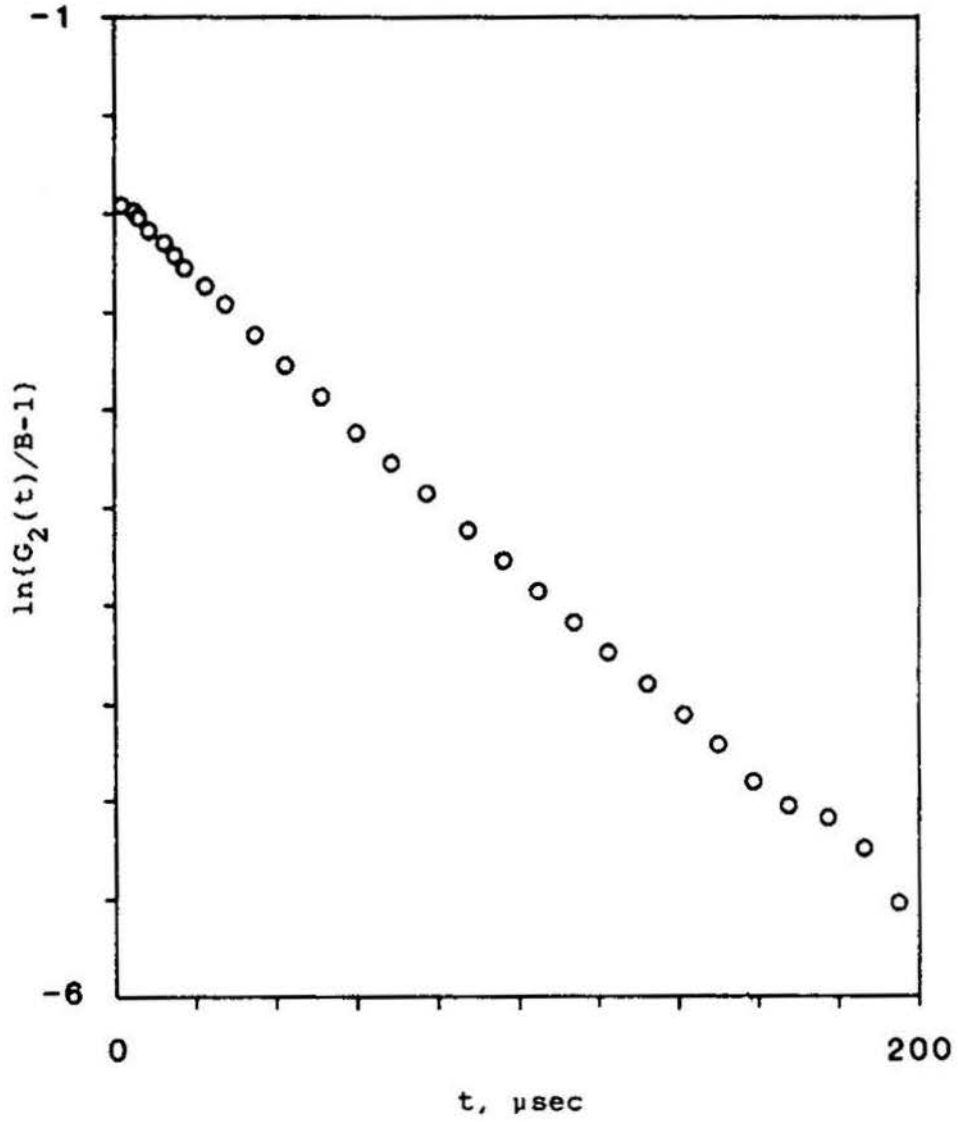

Figure 3b. Plot of $\ln\{G_2(t)/B-1\}$ vs. decay time, t.
Data from Figure 3a.

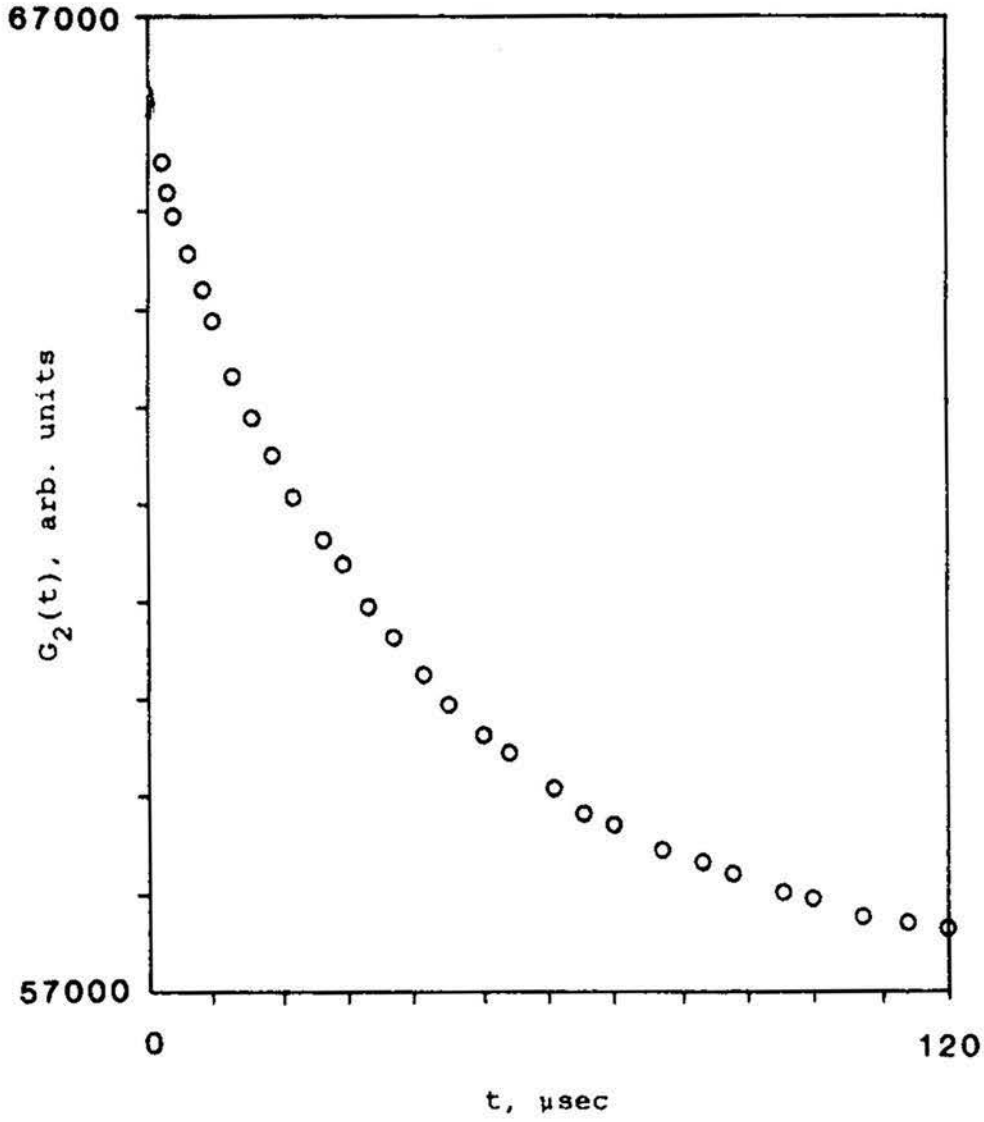

Figure 4a. Autocorrelation function of scattered light intensity from a microemulsion: ϕ=0.0373, Series A.

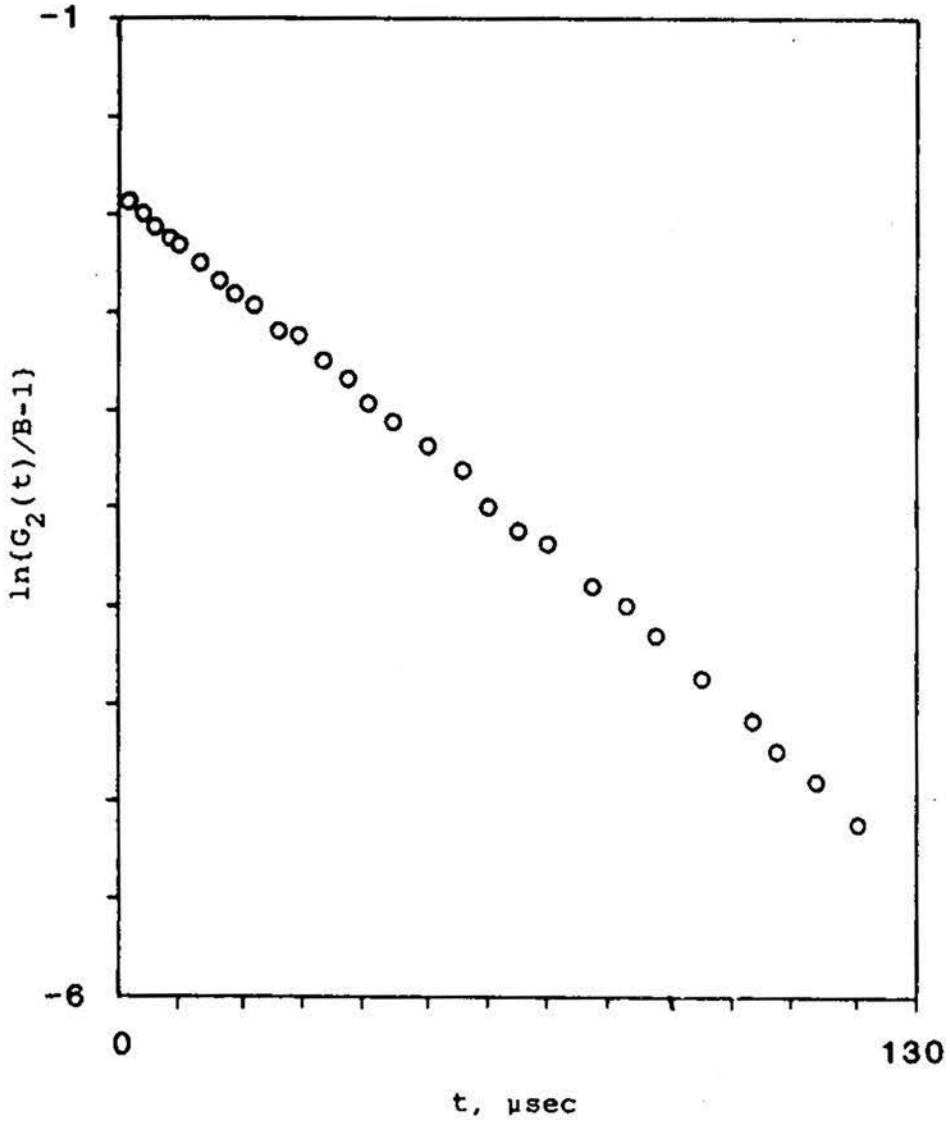

Figure 4b. Plot of $\ln\{G_2(t)/B-1\}$ vs. decay time, t.
Data from Figure 4a.

3b, and 4b show such straight lines. There are only very small deviations from linearity, indicating that our microemulsions are basically monodisperse. Indeed, fitting the same set of data with Eq. 24 up to the third moment using the cumulant method[47,48] usually yields a small value of the index of polydispersity as defined by Eq. 29. Values of about 0.05 are typical if the sample is clean.

If the diffusion coefficient of the diffusing particle is independent of scattering angle, Eq. 33 shows that the plot of Γ versus q^2 is a straight line passing through the origin with the slope equal to the diffusion coefficient. Measurements of diffusion coefficients at various angles are often necessary because for some microemulsion systems diffusion coefficients may be angle dependent.[16] Moreover, measurements at only one angle may sometimes lead to an incorrect conclusion due to dust, flare, etc., especially at angles below 90°. In our experiments we calculated diffusion coefficients from plots of Γ against q^2 and found that the diffusion coefficients were not dependent on scattering angle within the accuracy of the experiment. Fig. 5 shows such plots for Series A. All lines pass through the origin and have good linearity.

Diffusion coefficients for both series A and B are presented in Figs. 6, plotted vs. volume fraction of droplets. We see that they are on the order of $10^{-7}cm^2/sec$, in agreement with that commonly observed for microemulsions[11]. In the low concentration range, the diffusion coefficient decreases

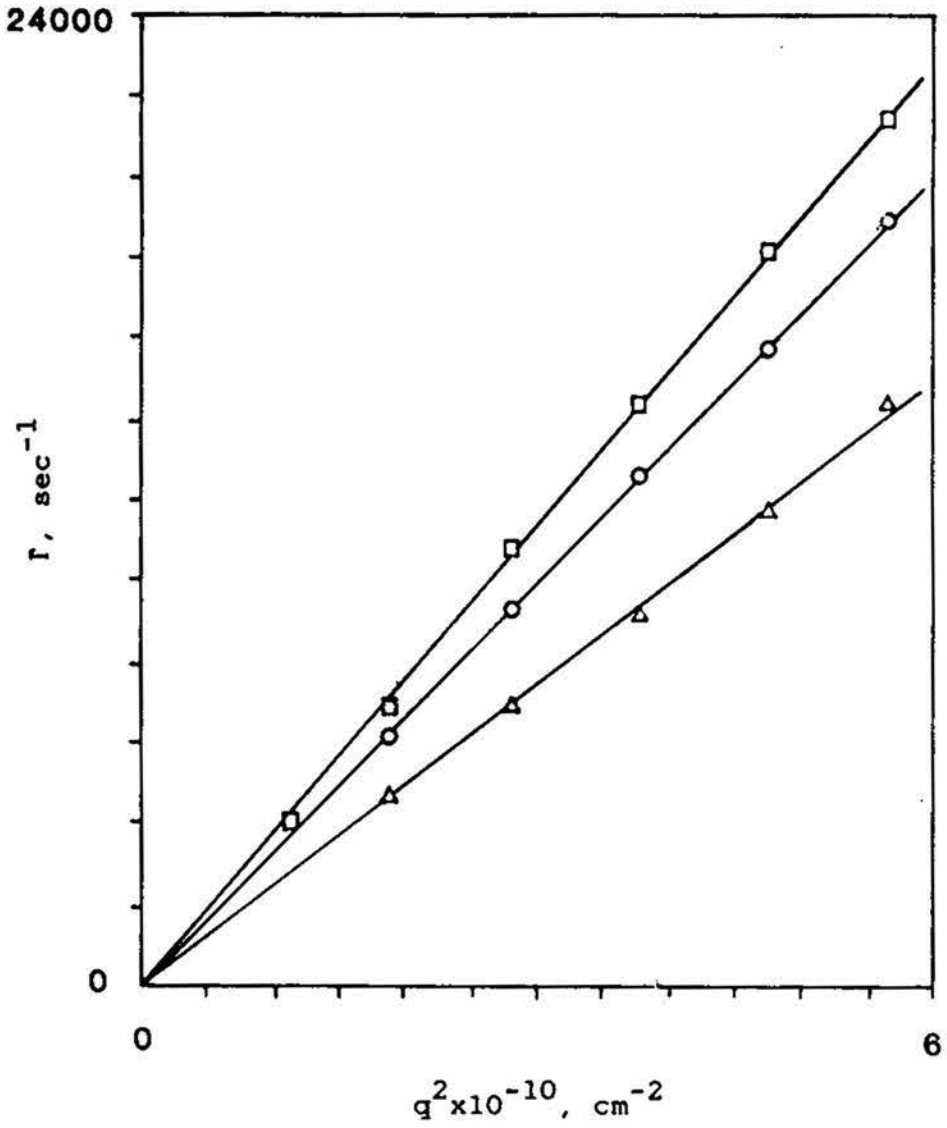

Figure 5a. Plots of Γ as a function of q^2 for Series A. Volume fraction, ϕ: □—0.0185; ○—0.0373; △—0.0564.

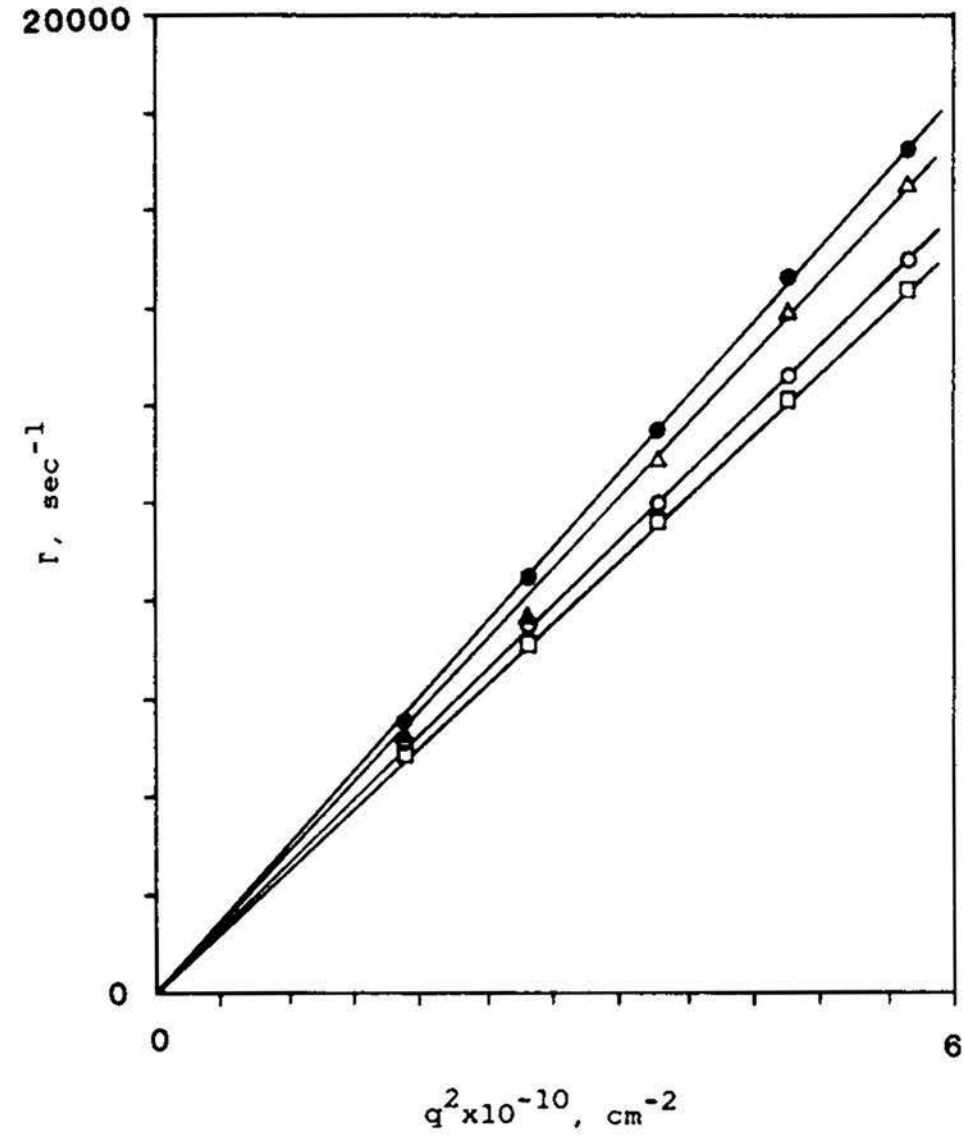

Figure 5b. Plots of Γ as a function of q^2 for Series A. Volume fraction, ϕ: □—0.0759; ○—0.158; △—0.201; ●—0.246.

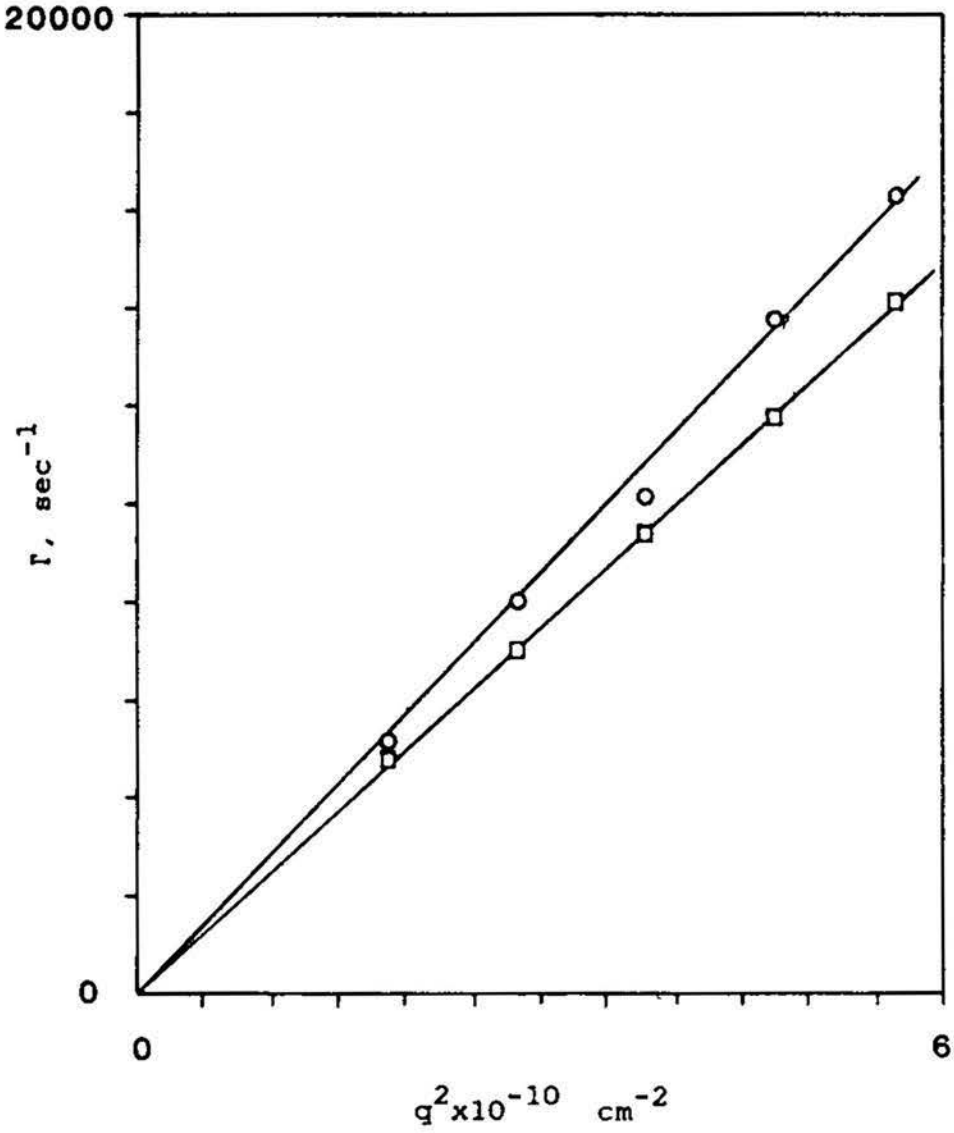

Figure 5c. Plots of Γ as a function of q^2 for Series A. Volume fraction, ϕ: □—0.116; ○—0.293.

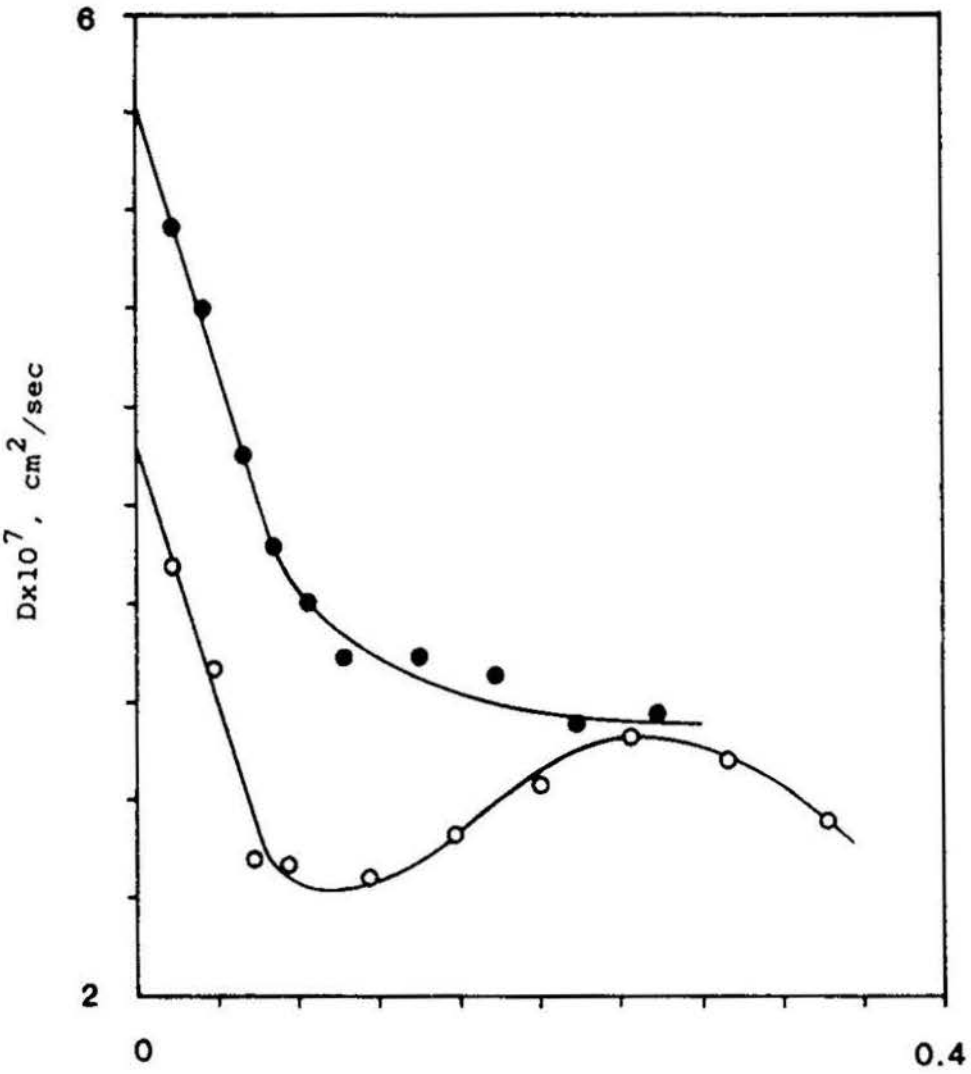

Figure 6. Diffusion coefficient, D, of the droplet as a function of volume fraction, ϕ. O—Series A; ●—Series B.

linearly with increasing volume fraction of droplets for both Series A and B. This linear relationship between diffusion coefficient and volume fraction at low concentrations is expected from Eq. 22. A negative slope was observed, indicating attractive interactions between droplets.[21] From the intercept at zero volume fraction, and the initial slope, the second virial coefficient of the diffusion coefficient, k_d, can be calculated. For Series A, k_d=-5.62, and for Series B the value is -4.75. These values are comparable to literature values[10,11,21,22] for some other W/O microemulsions. It is interesting to note that, for Series A, there is a minimum of D(ϕ) at a volume fraction of ~0.1. We will see that this minimum of the diffusion coefficient corresponds to a maximum of the excess reduced intensity, I(ϕ), given by Eq. 1. Such a shape of a D vs. ϕ plot has been observed for other W/O microemulsions with an alcohol as the cosurfactant.[10,11] For Series B there does not appear to be an obvious minimum. Interestingly, the maximum in I(ϕ) versus ϕ is not pronounced for this same series of microemulsons, as will be seen later. Another feature of Fig. 6 is that the diffusion coefficients for Series B are larger than those for Series A at the same volume fraction, corresponding to a smaller particle size. Extrapolation to zero concentration allows one to calculate the hydrodynamic radius of the droplet using the Stokes-Einstein law, Eq. 26. These radii together with other parameters are summarized in Table I. The hydrodynamic radius for Series A is 136 Å, and that for Series

B is 100 Å. This confirms the conclusion that the larger the molar ratio of water to surfactant, the greater the particle size.[8,10,11]

B. INTENSITY MEASUREMENTS

The excess reduced intensities measured at 90°, I(C), for Series A and B are shown in Figs. 7a and 7b, respectively. It is seen that at low concentrations, a linear relationship exists between I(C) and C, indicating ideal limiting behavior. For infinitely dilute concentrations, Eq. 2, written in terms of C (g/cm^3), gives

$$(\partial \Pi/\partial C)_{C \to 0} = RT/M \tag{35}$$

Substitution of this quantity into Eq. 1 gives

$$I_{C \to 0} = K_C MC \tag{36}$$

Therefore, from Eq. 36 the molecular weight, M, of the droplet can deduced from the initial slope of the plot of I(C) versus C. Similarly, if I is plotted versus ϕ, the molar volume, V_m, and thus the radius of the droplet, R_m, can be obtained. Values of the molecular weight and droplet radius calculated in this way are reported in Table I. Notice that the radius of the droplet obtained from the intensity measurement, R_m, is very close to the hydrodynamic radius deduced from dynamic light scattering.

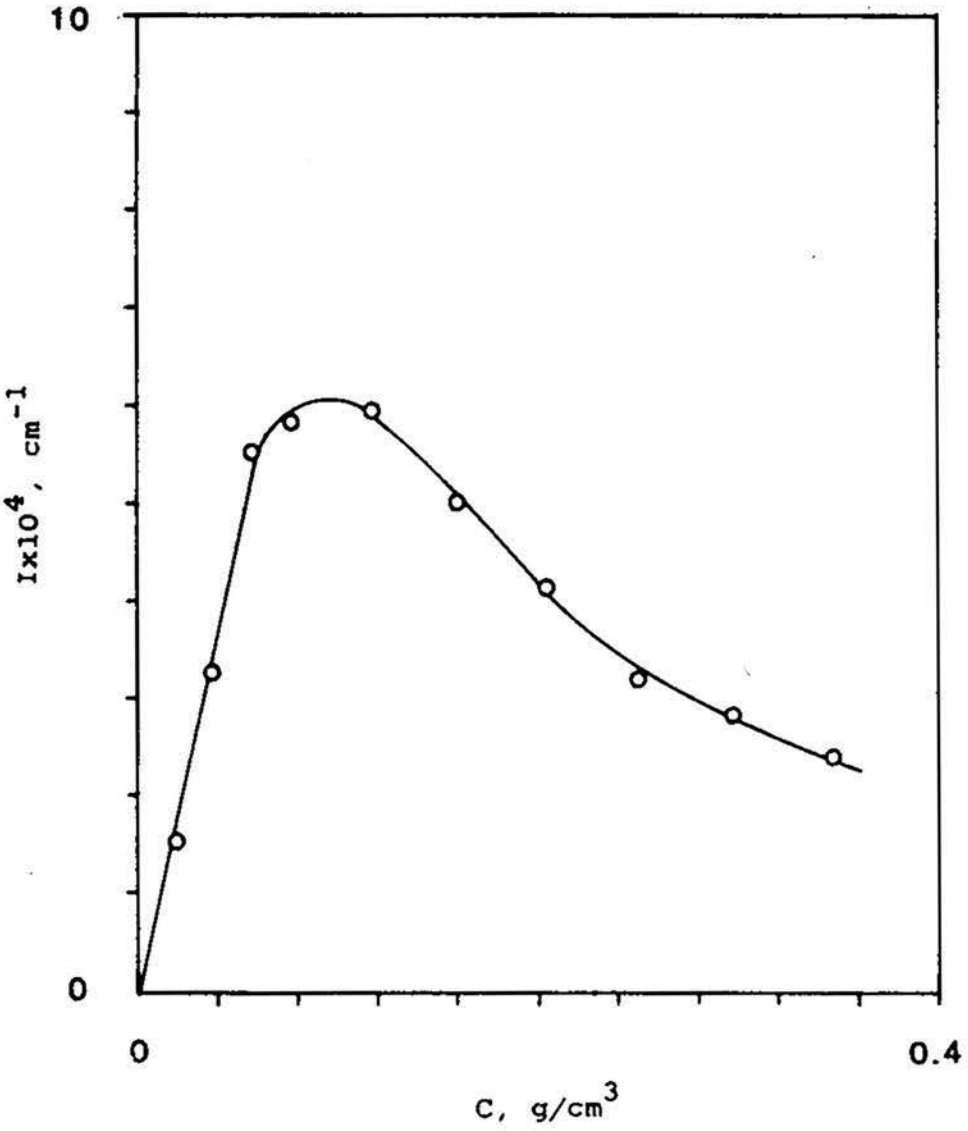

Figure 7a. Excess reduced intensity of scattered light at 90°, I, as a function of concentration of the disperse phase, C, for Series A.

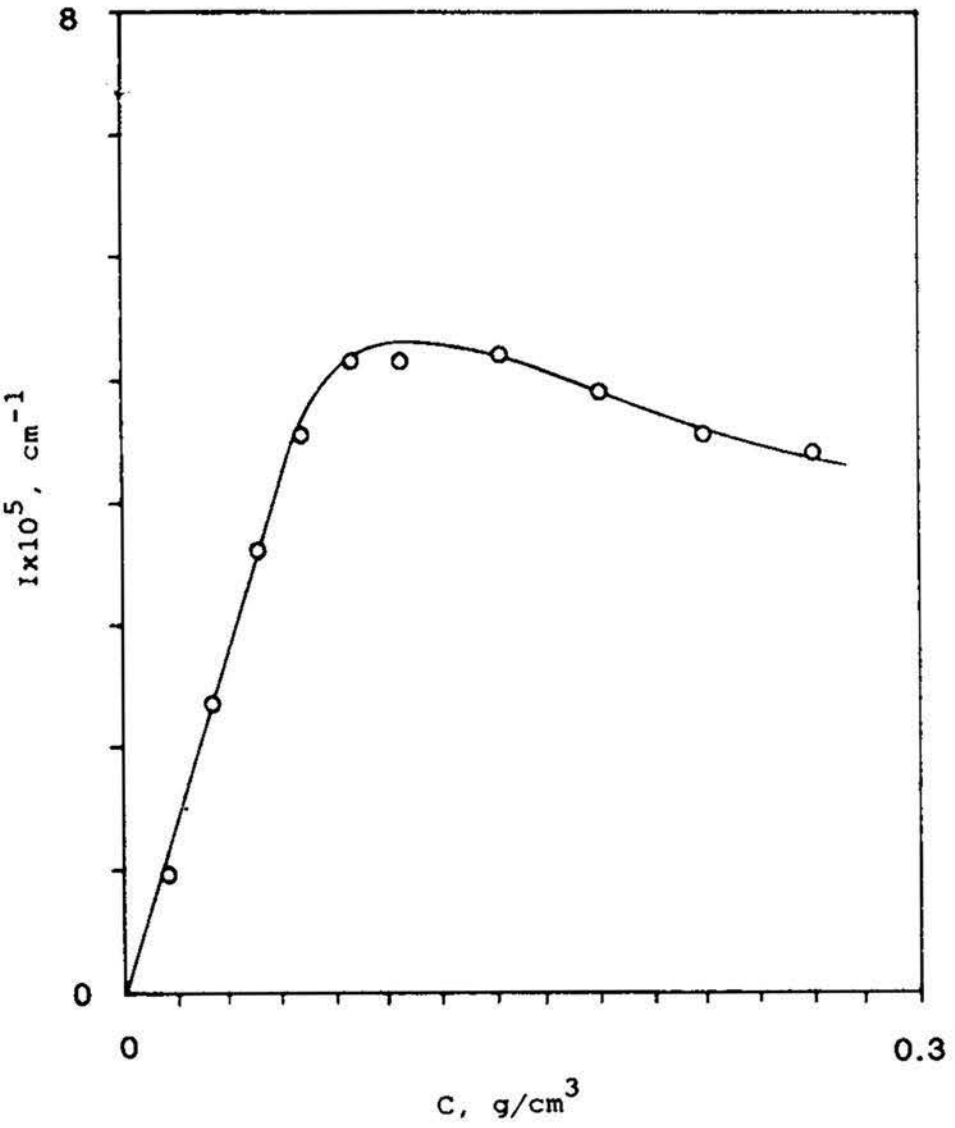

Figure 7b. Excess reduced intensity of scattered light at 90°, I, as a function of concentration of the disperse phase, C, for Series B.

It is interesting that, for Series A, I(C) shows a pronounced maximum as the concentration of droplets increases. This maximum very closely corresponds to the minimum of the diffusion coefficient, as pointed out previously. In the next section we will show that this maximum can be accounted for by the hard sphere model. It can also be explained according to Eq. 1. An examination of this latter equation indicates that a maximum will occur if $(\partial\Pi/\partial C)$ increases more rapidly with increasing C than does C itself. For Series B, we see that after passing through a maximum, I(C) decreases more slowly with C than for Series A. This maximum is not as pronounced as that for Series A. The behavior of scattered light intensity seems to match that of the diffusion coefficients.

Fig. 8 shows the plot of K_cC/I versus C according to Eq. 4. The extrapolated value of K_cC/I to zero concentration gives the reciprocal molecular weight of the droplet. Molecular weights obtained in this way are close to those obtained from the initial slope of I versus C, suggesting that the previous method of determining molecular weights is reliable. Notice that the relationship between K_cC/I and C is not linear, even in the low concentration range. This makes it difficult to obtain a reasonably precise second virial coefficient from such a plot.

From the measured intensity data, it is possible to calculate the osmotic compressibility from Eq. 1. Fig. 9 shows $\partial\Pi/\partial\phi$ plotted vs. volume fraction of droplets for both series

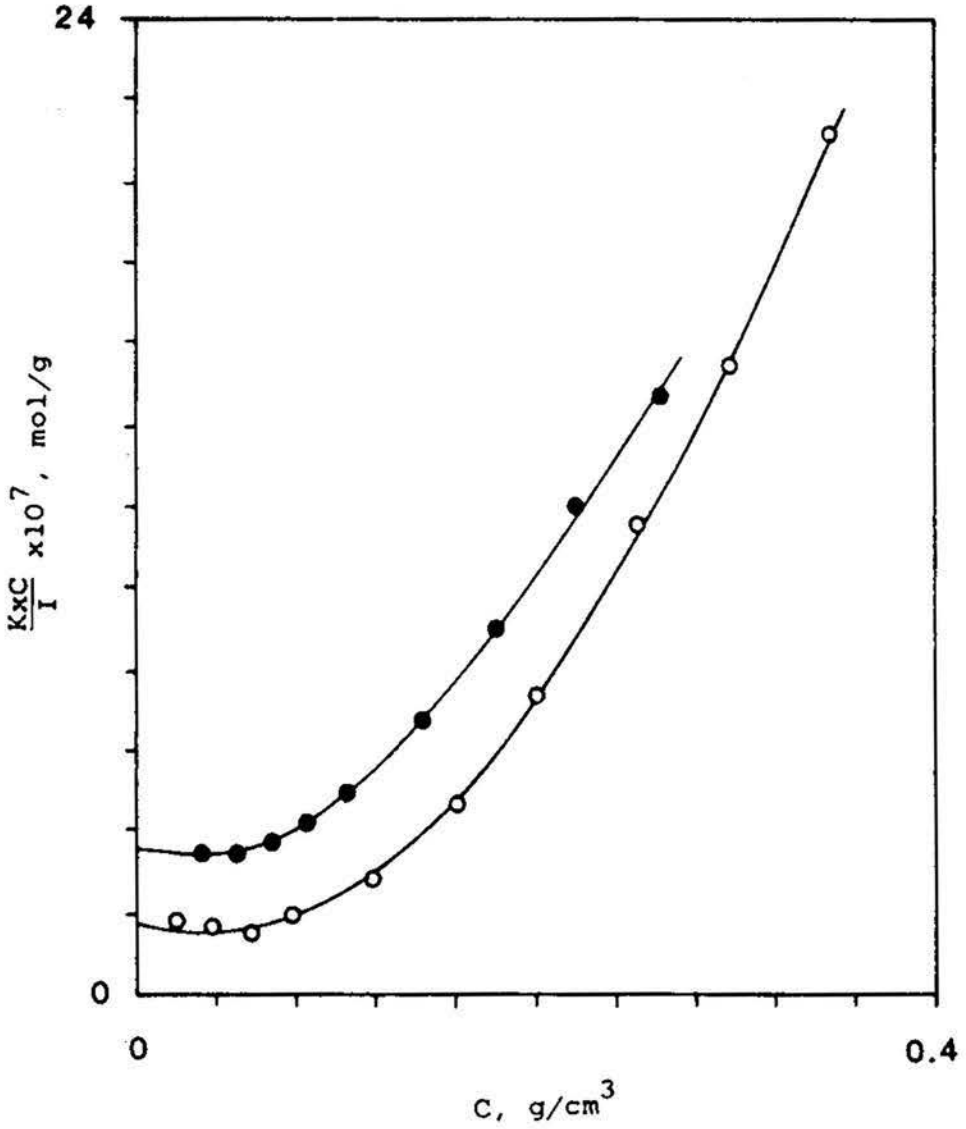

Figure 8. Plot of KxC/I versus C. O—Series A;
●—Series B.

of microemulsions. A theoretical curve of $(\partial \Pi_{hs}/\partial \phi_{hs})$ for the hard sphere model using Eq. 8 is also included in this figure. It is interesting to note that for Series A the data are fitted fairly well with the hard sphere model over a large concentration range. This suggests that the major contribution to the osmotic pressure is the hard sphere interactions. Data for Series B appear to deviate quite markedly from this model, showing that some other contributions to the osmotic pressure are also important for this Series.

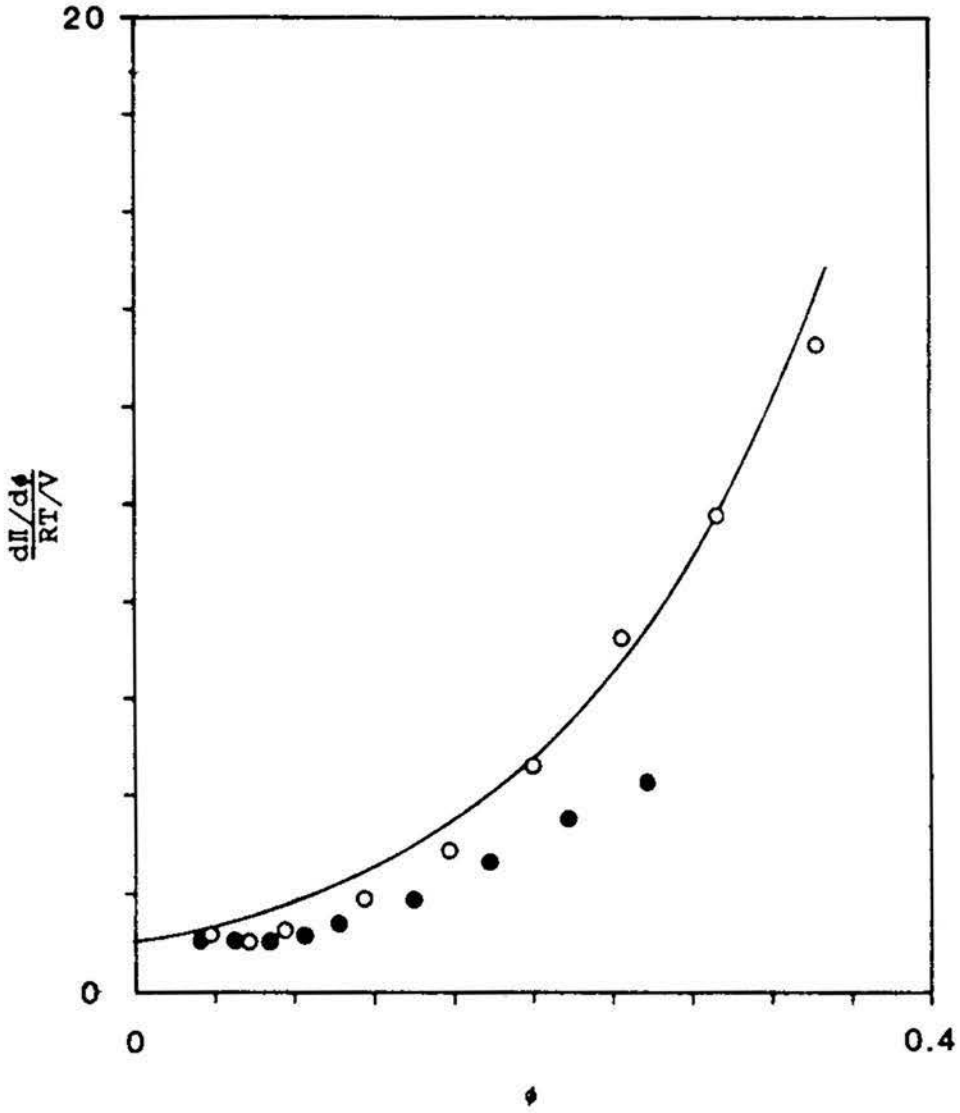

Figure 9. Comparison between the hard sphere model and the experimental results—Plot of $\frac{d\Pi/d\phi}{RT/V}$ vs ϕ. Solid line—theoretical hard sphere model; ○—experimental result of Series A; ●—experimental result of Series B.

TABLE I

Experimental Parameters of Microemulsion Series A and B

	Series A	Series B
n_w/n_s	70.2	50
$W_{Ha(c)}/W_{Hp}$	.040	.046
$n_{Ha(d)}/n_s$	1.80	1.81
$Mx10^{-6}$(g/mol)	6.15	2.86
R_m^o(A)	134	104
R_H^o(A)	136	100
R_w^o(A)	120	90
ℓ^o(A)	14	14
N_s	3404	2101
$N_{Ha}(d)$	6127	3812
N_{aq}	$2.43x10^5$	$9.99x10^4$
B_2	-3.94	-1.71
B_3	35.8	23.1
B_a	-11.5	-7.79
k_d	-5.62	-4.75
A_Hx10^{19}(J)	2.39	2.32
$A_{s-a}(A^{o2})$	19.1	17.2
$A_s(A^{o2})$	53.2	48.4

DISCUSSION

Fig. 10 shows a simplified model of a W/O microemulsion droplet. Based on this model it is possible to calculate the radius of the aqueous core, R_w, from light scattering measurements. Hence the effective thickness, t, of the interfacial film can be estimated since the radius of the whole droplet, R_m, is known from intensity measurements. The water core radius is given by the equation

$$R_w = \left[\frac{3Mf_{aq}\rho_t}{4\pi N_A \rho_{aq} C}\right]^{1/3} \qquad (37)$$

where f_{aq} and ρ_{aq} are the weight fraction and density, respectively, of the aqueous solution. The density of the microemulsion is ρ_t. This radius will not change during dilution. Aqueous core radii calculated from the above equation are listed in Table I. The difference between R_m and R_w gives the same value of the interfacial thickness, $t = 14$ Å, for both Series A and B, as would be expected. This result is in very good agreement with the value of ~13 Å obtained for a microemulsion system consisting of SDS, water, hexanol and cyclohexane by Cazabat et al [10] Hexylamine used in the present study should have a chain length very close to that of hexanol. It is not surprising that both systems give the same value of the interfacial thickness. Of course, a minor difference may exist due to the different hydrocarbons,

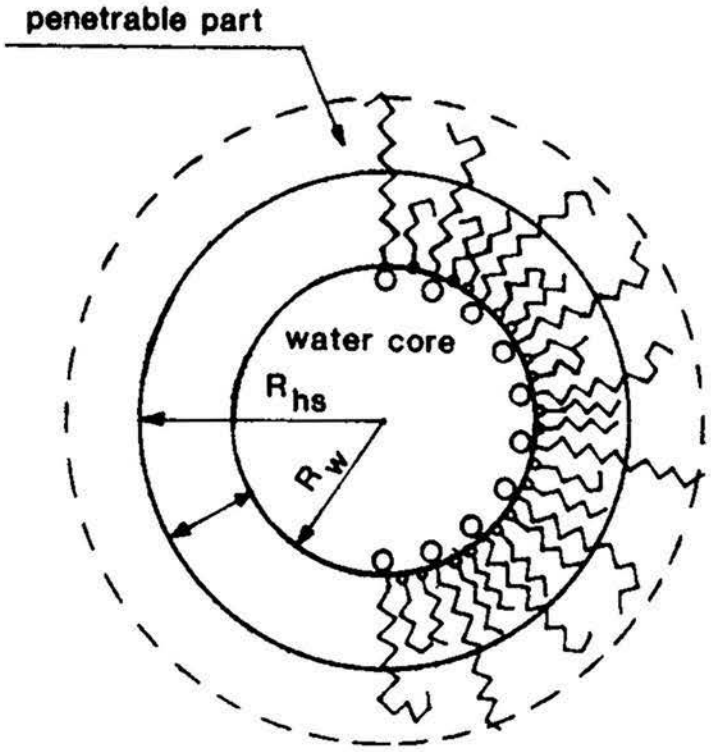

Figure 10. A schematic illustration of droplet structure in W/O microemulsions. Molecules with a long chain length are surfactant and those with a short chain length are cosurfactant.

especially if the composition of the interfacial film differs, since the chain lengths of the surfactant and cosurfactant are not the same. Note that this deduced interfacial film thickness is greater than the chain length of hexylamine(~7 Å) but shorter than that of SDS(~21 Å). This result is in agreement with that determined by low angle X-ray diffraction on the lamellar liquid crystalline phase,[29] in the absence of sodium chloride. There the thickness of the amphiphilic bilayer is about twice the ℓ value here. Since the effective interfacial film thickness is smaller than the SDS chain length, there exists a region where interpenetration may occur when two droplets approach each other. This region is the outer part of the interfacial monolayer of the droplet and on average has a thickness of 7 Å. It is believed that the attractive interaction between particles in a microemulsion is partly due to this partial interpenetration of the tails of surfactant molecules. Apparently, this attraction is short range.[9,13,62] Another possible contribution to the attractive potential is the long range London-van der Waals forces between aqueous cores immersed in the non-polar hydrocarbon medium. A theory for this long range attractive interaction is available from the literature.[8] We will use this theory to estimate the Hamaker constant for our system after we obtain the attractive contribution, B_a, to the second virial coefficient given by Eq. 10.

The composition of the droplet can be obtained from the molecular weight, the radius of the aqueous core, and the

molar ratio of SDS to hexylamine in the interfacial film. From the following equation, the number of molecules of SDS, hexylamine, and water in the droplet can be calculated.

$$m_d = N_s m_s + \gamma N_s m_a + \upsilon_{aq}\rho_{aq} \qquad (38)$$

N_s is the number of SDS molecules in the interfacial monolayer, m_d the mass of the droplet, m_s and m_a the mass of an SDS and a hexylamine molecule respectively, and υ_{aq} the volume of the aqueous core. The ratio $N_{Ha(d)}/N_s$ is γ where $N_{Ha(d)}$ is the number of hexylamine molecules in the interfacial monolayer. The calculated results are listed in Table I. Obviously, the aggregation number of the surfactant in our microemulsions is much larger than that in normal micellar solutions.[63] Of course, depending on the location in the phase diagram, microemulsions may have very small droplets, or even be molecular dispersions.[64]

Having calculated the number of the SDS and hexylamine molecules in the interfacial film, we can now estimate the average interfacial area per polar group of these amphiphilic molecules. Assume that the polar head of the hexylamine molecule is anchored together with the ionic group of the SDS molecule at the surface of the aqueous core. The average area per polar group, A_{s-a}, can be calculated from

$$(N_s + N_{Ha(d)})A_{s-a} = 4\pi R_w^2 \qquad (39)$$

which gives A_{s-a}=19.1 $\mathring{A}^2$ for Series A and 17.2 $\mathring{A}^2$ for Series B. These values are smaller than those determined from low angle

X-ray diffraction for the lamellar liquid crystalline phase.[29] Two possible reasons may be given. One is geometrical and the other electrostatic. The interfacial structure between the aqueous core and the amphiphilic monolayer in the microemulsion phase is different from that in the lamellar liquid crystalline phase. This interfacial film is bent in the case of a microemulsion since the droplet is spherical or has a curved surface. This geometrical factor provides more space between the hydrocarbon tails of SDS molecules so that hexylamine molecules in the interfacial film may slip back to some extent from the surface of the aqueous core and this effect will reduce the average interfacial area per polar group. Since in the present study brine was used instead of pure water, the screening effect of the electrolyte will reduce the repulsion between neighboring ionic heads of SDS molecules to allow a more compact arrangement. Therefore it seems possible to ignore the contribution of hexylamine molecules to the interfacial area in the monolayer. With this assumption we obtain an area per SDS molecule of 53.2 $\mathring{A}^2$ for Series A, and 48.4 $\mathring{A}^2$ for Series B. These values are very close to that obtained by Cazabat et al.[11] Comparing the A_s value between Series A and B, we see that the larger the molar ratio of water to SDS, the greater the interfacial area per polar group. This is also in good agreement with the results obtained from low angle X-ray diffraction of the lamellar liquid crystalline phase.[29]

To extract virial coefficients of osmotic pressure from intensity measurements of scattered light, Eq. 6 can be rearranged to give a linear form at not very high concentrations

$$(\phi/I - 1)/\phi = 2B_2 + 3B_3\phi \qquad (40)$$

The quantity ϕ/I has been scaled with $(\phi/I)_{\phi=0}$. This equation allows one to calculate the second and third virial coefficients, B_2, and B_3, from the intercept and the slope, respectively, of the plot of $(\phi/I-1)/\phi$ vs ϕ. Fig. 11 shows such plots. We see that the straight line is fairly good, especially for microemulsion Series A. For Series B, deviation from the straight line becomes significant at the two concentration extremes. Virial coefficients obtained from these plots are included in Table I. For both series, the second virial coefficient is negative, confirming the existence of attractive interactions between particles. Notice that Series A gives a more negative second virial coefficient than Series B, implying that attractive forces become stronger as the molar ratio of water to SDS increases. This tendency is in general agreement with Cazabat et al.[10] They used a different virial expression of osmotic pressure in that work.

From Table I we see that the third virial coefficient for both Series is positive. This positive third virial coefficient is known to be responsible for the occurrence of the maximum of $I(\phi)$ versus ϕ.[65] As mentioned previously, this

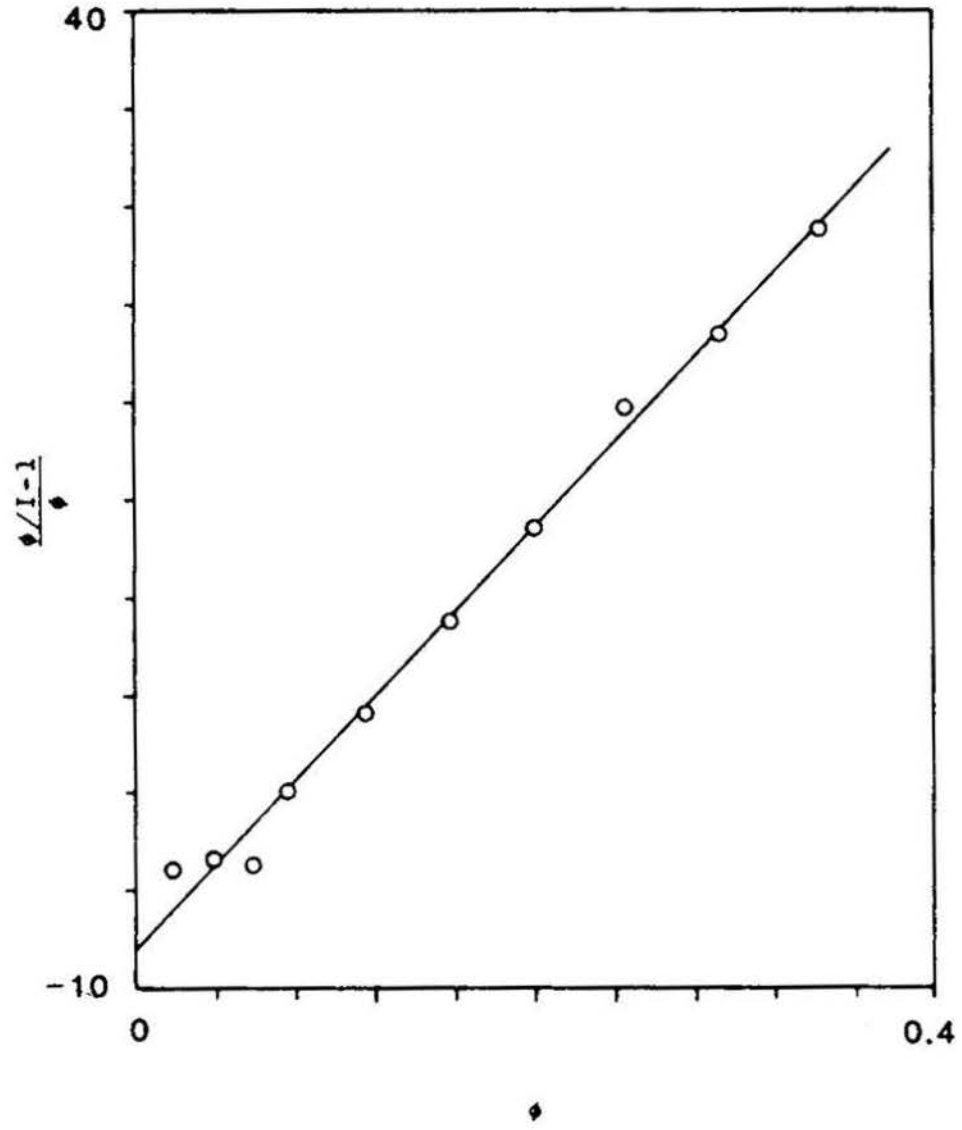

Figure 11a. Plot of $\frac{\phi/I-1}{\phi}$ vs. ϕ for Series A. ϕ/I is normalized.

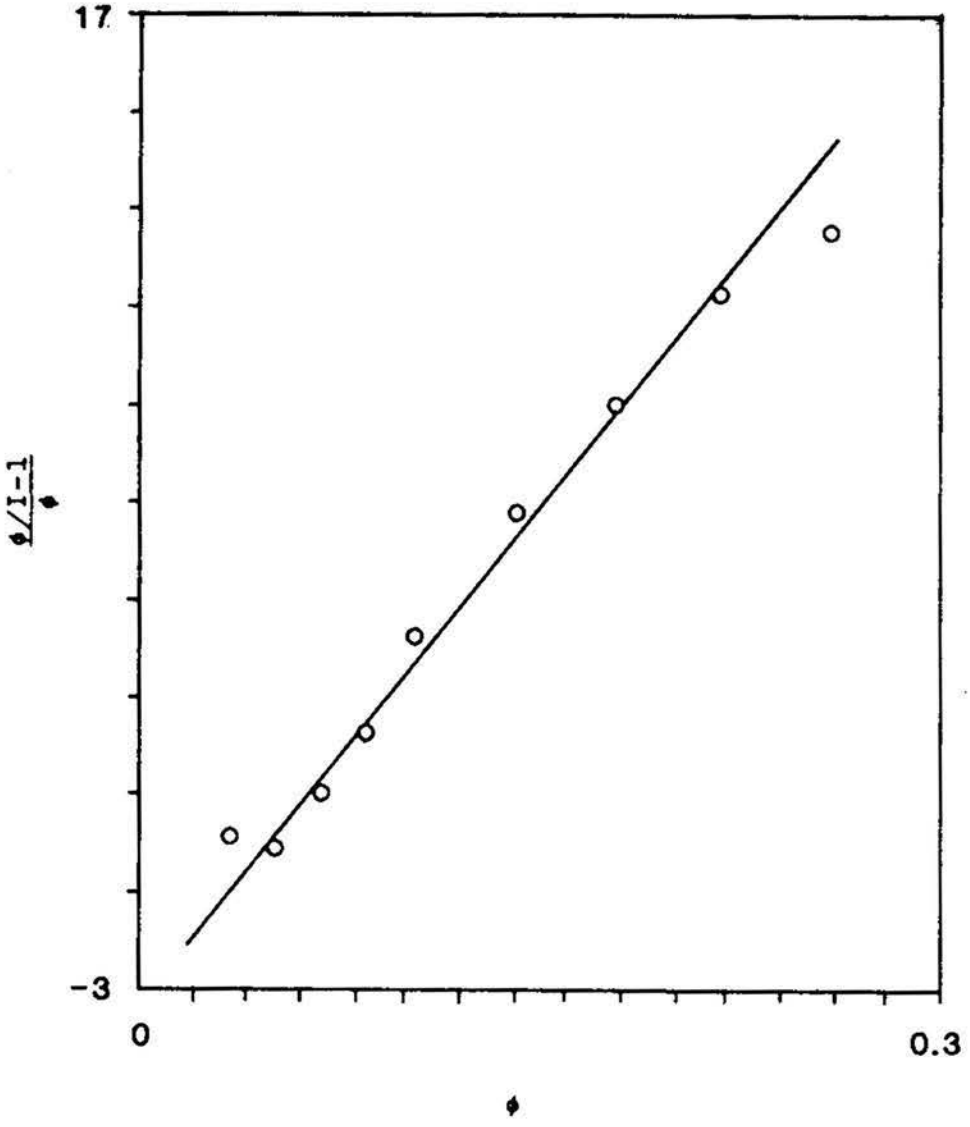

Figure 11b. Plot of $\frac{\phi/I-1}{\phi}$ vs. ϕ for Series B. ϕ/I is normalized.

maximum is mainly due to the hard sphere interactions between particles. Thus the third virial coefficient of the osmotic pressure due to these hard sphere interaction must be positive. This can be shown from Eq. 8 by expanding Π_{hs} as a power series in terms of volume fraction of hard spheres, ϕ_{hs}. By doing so one obtains

$$\Pi_{hs} = \frac{kT}{v_{hs}} \phi_{hs}(1+4\phi_{hs}+10\phi_{hs}^2+18\phi_{hs}^3+\ldots) \qquad (41)$$

which has a positive third virial coefficient of 10. This value is smaller than the experimental ones as would be expected since the system does not behave as a pure hard sphere one.

It is easy to show that if Eq. 8 is substituted into Eq. 1, a maximum of $I(\phi)$ occurs at a volume fraction of ~0.13, which is close to the observed values for both the microemulsion Series. Fig. 12 compares the intensity data between the hard sphere model and experimental results. The intensity has been normalized by $K_\phi V$. We now see why a maximum of scattered light intensity appears as the concentration of particles increases. It is mainly caused by hard sphere interactions. At low concentrations, both series behave like hard spheres. Deviations from this model become larger as the concentration increases. Series A comes to agreement with the model again at high concentrations while Series B does not.

It is possible to obtain the attractive part of the second virial coefficient, B_a, given in Eq. 9, by fitting data

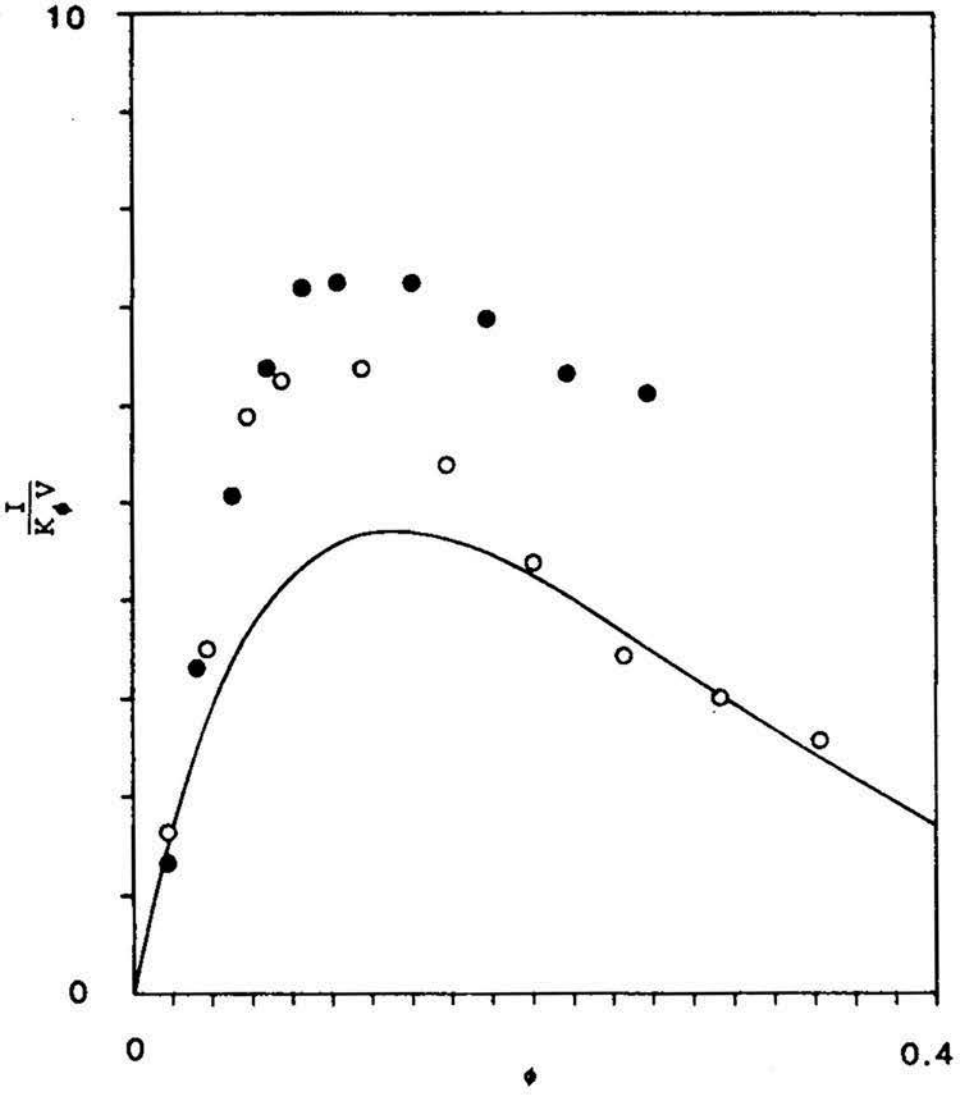

Figure 12. Comparison of intensity data between the hard sphere model and experimental results.
Solid line—the hard sphere model;
O—Series A; ●—Series B.

of $I(\phi)$ to Eq. 13. Alternatively, it may be obtained in the following way. Combination of Eq. 41 and Eq. 9 yields

$$\Pi = \frac{kT}{v_m} \phi \left[1 + (4x + B_a)\phi + 10x^2\phi^2 + \ldots\right] \quad (42)$$

Comparing this with Eq. 2, one obtains

$$\begin{aligned} B_2 &= 4x + B_a \\ B_3 &= 10x^2 \end{aligned} \quad (43)$$

The observed third virial coefficient is considerably larger than 10, which means that x deviates appreciably from 1. The attractive contribution to the osmotic pressure given by Eq. 9 is obviously oversimplified. B_a is given in Table I according to this treatment. Still, these B_a values are comparable to literature values.[11]

With B_a known we can now calculate the Hamaker constant for our microemusion system following the treatment of Vrij and coworkers.[8] According to Hamaker,[66] the potential of the long range London-van der Waals forces between aqueous cores suspended in a non-polar medium is given by the following equation

$$U_a(r) = -\frac{A_H}{12}\left[\frac{4}{S^2-4} + \frac{4}{S^2} + 2\ln\frac{S^2-4}{S^2}\right] \quad (44)$$

where A_H is the Hamaker constant for water across an oil medium and $S=r/R_w$, where r is the distance between the centers of aqueous cores. Substituting this potential into Eq. 12, one obtains

$$B_a = - \frac{2A_H}{kTS_o^3} \left[\frac{2}{3} \ln \frac{S_o-2}{S_o+2} - \frac{4S_o}{3} - \frac{S_o^3}{3} \ln \frac{S_o^2-4}{S_o^2} \right] \quad (45)$$

where $S_o=2R_m/R_w$. Since B_a has been determined experimentally, one can use Eq. 45 to calculate the Hamaker constant, A_H. The calculated values of A_H are included in Table I. Interestingly, we obtain the same value ($\sim 2.35 \times 10^{-19}$ J) of the Hamaker constant for both microemulsion series. This is required by the theory, since A_H is a material constant. Although the observed A_H value is still larger than the commonly adopted value[67] of $\sim 5 \times 10^{-20}$ J, it is in good agreement with those obtained by Vrij and coworkers whose values of A_H are not the same for different microemulsion series.[8] The reason for a larger experimental than theoretical Hamaker constant is said to be caused by use of a non-realistic radial distribution function, g(r), in Eq. 10.

Finally, it is possible to combine data for $I(\phi)$ with diffusion coefficients. As mentioned in the Results section, for a particular concentration dependence of $I(\phi)$, there is a corresponding pattern of the diffusion coefficient. From Eqs. 1 and 19, it is seen that $I(\phi)$ and $D(\phi)$ have a reverse relationship to the osmotic compressibility. Since the maximum of $I(\phi)$ has satisfactorily been accounted for by using the hard sphere model for the osmotic compressibility, this same factor should also be responsible for the occurrence of the minimum of the diffusion coefficient. Combining Eqs. 1 and 19, one obtains

$$f = \frac{K_\phi RT\phi}{D(\phi)I(\phi)} \tag{46}$$

which provides access to calculating the friction coefficient from the diffusion coefficient and excess reduced intensity measured for the same solution. Calculated results of f are presented in Fig. 13. It is interesting that f increases monotonically and does not show any abnormal behavior within the whole concentration range covered in spite of the existence of the maximum in $I(\phi)$ and minimum in $D(\phi)$. This is especially interesting when one realizes that the measurements of scattered light intensity and diffusion coefficients in the present study were done in separate experiments instead of being done simultaneously as was done by Cazabat et al.[11] Also notice that although the shapes of $I(\phi)$ and $D(\phi)$ for microemulsion Series A look quite different from those for Series B, the friction coefficient, f, shows a similar behavior. Apparently, the "regular" behavior of the friction coefficient proves that the "irregular" behavior of $I(\phi)$ and $D(\phi)$ is caused by the variation of the osmotic compressibility since when forming the product of $I(\phi)$ and $D(\phi)$ the effect of the osmotic compressibility cancels out.

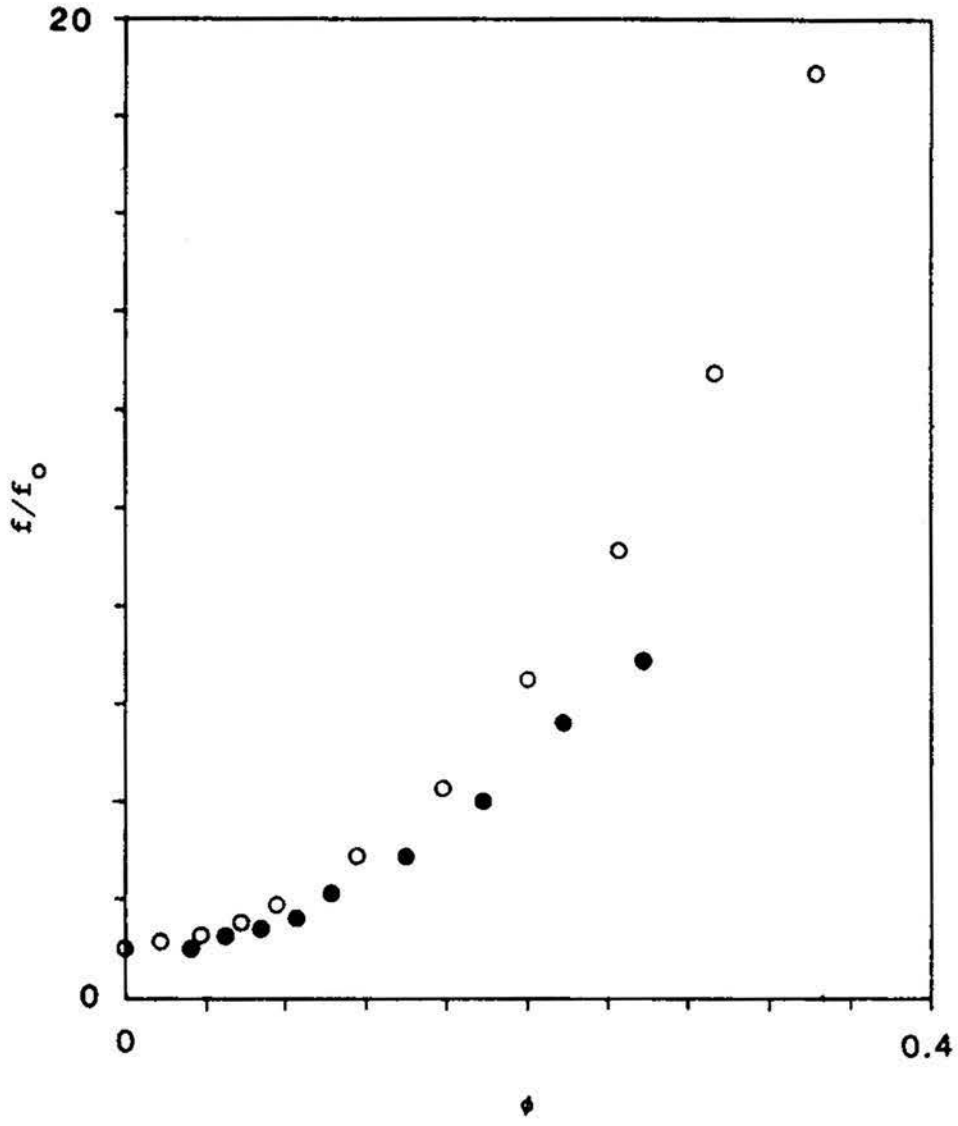

Figure 13. Normalized friction coefficient as a function of volume fraction of the disperse phase. O—Series A; ●—Series B.

SUMMARY

Dynamic and time-average light scattering measurements help us have a better understanding about the structure and interactions between liquid droplets in W/O microemusions composed of SDS, hexylamine, heptane, and brine. A proper dilution technique must be employed in order to interpret the data from light scattering. The molecular weight and radius of droplets have been obtained from the time average intensity measurements. Dynamic light scattering measurements allow one to calculate the hydrodynamic radius. It turns out that the radii obtained by these two scattering techniqes are very close to each other. Concentration dependence of the excess reduced intensity and diffusion coefficient has been interpreted satisfactorily using the hard sphere model. Virial coefficients for osmotic pressure and diffusion coefficents have been obtained. Combination of data of scattered light intensity and diffusion coefficients explains their behavior toward variation of volume fraction of droplets in the microemulsion.

ACKNOWLEDGEMENTS

We would like to thank Drs. Stig Friberg, Gary Bertrand, and Louis Biolsi for many helpful discussions. We are also deeply grateful to Dr. Stig Friberg for allowing us to use the light scattering instrument. This research has been partly supported by the Weldon Spring Endowment Fund of University of Missouri.

REFERENCES

1. Hoar, T. P.; Schulman, J. H. Nature(London) 1943, 152, 102.
2. Tadros, Th. F. in Surfactants in Solutions, Mittal, K. L.; Lindman, B., Eds; Plenum Press: New York, 1984; Vol. 3, p. 1501.
3. Langevin, in "Reverse Micelles", Luisi, P. L.; Straub, B. E. Eds.; Plenum press: New York, 1984; p. 287.
4. Shinoda, K.; Friberg, S. Adv. Colloid Interface Sci. 1975, 4, 281.
5. Friberg, S.; Venable, R. L. in Encyclopedia of Emulsion Technology; Becher, P., Ed.; Marcel Dekker: New York, 1983; Vol. 1, p. 287.
6. Scriven, L. E. in Micellization, Solubilization, and Microemulsions; Mittal Ed.; Plenum Press: New York, 1977; Vol. 2, p. 877.
7. Clausse, M.; Peyrelasse, J.; Heil, J.; Boned, C.; Lagourette, B. Nature 1981, 293, 636.
8. Agterof, W. G. M.; Van Zomeren, J. A. J.; Vrij, A. Chem. Phys. Lett. 1976, 43, 363.
9. Calje, A. A.; Agterof, W. G. M.; Vrij, A. in Micellization, Solubilization, and Microemulsions; Mittal, K. L., Ed.; Plenum Press: New York, 1977; Vol. 2, p. 179.

10. Cazabat, A. M.; Langevin, D.; Pouchelon, A. J. Colloid Interface Sci.1980, 73, 1.

11. Cazabat, A. M.; Lanvegin, D. J. Chem. Phys. 1981, 74, 3148.

12. Bellocq, A. M.; Biais, J.; Bothorel, P.; Clin, B.; Fourche, G.; Lalanne, P.; Lemaire, B; Lemanceau, B.; Roux, D. Adv. Colloid Interface Sci. 1984, 20, 167.

13. Brunetti, S.; Roux, D.; Bellocq, A. M.; Fourche, G.; Bothorel, P. J. Phys. Chem. 1983, 87, 1028.

14. Cebula, D. J.; Ottewill, R. H.; Ralston, J ; Pusey, P. N. J. Chem. Soc. Faraday Trans. 1981, 77, 2585.

15. Albers W.; Overbeek, J. T G. J. Colloid Interface Sci. 1959, 14, 510.

16. Bellocq, A. M.; Fourche, G; Chabrat, P.; Letamendia, L; Rouch, J.; Vaucamps, C. Optica Acta 1980, 27, 1629.

17. Graciaa, A.; Lachaise, J.; Chabrat, P.; Letamendia, L.; Rouch, J.; Vaucamps, C.; Bourrel, M.; Chambu, C. J. Phys. Lett.(Paris) 1977, 38, L-253.

18. Day, R. A.; Robinson, B. H.; Clarke, J. H. R.; Doherty, J. V. J. Chem. Soc. Faraday Trans. 1979 75, 132.

19. Cazabat, A. M.; Chatenay, D.; Guering, P.; Langevin, D.; Meunier, J.; Sorba, O. in Reverse Micelles; Luisi, P. L.; Straub B. E., Eds.; Plenum Press: New York, 1984, p. 121.

20. Nicholson, J. D.; Clarke, J. H. R. in Surfactants in Solutions; Mittal, K. L.; Lindman, B., Eds.; Plenum Press: New York, 1984; Vol. 3, p. 1663.

21. Finsy, R.; Devriese, A.; Lekkerkerker, H. J. Chem. Soc. Faraday II. 1979, 76, 767.

22. Kim, M. W.; Dozier, W.D.; Klien, R. J. Chem. Phys. 1986, 84, 5919.

23. Graciaa, A.; Lachaise, J.; Chabrat, P.; Letamendia, L. Rouch, J.; Vaucamps, C. J. Phys. Lett.(Paris) 1978, 39, L-235.

24. Pusey, P. N.; Tough, R. J. A.; Adv. Colloid Interface Sci. 1982, 16, 143.

25. Roux, D.; Bellocq, A. M.; Bothorel, P. in Surfactants in Solutions Mittal, K. L.; Lindman B., Eds.; Plenum Press: New York, 1984; Vol. 3, p. 1843.

26. Cazabat, A. M.; Chatenay, D.; Langevin, D.; Meunier, J.; Leger, L. in Surfactants in Solutions; Mittal, K. L.; Lindman, B., Eds.; Plenum Press: New York,1984; Vol. 3, p. 1729.

27. Mazer, N. A. in Dynamic Light Scattering; Pecora, R., Ed.; Plenum Press: New York, 1985, p. 305.

28. Venable, R. L.; Elders, K. L.; Fang, J. J. Colloid Interface Sci. 1986, 109, 330.

29. Fang, J.; Venable, R. L. J. Colloid Interface Sci., in press.

30. Debye, P. J. Phys. Colloid Chem. 1947, 51, 18.

31. Utiyama, H. in Light Scattering from Polymer Solutions; Huglin, M. B., Ed.; Academic Press: 1972; chapter 4.

32. Berry, R. S.; Rice, S. A.; Ross, J. Physical Chemistry; Wiley: New York, 1980; p. 929.

33. Mcquarrie, D. A. Statistcal Mechanics; Harper & Row: New York, 1976; Chapter 12.

34. Carnahan, N. F.; Starling, K. E. J. Chem. Phys. 1969, 59, 635.

35. Chu, B. Laser Light Scatering; Academic Press: New York, 1974, p. 204.

36. Berne, B. J.; Pecora, R. Dynamic Light Scattering; Wiley: New York, 1976; chapter 13.

37. Zero, K.; Pecora, R., in Dynamic Light Scattering; Pecora, R., Ed.; Plenum Press: New York, 1985.

38. Pusey, P. N. J. Phys. A 1975, 8, 1433; 1978, 11, 119.

39. Pusey, P. N.; Koppel, D. E.; Schaefer, D. W.; Camerini-Otero, R. D.; Koening, S. H. Biochem. 1974, 13, 952.

40. Foord, R.; Jakeman, E.; Oliver, C. J.; Pike, E. R.; Blagrove, R. J.; Wood, E.; Peacoke, A. R. Nature 1970, 227, 242.

41. Camerini-Otero, R. D.; Pusey, P. N.; Koppel, D. E.; Schaefer, D. W.; Frankelin, R. M. Biochem. 1974, 13, 960.

42. Cummins, H. J.; Pike, E. P. Photon Correlation and Light Beating Spectroscopy; Plenum Press: New York, 1974.

43. Felderof, B. U. J. Phys. A. 1978, 11, 929.

44. Batchelor, G. K. J. Fluid Mech. 1983, 131, 155.

45. Batchelor, G. K. J. Fluid Mech. 1976, 75, 379.

46. Reif, F. Fundamentals of Statistcal and Thermal Physics; McGraw-Hill: New York, 1965; Section 15.6.

47. Bloomfield, V. A. in Dynamic Light Scattering; Pecora, R., Ed.; Plenum Press: New York, 1985; chapter 10.

48. Koppel, D. E. J. Chem. Phys. 1972, 57, 4814.

49. Brow, J. C.; Pusey, P. N.; Dietz, R. J. Chem. Phys. 1975, 62, 1136.

50. Billmeyer Jr., F. W. Textbook of Polymer Science; Wiley: New York, 1984; 3rd ed., p. 18.

51. Huglin, M. B., Ed.; Light Scattering from Polymer Solutions; Academic Press: 1972.

52. Bowcott, J. E.; Schulman, J. H. Z. Elektrochem. 1955, 59, 283.

53. Schulman H. H.; Friend, J. A. Kolloid Z. 1949, 115, 67.

54. Graciaa, A.; Lachaise, J. ; Martinez, A.; Bourrel, M.; Chambu, C. C. R. Acad. Sci., Ser B, 1976, 282, 547.

55. Cazabat, A. M. J. Phys. Lett.(Paris) 1983, 44, L-593.

56. Talmon, Y.; Prager, S. J. Chem. Phys. 1978, 69, 2984.

57. Granz, A. M.; Boeger, B. E. J. Colloid Interface Sci. 1986, 109, 499.

58. Graciaa, A.; Lachaise, J.; Bourrel, M.; Schechter, R. S.; Wade, W. H. J. Colloid Interface Sci. 1986, 113, 583.

59. Dominguez, J. G.; Wilhite, G. P.; Green, D. W. in Solution Chemistry of Surfactants; Mittal, K. L., Ed.; Plenum Press: New York, 1979; Vol. 2, p. 673.

60. Ruckenstein, E. J. Dispersion Sci. Technol. 1981, 2, 1.

61. Dvolaitzky, M.; Guyot, M.; Lagues, M.; Le Pesant, J. P.; Ober, R.; Sauterey, C.; Taupin, C. J. Chem. Phys. 1978, 69, 3279.

62. Huang, J. S.; Safran, S.; Kim, M. W.; Grest, G. S.; Kotlarchyk, M.; Quireke, N. Phys. Rev. Lett. 1984, 53, 592.

63. Philips, J. N.; Trans. Faraday Soc. 1955, 51, 561.

64. Sjoblom, E., and Friberg, S., J. Colloid Interface Sci. 1978, 67, 16.

65. Dautzenberg, J. Polym. Sci. 1974, C39, 125.

66. Hamaker, H. C. Physica 1937, 4, 1058.

67. Hiemenz, P. C. Principles of Colloid and Surface Chemistry; Marcel Dekker: New York, 1986, 2nd ed., chapter 11.

VITA

Jiafu Fang was born on November 30, 1952 in Yunxiao, Fujian, The People's Republic of China. He received his primary and secondary education in Yunxiao, Fujian and graduated from Xiamen(Amoy) University, Xiamen, Fujian, The People's Republic of China, with a Bachelor of Science degree in chemistry.

He has been enrolled in the Graduate School of University of Missouri-Rolla since January 1984.